UC San Diego
UC San Diego Electronic Theses and Dissertations

Title
Topological Phases and Strongly Correlated Fermions in Many-Body Systems

Permalink
https://escholarship.org/uc/item/5022z7tn

Author
Ben-Zion, Daniel

Publication Date
2019

Peer reviewed|Thesis/dissertation

eScholarship.org Powered by the California Digital Library
University of California

UNIVERSITY OF CALIFORNIA SAN DIEGO

Topological Phases and Strongly Correlated Fermions in Many-Body Systems

A dissertation submitted in partial satisfaction of the
requirements for the degree
Doctor of Philosophy

in

Physics

by

Daniel Ben-Zion

Committee in charge:

Professor John McGreevy, Chair
Professor Daniel Arovas
Professor Tarun Grover
Professor Kenneth Intrilligator
Professor Justin Roberts

2019

Copyright
Daniel Ben-Zion, 2019
All rights reserved.

The dissertation of Daniel Ben-Zion is approved, and it is acceptable in quality and form for publication on microfilm and electronically:

_____

_____

_____

_____

_____

Chair

University of California San Diego

2019

DEDICATION

This thesis is dedicated to my parents, and to my cat Lenny.

EPIGRAPH

”It’s the job that’s never started as takes longest to finish."

J.R.R. Tolkien, The Lord of the Rings

TABLE OF CONTENTS

Signature Page iii

Dedication iv

Epigraph v

Table of Contents vi

List of Figures ix

List of Tables xi

Acknowledgements xii

Vita xiii

Abstract of the Dissertation xiv

Chapter 1 Introduction 1
1.1 Outlook 1

Chapter 2 Exactly solvable models of spin liquids with spinons, and of 3d topological paramagnets 8
2.1 Context 8
2.2 Snake monster 11
2.2.1 Generalization to other quantum double models 14
2.3 Cluster states as 1d SPT states 16
2.3.1 Stability of the edge states 18
2.4 An exactly solvable spin liquid with spinons 19
2.4.1 Unitary symmetry 20
2.4.2 String operators and anyons 20
2.4.3 Time-reversal-invariant cluster snake 22
2.5 Exactly solvable models of topological paramagnets 23

2.5.1 Pure loop model review 24
2.5.2 Cluster snake paramagnet 26
2.5.3 Nontriviality of the snake paramagnet 27
2.5.4 Relation to coupled layer construction 29
2.6 Discussion 30

Chapter 3 Strange metal from local quantum chaos 32
3.1 Introduction 32
3.2 Large-N analysis 37
3.2.1 SYK review 37
3.2.2 Using SYK clusters to kill the quasiparticles and take their momentum 39
3.2.3 Replica analysis 42
3.3 Towards finite N 44
3.3.1 Renormalization group analysis of impurity problem 44
3.3.2 Possibilities for the phase diagram 46
3.4 Coupling a Fermi surface to $\mathrm{SYK}_{2.0001}$ clusters 47
3.5 Numerical analysis 50
3.6 Conclusions 55
3.7 Acknowledgements 57

Chapter 4 Disentangling quantum matter: Applications to scars, heavy fermions, and gapless topological phases 60
4.1 Context 60
4.2 SPT physics in the presence of gaplessness 61
4.3 An operator-agnostic QDL measurement 64
4.4 Disentangling heavy Fermi liquids 71
4.5 Acknowledgements 74

Appendix A 75
A.1 Cluster states for $\mathbb{Z}_N$ 75
A.2 Stability of the physics of the snake monster 77
A.3 Triviality of the cluster paramagnet with unitary symmetry 79

A.4 Self-dual models of confinement 82
A.4.1 $\mathbb{Z}_N$ self-dual models of confinement 83

Appendix B 87
B.1 $1/N$ corrections to the cluster-fermion propagator 87
B.2 Other numerical results 90

Bibliography 92

LIST OF FIGURES

Figure 2.1: Kitaev's toric code in two dimensions 11

Figure 2.2: In the coupled layer construction, three anyons on neighboring surfaces are condensed, destroying topological order in the bulk. 29

Figure 3.1: A cartoon of the model we study in this paper. Each blob represents an independent SYK model. The vertical edges represent the random couplings g_{ix}. The horizontal edges represent the translation-invariant hopping amplitudes t. 35

Figure 3.2: A diagram of the model in two spatial dimensions. The vertical (blue) bonds represent the random hybridization couplings g_{xi}. The black horizontal bonds are the uniform hoppings, t. 37

Figure 3.3: Proposed phase diagram of the FS $\times$ SYK model 38

Figure 3.4: The self-energy diverges at $\omega = 0$, leading to a *zero* of the Green's function, and of the spectral density $A(k,\omega)$, exactly at the Fermi surface. 40

Figure 3.5: Diagrams contributing to cluster fermion green's function 41

Figure 3.6: The corrections to the localized-fermion propagator $\mathscr{G}$ at order $1/N$. . . . 42

Figure 3.7: When $g \gg J$, we can neglect the SYK interactions, and our problem becomes quadratic. Hybridizing a localized fermion (flat band) with an itinerant fermion produces this bandstructure. 46

Figure 3.8: Possible behaviors of the beta function for g, given the known asymptotics. Arrows point toward the infrared. 46

Figure 3.9: Behavior of the half-chain entanglement entropy in scenarios 1 and 3 of Fig. 3.8. 47

Figure 3.10: The half-chain entanglement $S(L/2) - S(2)$ at fixed $L = 52$, as a function of g, averaged over up to 600 samples. 52

Figure 3.11: Half chain entanglement entropies of the SYK $\times$ FS chain 53

Figure 3.12: Finite size entanglement of the FS $\times$ SYK chain 54

Figure 3.13: Correlation functions of local fermions 58

Figure 3.14: Half chain entanglement entropy of disordered free fermions 59

Figure 4.1: Leftmost: Entanglement spectrum across the center bond of the full wave function. Right plots: Entanglement spectrum across the center bond for the projected wave function $|\Psi_s\rangle$ for three randomly chosen hole configurations. The system size is $L = 96$, with couplings $J = 0.1$ and $D = 0.01$. Also shown is the mean spacing between pair levels in the entanglement spectrum $\langle\Delta\rangle$. 62

Figure 4.2: QDL Measure $S^{s/c}$ across the phase diagram. Left) Topological phase: entanglement entropy of post-projection spin wavefunction collapses to an area law. Middle) Critical point: entanglement entropy of post-projection spin wavefunction shows critical behaviour with $c = 1$. Right) Trivial phase: entanglement entropy of post-projection spin wavefunction collapses to an area law. 64

Figure 4.3: Entanglement entropy and CMI measurements on one dimensional Hubbard model as a function of bipartioning cut at couplings $U = 4$, $V = 3/4$. Left: Ground state. Middle: A generic state in the charge band. Right: A state in the spin band. Colors corresonpond to the same legend as the other two plots. 67

Figure 4.4: Subsystem mutual informations representing the refined QDL protocol . . . 71

Figure 4.5: Conditional mutual information calculated in the paramagnetic HFL phase. Left: Conditional mutual information of f electrons as a function of linear size of region A. Right: Conditional mutual information of c electrons. The system is bipartitioned into left and right halves. 72

Figure 4.6: Left: Conditional mutual information calculated in the AFs phase. Right: Conditional mutual information at $n_c = 1$ in the HFL phase. 73

Figure A.1: As the quasiparticles hop around, they acquire phases dependent on the flux through the plaquettes. 77

Figure B.1: $S_{1/2}$ vs Log(L) calculating using standard DMRG at small g. 90

Figure B.2: A check on the validity of the truncation method. 91

LIST OF TABLES

Table 2.1: Action of $g^{o/e}$ on the anyons. 21
Table 2.2: Spectrum of anyons in the $eTmT$ model 27

Table A.1: Sublattice-dependent symmetry action on anyons 80
Table A.2: Flux fusion table for gauged cluster paramagnet 81

ACKNOWLEDGEMENTS

First and foremost I would like to thank my advisor John McGreevy. Throughout my journey through graduate school John provided me with continuous mentorship, discussion, collaboration, and support. His door was always open, and over the six years we worked together I cannot remember a single occasion where he did not put down whatever he was working on at the time to entertain my questions. Thank you for the constant guidance, teaching, and for challenging me to find interesting questions.

Another instrumental person during my time in graduate school was Dan Arovas - for all of the amazing classes I took from him, and for many helpful discussions. But most importantly, for expanding my horizons regarding spicy food, and for sharing his repertoire of excellent jokes. I would also like to thank Tarun Grover for stimulating collaborations and for pushing me to be a better physicist. Finally I would like to thank all of the friends I made along the way, especially Shenglong Xu, who probably taught me as much as any professor.

Chapter 2 is, in part, a reprint of material from published work done in collaboration with John McGreevy and Diptarka Das, as it appears in Physical Review B, as well as on the arXiv. D. Ben-Zion, D. Das, and J. McGreevy, "Exactly solvable models of spin liquids with spinons, and of three-dimensional topological paramagnets," *Phys. Rev. B* **93** 155147. The dissertation author was the primary investigator and author of this material.

Chapter 3 is, in part, a reprint of material from published work done in collaboration with John McGreevy, as it appears on Physical Review B. D. Ben-Zion and J. McGreevy, "Strange Metal from Local Quantum Chaos," *Phys. Rev. B* **97** 155117 . The dissertation author was the primary investigator and author of this material.

Chapters 4 is, in part, a reprint of material from work done in collaboration with Tarun Grover and John McGreevy, as it will appear on the arXiv. The dissertation author was the primary investigator and author of this material.

The work in this dissertation was supported in part by DOE grant DE-SC0009919.

VITA

2013	B. S. in Physics, University of Southern California, Los Angeles
2019	Ph. D. in Physics, University of California San Diego

PUBLICATIONS

Daniel Ben-Zion,Diptarka Das, and John McGreevy, "Exactly solvable models of spin liquids with spinons, and of three-dimensional topological paramagnets," *Phys. Rev. B* **93** 155147 (2016), arXiv:1511.01539.

Daniel Ben-Zion and John McGreevy, "Strange Metal from Local Quantum Chaos," *Phys. Rev. B* **97** 155117 (2018), arXiv:1611.01229.

Daniel Ben-Zion, Tarun Grover, and John McGreevy, "Disentangling quantum matter: Applications to scars, heavy fermions, and gapless topological phases," *in preparation*

ABSTRACT OF THE DISSERTATION

Topological Phases and Strongly Correlated Fermions in Many-Body Systems

by

Daniel Ben-Zion

Doctor of Philosophy in Physics

University of California San Diego, 2019

Professor John McGreevy, Chair

In this dissertation we study the properties of quantum many-body systems whose behavior is governed by strong correlation effects between large numbers of degrees of freedom. We begin with a review of various types of condensed matter settings and a general discussion of how interactions can lead to qualitatively new properties. In Chapter 2 we discuss a class of spin models which generate nontrivial realizations of a global symmetry, both in the presence and absence of topological order. In Chapter 3, we examine a model of a non-Fermi liquid. This model is built out of electron-like degrees of freedom and has a Fermi surface, yet has no stable quasiparticle excitations. In Chapter 4 we discuss some aspects of entanglement entropy in gapless multi-component systems, and suggest a way of measuring the topological properties of

Kondo lattice wavefunctions.

Chapter 1

Introduction

1.1 Outlook

The development of quantum mechanics in the early 1900's and its subsequent application to condensed matter systems has led to an unprecedented level of understanding of the properties of a wide class of materials. In many cases, a satisfactory explanation of the behavior of a system can be obtained by assuming that the particles comprising the system are noninteracting, or only weakly interacting. Noninteracting - or free - theories are able to account for many exotic phenomena including Bose-Einstein condensation, the existence of metals, and topological insulators.

Adding a small amount of interactions to a free theory often results in a weakly coupled theory which may be studied by perturbation theory. The idea is that the properties of the weakly interacting system are almost like that of the free system, but just a little bit different. A description in terms of a weakly coupled theory is relevant to huge fraction of materials we encounter in the real world.

What does it mean for interactions to be 'weak' or 'strong'? For the moment we specialize to the case of electrons, since many condensed matter systems are either themselves models of

electrons, or descend in one way or another from a model of electrons. If we wish to estimate the magnitude of correlation effects, we can compare the typical kinetic energy (KE) and potential energy (U) an electron experiences. If the ratio KE/U is large, then interactions will not have a very strong affect and the system will behave more or less like a system of free electrons. On the other hand if U is comparable in magnitude to KE, then it is likely that the electronic degrees of freedom will undergo some qualitative reorganization in order to lower their potential energy.

Within the Jellium model of a homogenous electron gas, the average kinetic energy is $\frac{3}{5}E_f$, where E_f is the Fermi energy, and the average potential energy of an electron is $U = e^2/\langle r \rangle$. The mean inter-electron separation may be related to the electron density through the relation $\frac{4}{3}\pi\langle r^3 \rangle n = 1$. Similarly, the Fermi energy is related to the density via

$$E_f = \frac{1}{2m_e}\left(3\pi^2 n\right)^{2/3}$$

in three dimensions. We thus find that $E_f/U \sim n^{1/3}$, so in systems with a high density of electrons the kinetic term dominates. On the other hand, when the density of electrons is low, correlation effects play an increasingly important role in determining the properties of the system. For example, it may be favorable for the electrons to form a Wigner crystal [1] in order to maximize the typical nearest-neighbor distance.

One paradigmatic example of how competition between kinetic and potential energy can lead to strongly correlated physics is the Mott insulator, in which an electronic system at half filling becomes insulating due to the repulsion between electrons. At half filling, there is exactly one electron per site. In general the electrons would like to move around in order to reduce their kinetic energy. To do so, they must pay a price corresponding to the energy it costs to put two electrons on the same site. As a consequence, the system forms an incompressible insulating state. The existence of this insulating state is due entirely to correlation effects; in the absence of the coulomb interaction the system would be a metal.

This simple picture of a Mott insulator is a starting point for understanding a variety of spin related phenomena such as magnetism [2], and spin liquids [3]. The charge degrees of

freedom are quenched to one electron per site, effectively leaving behind a lattice with a spin half degree of freedom on every site. Within degenerate perturbation theory, virtual hopping processes of electrons give rise to an effective Heisenberg interaction between spins. To understand the magnetic properties of these systems, we may therefore consider an effective model of spins residing at the sites of the lattice.

Spin models have a storied history in condensed matter physics dating back to the Ising model, which was first proposed as a toy model of ferromagnetism in 1920 [4]. The traditional way of characterizing the phase diagram of a spin model is through the use of symmetries, as pioneered by Landau [5]. When it comes to ground states of quantum mechanical systems things are more subtle, and it is possible for two states to realize the symmetries in the same way yet belong to distinct phases of matter. Two notable examples of this is are states with topological order [6], and symmetry protected topological phases [7].

State with topological order differ from those without - typically referred to as *trivial* - through some global properties of the wavefunction. As such, they cannot be distinguished by local measurements. This is related to their famous robustness. In the same way that local measurements cannot access global properties of the wavefunction, local perturbations cannot affect the topological order of the state. Topologically ordered states have an energy gap and host stable fractional excitations known as anyons. In the most exotic cases, braiding various anyons around each other acts as a unitary operator on the state. This property, combined with the robustness of the topological information stored in a state, make such states prime candidates as platforms for quantum computation.

One of the most well known spin models which exhibits topological order is Kitaev's Toric Code [8], an exactly solvable model of a state with $\mathbb{Z}_2$ topological order. This model can be constructed by placing Ising spins on the links of a square lattice in two dimensions. The

Hamiltonian for the system can be written as sum over sites i and plaquettes p as

$$H_{TC} = -\sum_i A_i - \sum_p B_p = -\sum_i \prod_{l(i)} \sigma_l^z - \sum_p \prod_{l \in p} \sigma_p^x.$$

The product in the first term means a product over links emanating from site i and the product in the second term means product over links bordering a plaquette p.

The ground state of this Hamiltonian has a simple interpretation as a uniform superposition of closed string configurations. There are two kinds of quasiparticle like defects - 'electric' defects corresponding to sites where strings end, and 'magnetic' defects corresponding to plaquettes with π flux through them. By repeated use of the Pauli matrix commutation relations, it is possible to verify that upon bringing an electric defect around a magnetic one, the wave function acquires a phase of -1. The nontrivial mutual statistics of e and m defects is a characteristic of the topological order of this wavefunction.

In Chapter 2, exactly solvable models are constructed using Toric Code like hamiltonians as a base. These models have additional global symmetries and it is shown that the electric defects form projective doublets under the new symmetry. The enrichment of the Toric Code by an additional symmetry which acts nontrivially on the anyons leads to a state with so-called symmetry enriched topological (SET) order. Destroying the topological order results in a symmetry protected topological (SPT) phase which can be understood in terms of a decorated domain wall picture.

Spin models provide a wide variety of contexts for studying correlated phases of matter, but understanding strongly correlated states of fermions where the charge degrees of freedom are not quenched remains a major challenge in modern condensed matter theory. The standard lore of Landau Fermi Liquid theory (FLT) [9] holds that a system of interacting electrons is adiabatically connected to a system of noninteracting electron-like quasiparticles. This result can be very elegantly understood in terms of a renormalization group calculation which shows that in the presence of a Fermi surface, the four-fermion interaction term is for the most part irrelevant [10, 11]. The effect of interactions is to renormalize thermodynamic properties away from their noninteracting values, but qualitatively the behavior is that of a noninteracting Fermi surface.

The quasiparticles can be partially characterized by the quasiparticle weight Z, which roughly speaking measures the overlap between the quasiparticle and the bar electron.

Despite the success of this quasiparticle picture, it is an indisputable fact that there exist fermionic systems which are not described by Fermi liquid theory. A class of examples which has garnered an enormous amount attention is the strange metal phase observed in several high temperature superconducting materials such as $YBa_2Cu_4O_8$ and $La_{2-x}Sr_xCuO_4$ [12]. One of the most noteworthy properties of these materials is that they exhibit a resistivity which is linearly proportional to the temperature over a range of temperatures spanning several hundred Kelvin. Although there are mechanisms for linear-in-T resistivity over parts of the temperature range (scattering from classical phonons, for example), a satisfactory explanation of this phenomena is not possible within the framework of Fermi liquid theory.

One of the reasons for this is that the central assumption of FLT, the existence of long lived quasiparticles, places certain constraints on the transport behavior. Requiring the quasiparticle lifetime to be much larger than the mean collision time leads to the Mott-Ioffe-Regel (MIR) limit which gives the maximum resistivity possible in a system described by quasiparticles [13]. A resistivity in excess of the MIR limit implies that the quasiparticle picture is breaking down and a new description is required. Experimentally, the resistivity of strangle metals is found to cross the MIR limit with impunity.

There have been many attempts at providing a theory of non-Fermi liquids. One successful approach has been coupling the Fermi surface to some bosonic modes which are tuned to a quantum critical point [14]. This has the effect of modifying the fermion greens function in such a way that the quasiparticle weight vanishes, which means that the electron operator has zero overlap with any stable quasiparticle state. Another way of saying this is that the quasiparticle lifetime becomes zero.

With regards to transport properties however, there is a distinction between the quasiparticle lifetime and the transport lifetime, which also takes into account the angular deflection due to

scattering. Scattering off of gapless bosonic modes primarily takes place at small momentum transfer, therefore this scattering mechanism is not sufficient to qualitatively alter the transport lifetime. In Chapter 3, an alternative theory of a non-Fermi liquid is formulated by coupling a Fermi surface to locally critical fermionic modes. One useful feature of this formulation is that the transport lifetime is equal to the quasiparticle lifetime. The work builds on exciting recent developments at the intersection between high energy theory and condensed matter known as the SYK model [15, 16].

Another context for obtaining exotic physics due to correlation effects in fermionic systems can be found in Kondo lattice models. These models are given by the schematic Hamiltonian

$$H_{KLM} = \sum_{k\sigma} \varepsilon_k c^\dagger_{k\sigma} c_{k\sigma} + J \sum_i \vec{S}_i \cdot \vec{s}_i$$

where $\vec{S}_i$ represents a spin $1/2$ local moment on site i and $\vec{s}_i = c^\dagger_{i\alpha} \vec{\sigma}_{\alpha\beta} c_{i\beta}$ is the electron spin operator. This effective model is thought to describe the physics of heavy fermion materials, in which itinerant conduction electrons interact with an array of local moments representing a partially filled f state [17]. The conduction electrons mediate RKKY interactions between the local moments, and the physics of this model is determined by the competition between Kondo screening and a tendency towards antiferromagnetic order.

One approach to understanding the properties of this model begins by expressing the spin operator in terms of slave fermions as $\vec{S}_i = f^\dagger_{i\alpha} \vec{\sigma}_{\alpha\beta} f_{i\beta}$. This representation must be supplanted by the constraint $n_f = 1$ on every site to be exact. The mean field solution to this Hamiltonian consists of decoupling the interaction term with a parameter $b = \langle c^\dagger f \rangle$ which represents the hybridization between conduction electrons and the f slave fermions. It is important to note that within mean field theory the constraint $n_f = 1$ is implemented only on average rather than exactly on every site. Enforcing the constraint exactly amounts to including gauge fluctuations of an emergent gauge field representing the transformation $f_i \to f_i e^{i\theta(i)}$. Crucially, the mean field parameter b is not gauge invariant, so under an exact treatment of this model the quantity $\langle c^\dagger f \rangle$ always vanishes. Therefore, it is desirable to have some other quantity to serve as a kind of 'order

parameter' for the heavy fermi liquid (HFL) phase.

Another interesting aspect of Kondo lattice models concerns the fate of the local moments outside of the HFL phase. If the coupling J is below some threshold value, then it is expected that itinerant fermions and local moments approximately decouple at low energies. One possibility is that the spins order antiferromagnetically. This is the so-called AFs phase, in which a small fermi surface of conduction electrons coexists with antiferromagnetically ordered spins. In the absence of magnetic order, the Lieb-Shultz-Mattis-Hastings-Oshikawa theorem places strong constraints on the form of the spin wavefunction [18, 19, 20, 21]. In particular, it forbids the existence of a trivial featureless state. In this scenario, the spins are forced into a state with topological order.

In Chapter 4, we partially address some of these questions by studying entanglement in Kondo lattice models. We apply recent ideas regarding quantum disentangled states [22] to serve as an order parameter for the HFL phase. More generally, we explore the usage of quantum disentangled measurements and conditional mutual information as a tool for characterizing entanglement in gapless phases. In the context of Kondo systems, we find that the conditional mutual information serves as a diagnostic for whether the local moments participate in the fermi surface or not. Importantly, this is a more general quantity than the non-gauge-invariant mean field parameter and could in principle be measured in Monte Carlo simulations where the constraint $n_f = 1$ is implemented exactly on every site. We also conjecture as to the applying these ideas for measuring the topological order in the aforementioned FL^* phase.

Chapter 2

Exactly solvable models of spin liquids with spinons, and of 3d topological paramagnets

2.1 Context

Worldsheet matter for electric flux strings. The idea that worldsheets of strings may have dynamical degrees of freedom living upon them (in addition to the fields which encode their embedding in space(time)) is crucial for fundamental string theory [23]. This possibility is realized in other contexts as well, such as in the worldvolume theory of domain wall strings in the 2d Ising model [24].

In this paper we are going to show how to glue (1+1)-dimensional topological states to the electric flux lines of a gauge theory, in an exactly solvable way. The signature of a nontrivial 1d topological state is some degeneracy at the edge of an open chain, generally representing projectively a symmetry of the system. Since the ends of electric flux lines are electric charges, our construction provides a machine for imbuing the charges of a gauge theory with nontrivial symmetry properties.

The information we need to accomplish this goal is just a certain “circuit construction" of

the 1d topological state, *i.e.* a collection of unitary operators associated to the links which create and destroy the desired 1d state out of a background bath of product states.

Previously, frustration free parent hamiltonians and representative wave functions have been constructed and used to study the nontrivial symmetry properties [25, 26, 27]. Here, we systematically generalize this idea to produce a variety of interesting decorated string net models whose entire spectrum is known. In particular, we can guarantee that the spectrum is gapped. We will occasionally refer to these models as snake monsters. The name is motivated by the idea that we are imparting dynamics to these one-dimensional creatures with all the action at the ends. We focus most of our attention on two and three spatial dimensions, although extensions to higher dimensions are readily possible.

What are these models for? It has been known for some time that the possibilities for phases of quantum matter extend far beyond Landau's symmetry-breaking paradigm [28]. Two groundstates can preserve the same symmetry yet nonetheless belong to distinct phases. Even in the absence of symmetry, different patterns of long range entanglement can lead to distinct types of topological order.

By now there exist several partial classification schemes for topological phases [29, 30, 31, 32]; it is not clear that these schemes are complete. Furthermore, these methods are quite formal and do not necessarily lead to an intuitive understanding of the physics. Therefore, it is worthwhile to search for tractable examples which realize interesting phases.

Along the same lines, one would like to have a constructive method of building models which realize distinct phases. One such method is due to Walker and Wang [33]. In some ways our construction is an alternative to theirs in the sense that we bootstrap a given SPT order onto a higher dimensional gauge theory, which may be more suitable for the study of SETs.

Herding snakes. In section 2.2 we introduce the scheme in somewhat general terms. Since this construction is rather versatile and has already led us to a variety of examples, we first provide some organizing discussion and explain how they differ in physics and in technical

aspects. The models we discuss can be organized along several axes:

1. *Do they have topological order, and of what nature?*

   The models discussed in sections 2.2-2.4 have (abelian) topological order. These are therefore solvable representatives of symmetry-enriched topological (SET) phases. Previous examples of solvable models (and indeed partial classifications) of such phases have appeared in [34, 35], but our approach is quite different. In this context, the novelty of our construction is its simplicity and flexibility.

   In section 2.5 we extend a construction [36] of 3d models made from fluctuating strings *without* topological order. We use this to make solvable models of some topological paramagnets, and discuss their nontriviality as symmetry-protected topological (SPT) states[1]. The phases represented by this framework go beyond the group cohomology classification of [29].

2. *What symmetry protects their nontriviality?*

   In section 2.3 we provide a detailed review of cluster states, an example of a 1d SPT. These enjoy a solvable Hamiltonian which is protected from triviality either by time-reversal symmetry or (on a bi-partite graph) by a unitary $\mathbb{Z}_2 \times \mathbb{Z}_2$ symmetry.

3. *Is it a model of bosons/spins or one with microscopic fermions?*

   An example of the former may be obtained from an example of the latter by gauging the fermion parity symmetry. (A recent discussion of this connection appears in [43].)

   In this paper, all of our examples are models of bosonic SPTs. One can construct fermionic SPTs along similar lines, but we leave that for the future.

[1] For reviews of SPT and SET physics, see [37, 38]. Exactly solvable models have been constructed for some examples in [39, 40, 41, 42].

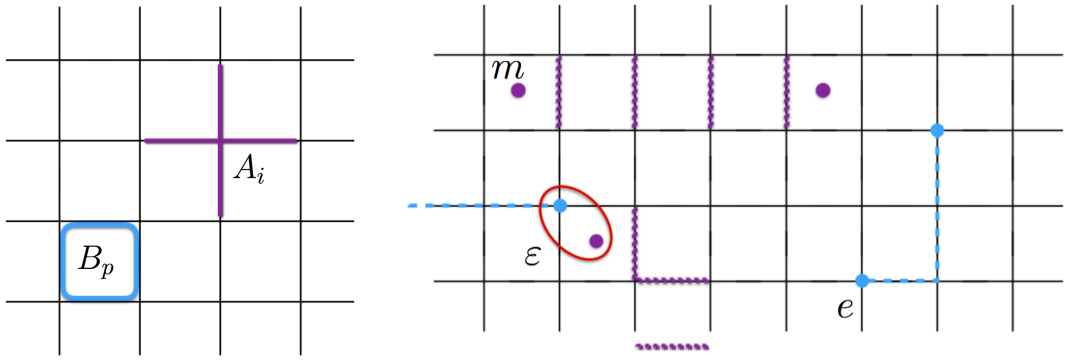

Figure 2.1: Kitaev's toric code in two dimensions. The hamiltonian consists of a sum of 'star' and 'plaquette' terms, shown in (a). In a particular choice of basis, blue lines represent the operator σ^x and purple lines represent σ^z. The elementary excitations of the model are shown in (b). 'Electric' defects are created by acting with a string of σ^x along a curve on the lattice. 'Magnetic' defects are created by acting with a string of σ^z along a curve of the dual lattice. The e and m particles are self-bosons with mutual semion statistics, and their bound state $e \times m = \varepsilon$ is a fermion.

2.2 Snake monster

We start with an exactly solvable lattice gauge theory. We introduce additional degrees of freedom coupled to the gauge fields in a nontrivial way to imbue the gauge theory with further symmetry properties. As a result of this procedure, anyons carry projective representations of the symmetry and we show that these models realize distinct phases. The simplest context in which to introduce our construction is $\mathbb{Z}_2$ lattice gauge theory.

Toric code review. To establish notation, recall the toric code [44], a system of qbits on the links of a graph which emerges $\mathbb{Z}_2$ gauge theory. The toric code is governed by the following hamiltonian:

$$\mathbf{H}_{\mathrm{TC}} = -\sum_p B_p - \sum_j A_j$$

where j runs over sites of the graph, and p runs over the faces[2] and

$$B_p \equiv \prod_{l \in \partial p} \sigma_l^x, \quad A_j \equiv \prod_{l \in v(j)} \sigma_l^z.$$

[2]Actually we are using a bit more structure than just a graph. The required information is a simplicial complex: a list of p-dimensional subspaces Ω^p and a boundary map $\partial : \Omega^p \to \Omega^{p-1}$ which says who is the boundary of whom. For $\mathbb{Z}_2$, the orientations do not matter.

(Here ∂p denotes the collection of links in the boundary of the plaquette p and $v(j)$ is the 'vicinity operator' which gives the collection of links whose boundary contains the site j.) These operators commute and can be simultaneously diagonalized. A useful description of a state is to imagine a link as occupied by a string if $\sigma_l^z = -1$ and unoccupied if $\sigma_l^z = +1$. Then satisfying the 'star terms' ($A_i|\psi\rangle = |\psi\rangle \forall i$) means that strings do not end; arbitrary superpositions of closed strings are the ground states.

The closed-string states of the link variables are

$$|C\rangle = \prod_{l \in C} \sigma_l^x \otimes_l |\sigma^z = 1\rangle$$

where C denotes a collection of occupied links. Their degeneracy under $\sum_j A_j$ is split by the action of B_p, which acts as a kinetic term for the strings:

$$B_p|C\rangle = |C + \partial p\rangle$$

The eigenvalue condition $B_p = 1$ then demands that the groundstate wavefunctions $\Psi(C) \equiv \langle C|\text{groundstate}\rangle$ have equal values for cycles C and $C' = C + \partial p$. This is the equivalence relation defining the 1st homology of the simplicial complex: distinct, linearly-independent groundstates are the labelled by homology classes with coefficients in $\mathbb{Z}_2$. On a simply connected space, there is a unique groundstate

$$|\text{gs}\rangle = \frac{1}{\sqrt{\mathcal{N}_C}} \sum_{\text{closed string collections, } C} |C\rangle$$

where $\mathcal{N}_C$ is the number of closed string configurations.

Circuit description of 1d states. Suppose we are given a *circuit construction* of a nontrivial state of a chain c of quantum spins:

$$|c\rangle = U \otimes_j |\rightarrow_j\rangle. \tag{2.1}$$

The operator $U \equiv \prod_l u_l$ is a product of local unitaries acting on the links which creates the state $|c\rangle$ from a reference product state. We consider here the case where the 1d state is classified by $\mathbb{Z}_2^n$ for some n. We assume the following properties of the link unitaries:

- $u_l^2 = 1$.

- $[u_l, u_{l'}] = 0$.

- When we say that the 1d state is nontrivial, we mean that it cannot be turned into a product state by acting with any finite-depth circuit which respects some given symmetry operation. This in turn imposes that individual link operators u_l fail to commute with the symmetry operation.

We give an example of a collection of link unitaries satisfying our demands in §2.3.

Snake monster. Finally, consider a system with both $\mathbb{Z}_2$ link variables (whose Pauli operators we call σ^x, σ^z as above) and site variables (whose Hilbert space we do not specify yet, but on which the u_l act). Let

$$\mathscr{B}_p \equiv B_p \prod_{l \in \partial p} u_l$$

and

$$h_j \equiv \prod_{l \in v(j)} u_l^{s_l} h_j^0 \prod_{l \in v(j)} u_l^{-s_l}.$$

Here $s_l \equiv \frac{1}{2}(1 - \sigma_l^z)$ counts the number of electric flux lines on the link l which in a $\mathbb{Z}_2$ gauge theory takes values $\{0, 1\}$. The general snake monster hamiltonian is:

$$\mathbf{H} = -\sum_p \mathscr{B}_p - \sum_j A_j + \sum_j h_j P_j \tag{2.2}$$

where $P_j \equiv \frac{1}{2}\left(1 + A_j\right)$ is the projector onto locally closed strings at site j.

The Hamiltonian is a sum of commuting terms and is therefore exactly solvable, as long as h_j^0 is exactly solvable. This statement is otherwise independent of the form of h_j^0. [3] We choose h_j^0 such that its unique ground state is a product state.

[3] To see this explicitly, consider a plaquette sharing two links l_1, l_2 with a site term H_s. Then, ignoring terms which commute trivially,

$$\begin{aligned}
\mathscr{B}_p h_j &= u_{l_1}^{(s_{l_1}-1)} u_{l_2}^{(s_{l_2}-1)} u_{l_1} u_{l_2} .. h_j .. u_{l_1}^{-s_{l_1}+1} u_{l_2}^{-s_{l_2}+1} \sigma_{l_1}^x \sigma_{l_2}^x .. \\
&= (u_{l_1} u_{l_2})^{1-1} \underbrace{u_{l_1}^{(s_{l_1})} u_{l_2}^{(s_{l_2})} .. h_j .. u_{l_1}^{-s_{l_1}} u_{l_2}^{-s_{l_2}}}_{=h_j} \underbrace{u_{l_1} u_{l_2} .. \sigma_{l_1}^x \sigma_{l_2}^x ..}_{=\mathscr{B}_p} \\
&= h_j \mathscr{B}_p.
\end{aligned} \tag{2.3}$$

The groundstate. Let $U_C = \prod_{l\in C} u_l$ denote the product of link unitaries over links in a collection of strings C. The groundstate of $\mathbf{H}$ on a simply connected space is:

$$\begin{aligned} |\mathrm{gs}\rangle &= \frac{1}{\sqrt{\mathscr{N}_C}} \sum_{\text{closed string collections},C} |C\rangle \otimes U_C \otimes_i |\rightarrow_i\rangle \\ &= \frac{1}{\sqrt{\mathscr{N}_C}} \sum_C \left(\prod_{l\in C} \sigma_l^x u_l \right) \left(\otimes_l |\sigma_l^z = 1\rangle \otimes_i |\rightarrow_i\rangle \right) \\ &= \frac{1}{\sqrt{\mathscr{N}_C}} \sum_C \prod_{p\in R|\partial R = C} \mathscr{B}_p \Big(\otimes_l |\sigma_l^z = 1\rangle \otimes_i |\rightarrow_i\rangle \Big) \,. \end{aligned} \tag{2.4}$$

To summarize the preceding construction, the groundstate of the site hamiltonian h_s puts the site variables along electric flux lines of the gauge theory into the state $|c\rangle$ in (2.1), while putting the rest into a product state. The plaquette and site terms commute because $\mathscr{B}_p$ simultaneously moves the flux line and the path along which $|c\rangle$ is laid.

Notice that we have not had to specify the number of spatial dimensions. In two dimensions, our construction is similar to decorated-domain-wall models, in that it involves the decoration of fluctuating closed strings. In three dimensions, domain walls are two dimensional surfaces rather than strings, so this analogy fails. Furthermore, domain walls are by definition contractible, whereas non-contractible string configurations are allowed and present in the cases we consider. Our scheme therefore naturally extends the idea of decorated domain walls to realize decorated string nets.

2.2.1 Generalization to other quantum double models

An extension to $\mathbb{Z}_n$ gauge theory will occasionally be useful [45]. Now we must choose an orientation for each element of our simplicial complex, and the boundary map keeps track of signs. Place an n-state hilbert space on each link, with clock operators $\sigma^x\sigma^z = \omega^{-1}\sigma^z\sigma^x, \omega \equiv e^{2\pi \mathbf{i}/n}$.

$$\mathbf{H} = -\sum_p (\mathscr{B}_p + h.c.) - \sum_j \big(A_j + h.c.\big) + \sum_j h_j P_j \tag{2.5}$$

Here $A_j = \prod_{l\in v(j)} \sigma_l^z$ – in this product, the links are taken to point away from the site j – and $\mathscr{B}_p = B_p U_{\partial p}$ with $B_p = \prod_{l\in\partial p} \sigma_l^x$ and $U_{\partial p} = \prod_{l\in\partial_p} u_l$. The link unitaries u_l act on site variables

at the ends of the links and we assume that[4]

- $[u_l, u_{l'}] = 0$.
- $u_l^n = 1$.
- $u_{jk} = u_{kj}^{-1}$.

Then we choose a reference site hamiltonian h_j^0 (whose groundstate is a product state $\otimes_j |0_j\rangle$) and take

$$h_j = \prod_{l\in v(j)} u_l^{s_l} h_j^0 \prod_{l\in v(j)} u_l^{-s_l} + h.c.$$

and $P_j = \frac{1}{n}\sum_{k=0}^{n-1} A_j^k$ is the projector onto $A_j = 1$. Again the product over links $\prod_{l\in v(j)}$ is taken with the links pointing out of the site.

These terms commute[5] and the groundstate is a uniform sum of closed $\mathbb{Z}_n$ string nets occupied by the $\mathbb{Z}_n$ state

$$\prod u_l^{s_l} \otimes_j |0_j\rangle.$$

That is, the groundstate of the full monster is (up to normalization)

$$|\mathrm{gs}\rangle = \sum_C \prod_{l\in C} \sigma_l^x u_l \Big(|0\rangle \otimes \prod_j |0_j\rangle \Big).$$

where, C is closed $\mathbb{Z}_n$ net and $|0\rangle$ is the state with no strings. Note that for $n > 2$ we have *junctions*.

[4]The construction could be generalized for unitaries which only represent $\mathbb{Z}_n$ on closed chains: $((\prod_{l\in C} u_l)^n = 1$ if C is a closed chain). This condition means that $u_{jk}^n = v_j w_k$, *i.e.*, that u is a $\mathbb{Z}_n$ operation modulo an on-site basis change.

[5]Let $-l$ denote the link l traversed in the opposite direction, so $s_{-l} = (-s_l)_n, u_{-l} = u_l^{-1}$. $(a)_n$ denotes a modulo n. The version of (2.3) where we keep track of s mod n (and regard the links as outgoing from the site s) is:

$$\begin{aligned}
\mathscr{B}_p h_s &= \left(\sigma_{l_1}^x \sigma_{-l_2}^x u_{l_1} u_{-l_2} \ldots\right) \left(u_{l_1}^{s_{l_1}} u_{l_2}^{s_{l_2}} \ldots\right) h_s \left(u_{l_1}^{s_{l_1}} u_{l_2}^{s_{l_2}} \ldots\right)^\dagger \\
&= u_{l_1} u_{-l_2} u_{l_1}^{(s_{l_1}-1)} u_{l_2}^{(s_{l_2}+1)} .. h_s .. u_{l_1}^{-s_{l_1}+1} u_{l_2}^{-s_{l_2}-1} \sigma_{l_1}^x \sigma_{-l_2}^x ..\\
&= (u_{l_1} u_{l_2})^{1-1} \underbrace{u_{l_1}^{s_{l_1}} u_{l_2}^{s_{l_2}} .. h_s .. u_{l_1}^{-s_{l_1}} u_{l_2}^{-s_{l_2}}}_{=h_s} \underbrace{u_{l_1} u_{-l_2} .. \sigma_{l_1}^x \sigma_{-l_2}^x ..}_{=\mathscr{B}_p} \\
&= h_s \mathscr{B}_p. \qquad (2.6)
\end{aligned}$$

2.3 Cluster states as 1d SPT states

Here we provide an example of a nontrivial 1d system for which we know a circuit description meeting the demands above. In the quantum information literature, these states are called *cluster states* or *graph states*. They optimize various measures of multipartite entanglement and are the basis of the measurement-based quantum computing scheme. For some further pedagogical discussion, see chapter 10 of [46].

Consider an open chain of N qbits with

$$h \equiv -\sum_{i=2}^{N-1} Z_{i-1} X_i Z_{i+1}. \tag{2.7}$$

This hamiltonian is a sum of commuting terms and has a $\mathsf{G} \equiv \mathbb{Z}_2 \times \mathbb{Z}_2$ symmetry generated by

$$\mathsf{g}^{e/o} = \prod_{i,\ \text{even/odd}} \mathbf{X}_i.$$

The operators [47]

$$\Sigma_L^x \equiv X_1 Z_2, \;\; \Sigma_L^y \equiv Y_1 Z_2, \;\; \Sigma_L^z \equiv Z_1$$

satisfy the $\mathsf{SU}(2)$ algebra, commute with the hamiltonian[6] and do not commute with G. The same statements apply to the other end:

$$\Sigma_R^x \equiv Z_{f-1} X_f, \;\; \Sigma_R^y \equiv Z_{f-1} Y_f, \;\; \Sigma_R^z \equiv Z_f$$

All the states of the chain are therefore fourfold degenerate. No perturbation which preserves G can split this degeneracy, so the symmetry protects the nontriviality of the state.

A useful description of the ground states is obtained as follows. First observe (*e.g.* [39]) that

$$h = -\mathbf{U} \sum_i X_i \mathbf{U}^\dagger$$

where

$$\mathbf{U} \equiv \prod_i \mathbf{CZ}_{i,i+1} \equiv \prod_i e^{\pi \mathbf{i} \left(\frac{1-Z_i}{2}\right)\left(\frac{1-Z_{i+1}}{2}\right)}. \tag{2.8}$$

(For PBC, the product may run $i = 1..N$, with $N+1 \equiv 1$; for the open chain it is $i = 1..N-1$.)

[6] For this property, it is important that we do not include the first term $X_1 Z_2$, which is a an external field for the effective edge spin.

There is some ambiguity in the form of $\mathbf{U}$, in the form of on-site unitary rotations of the link unitaries:

$$u_{i,i+1} \to v_i w_{i+1} u_{i,i+1} w_{i+1}^\dagger v_i^\dagger .$$

For example, the form of the link unitaries used in [39] is $\tilde{u}_{i,i+1} = e^{\frac{\pi \mathbf{i}}{4}(1-Z_i Z_{i+1})}$.

A groundstate is obtained by acting with $\mathbf{U}$ on a groundstate of the symmetric trivial paramagnet

$$h^0 = -\sum_{j=2}^{N-1} X_j . \tag{2.9}$$

For an open chain as in (2.9), this hamiltonian is independent of the first and last spins, so we obtain the four states

$$|\alpha_1, \alpha_N\rangle = \mathbf{U}\left(|\alpha_1\rangle \otimes_{i=2}^{N-1} |\to\rangle_i \otimes |\alpha_N\rangle\right)$$

where $X_{1,N}|\alpha_{1,N}\rangle = \alpha_{1,N}|\alpha_{1,N}\rangle$. These states are eigenstates of $\Sigma^x_{L,R}$ with eigenvalues $\alpha_{1,N}$. [7]

For closed chains, the Hamiltonian

$$h = -\mathbf{U}\sum_{j=1}^{N} X_j \mathbf{U} = -\sum_{j=1}^{N} Z_{j-1} X_j Z_{j+1}$$

(with periodic boundary conditions, $N+1 \simeq 1$) has a unique ground state

$$\mathbf{U} \otimes_j |\to_j\rangle = \sum_{Z\text{-basis states}, z=\pm} (-1)^{\frac{1}{2}\text{number of domain walls}(z)} \prod_{j=1}^{N} z_j |z\rangle .$$

Another symmetry of the solvable model is time reversal symmetry. That is,

$$\mathscr{T} = k \otimes \prod_j X_j \tag{2.10}$$

(where k is complex conjugation) is an antiunitary symmetry of the cluster hamiltonian (2.7). The individual link unitaries $u_{\langle jk\rangle} = \mathbf{CZ}_{jk}$ transform as

$$\mathscr{T} : \mathbf{CZ}_{jk} \mapsto -Z_j \mathbf{CZ}_{jk} Z_k .$$

[7] It is possible to show more directly that

$$\mathbf{U} \otimes_i |\alpha_i\rangle_i$$

is an eigenstate of h using the fact that

$$X_i \mathbf{CZ}_{i,i+1} = Z_{i+1} \mathbf{CZ}_{i,i+1} X_i, \quad X_{i+1} \mathbf{CZ}_{i,i+1} = Z_i \mathbf{CZ}_{i,i+1} X_{i+1} .$$

A chain of link unitaries only transforms at the endpoints

$$\mathscr{T} : \prod_{j=1}^{N} \mathbf{CZ}_{j,j+1} \mapsto (-1)^{N-1} Z_1 \prod_{j=1}^{N} \mathbf{CZ}_{j,j+1} Z_N.$$

A closed circuit therefore maps to itself up to a sign. A $\mathbb{Z}_N$ generalization of the cluster model is discussed in Appendix A.1 and has also been discussed in [27].

2.3.1 Stability of the edge states

The degeneracy of the ground states is protected by the symmetry; no perturbation of the chain hamiltonian which preserves the G can mix the states forming the doublet of the edge spin $\mathsf{SU}(2)$ at one end. The edge states of an SPT form irreducible projective representations of the symmetry group. The irreducible property means that they do not mix with other states under application of any elements of the group, and further, that only the elements of the group mix them with each other. Therefore, an operator which mixes them cannot commute with the whole symmetry group. So only non-symmetry-preserving perturbations can lift the degeneracy.

Let us illustrate this general statement explicitly in the example of the cluster model. The cluster model supports two states at each edge which we can label as $|\uparrow\rangle, |\downarrow\rangle$. For an open chain with an odd number of sites (a chain with an even number of sites can be analyzed similarly), the action of the symmetry generators on these states is given by

$$\mathrm{g}_o|\uparrow/\downarrow\rangle = \pm|\uparrow/\downarrow\rangle \qquad\qquad \mathrm{g}_e|\uparrow/\downarrow\rangle = |\downarrow/\uparrow\rangle. \tag{2.11}$$

A symmetry preserving perturbation $\hat{O}$ satisfies $\mathrm{g}_e^\dagger \hat{O} \mathrm{g}_e = \mathrm{g}_o^\dagger \hat{O} \mathrm{g}_o = \hat{O}$. Then it follows that

$$\begin{aligned} \langle\uparrow|\hat{O}|\uparrow\rangle &= \langle\uparrow|\mathrm{g}_e^\dagger \hat{O} \mathrm{g}_e|\uparrow\rangle = \langle\downarrow|\hat{O}|\downarrow\rangle \\ \langle\uparrow|\hat{O}|\downarrow\rangle &= \langle\uparrow|\mathrm{g}_o^\dagger \hat{O} \mathrm{g}_o|\downarrow\rangle = -\langle\uparrow|\hat{O}|\downarrow\rangle = 0 \end{aligned} \tag{2.12}$$

As a result, perturbing by the operator $\hat{O}$ will not split the degeneracy between the edge states. The operator which mixes the states $|\uparrow\rangle, |\downarrow\rangle$ is the symmetry generator g_e, a nonlocal operator spanning the whole chain. Therefore the splitting of the states by a local perturbation is exponentially small in the system size.

2.4 An exactly solvable spin liquid with spinons

Exactly solvable models such as Kitaev's toric code and honeycomb models [48, 44] have played an important role in our understanding of spin liquids[8]. However, these models have no essential symmetries, in the sense that although the solvable limit of the models do have various global symmetries, their actions on the quasiparticles are not the defining characteristics of the phase.

On the other hand, electrons carry spin and their interactions often preserve spin rotation invariance. Real spin liquids, when we find them, may have excitations which carry spin quantum numbers, namely *spinons*, and it would be useful to have solvable examples of this phenomenon.

To our knowledge there is so far no known exactly solvable model of a spin liquid with spinons, in this sense, above one dimension. In 1d, the spin-half-odd Heisenberg chain provides an example.

There are well-known models of spin liquids, which have also played an important role in the history of the subject, whose exact *groundstate* is known [50, 51]. That is, the associated parent hamiltonians are *frustration free*: each term independently annihilates the groundstate. Some frustration-free models exhibit phenomena similar to what we describe below [52, 53, 54]. In particular, [55] discusses a quantum dimer model which preserves spin rotation symmetry.

The interplay between global symmetry and topological order lies at the heart of the study of symmetry enriched topological (SET) phases. In a model with both topological order and global symmetries, anyons carry fractional quantum numbers. The type of fractionalization characterizes a particular SET phase [34, 35].

In this section, we show that the model defined by the hamiltonian (2.2) with the cluster state link unitaries (2.8) represents a gapped spin liquid with spinons. In the example we will study, the elementary degrees of freedom are effectively integer-spin excitations, while the quasiparticles in the spin liquid phase have half-integer spin.

[8] A useful review of models of spin liquids for our purposes is [49].

2.4.1 Unitary symmetry

Explicitly, the Hamiltonian is given by

$$\mathbf{H} = -\sum_i A_i - \sum_p \mathscr{B}_p - \sum_i X_i \prod_{\langle i|j\rangle} Z_j^{s_{ij}} \left(\frac{1+A_i}{2}\right) \tag{2.13}$$

The cluster hamiltonian 2.7 for a *closed* chain has a $\mathsf{G} = \mathbb{Z}_2 \times \mathbb{Z}_2$ symmetry generated by $\mathrm{g}^{e/o}$. This is respected by the star term, which doesn't involve the site variables. The plaquette term in $\mathbf{H}$ does not obviously respect this symmetry, since it involves products of Zs on the two sublattices. A crucial fact here is that any bipartite lattice has an even number of sites $2n$ around every plaquette.

$$\begin{aligned}(\mathrm{g}^o)^\dagger S_\square \mathrm{g}^o &= X_1 X_3 \cdots X_n \prod_{j=1}^{2n} \mathbf{CZ}_{j,j+1} X_1 X_3 \cdots X_n \\ &= (Z_2 Z_4)(Z_4 Z_6)\cdots(Z_{2n} Z_2) S_\square = S_\square \end{aligned} \tag{2.14}$$

so it is actually invariant.

The site hamiltonian $h_i = X_i \prod_{\langle v|j\rangle} Z_j^{s_{ij}}$ on an *open* string is not $\mathbb{Z}_2 \times \mathbb{Z}_2$ symmetric; it does not commute with the endpoint terms.

$$[\mathrm{g}^e, X_1 Z_2] \neq 0, \quad [\mathrm{g}^\alpha, Z_{f-1} X_f] \neq 0$$

Here $\alpha =$ odd/even for f even/odd respectively. Multiplying the site hamiltonian by a projector onto locally closed strings guarantees that only symmetric terms appear.

2.4.2 String operators and anyons

The magnetic string operator is unmodified relative to the toric code: $M_{\check{C}} = \prod_{l \perp \check{C}} \sigma_l^z$. Notice that if the curve in the dual lattice $\check{C}$ just goes around one site in the primal lattice, this reproduces the star operator, as usual. For closed $\check{C}$, this operator commutes with $\mathbf{H}$; if $\check{C}$ ends, $M_{\check{C}}$ violates the plaquette operators at the endpoints. This will mean that the anyons have the same statistics as in the toric code since only the link variables can participate in the commutator.

The demand that $W_{C=\partial p} = \mathscr{B}_p$ suggests that that the electric string operator is

$$W_C = \prod_{l \in C} \sigma_l^x \mathbf{CZ}_l.$$

This operator indeed commutes with $\mathbf{H}$ for closed curves.

Consider next the operator $W_C^{1,f}$ associated with an open string C with endpoints $1, f$:

$$W_C \equiv \prod_{l \in C} \sigma_l^x \mathbf{CZ}_{12} \mathbf{CZ}_{23} ... \mathbf{CZ}_{f-1,f}.$$

Acting on the groundstate of the snake monster, this violates the star constraint at sites $1, f$ (that is, $W_C A_{1,f} = -A_{1,f} W_C$).

We may modify our string operator by decorating it with site operators localized at the endpoints. Thus, we have found *four* states associated with each open string, a two-dimensional Hilbert space for each endpoint spanned by $\{W_C^{a,b}|\mathrm{gs}\rangle, Z_a W_C^{a,b}|\mathrm{gs}\rangle\}$. These states are eigenvectors of the end-point-site hamiltonians $h_{a,b}$ with eigenvalue $+1$ and -1 respectively, and we will occasionally refer to them as $|+\rangle$ and $|-\rangle$. The projector onto $A_i = 1$ annihilates these states, so they are degenerate.

To see that these states form an orbit of the $\mathbb{Z}_2 \times \mathbb{Z}_2$ symmetry we act on them with the generators. Straightforward calculations involving the algebra of X and $\mathbf{CZ}$ yield

$$\begin{aligned} \mathrm{g}_o W_{e,e}|\mathrm{gs}\rangle &= Z_1 Z_f W_{e,e}|\mathrm{gs}\rangle \\ \mathrm{g}_e W_{e,e}|\mathrm{gs}\rangle &= W_{e,e}|\mathrm{gs}\rangle \end{aligned} \tag{2.15}$$

where the subscripts on the open string operator W indicate on which sublattice the string begins and ends. Furthermore, g_e anticommutes with Z_i when site i is on the even sublattice. We can therefore summarize the action of the symmetry on the anyon states as shown in Table 2.1.

Table 2.1: Action of $g^{o/e}$ on the anyons.

$\bullet = e, \circ = o$	g_e	g_o
$\bullet$ - - - $\bullet$	$\mathbf{Z} \otimes \mathbf{Z}$	$\mathbf{X} \otimes \mathbf{X}$
$\bullet$ - - - $\circ$	$\mathbf{Z} \otimes \mathbf{X}$	$\mathbf{X} \otimes \mathbf{Z}$
$\circ$ - - - $\bullet$	$\mathbf{X} \otimes \mathbf{Z}$	$\mathbf{Z} \otimes \mathbf{X}$
$\circ$ - - - $\circ$	$\mathbf{X} \otimes \mathbf{X}$	$\mathbf{Z} \otimes \mathbf{Z}$

This table encodes the projective representation of $\mathbb{Z}_2 \times \mathbb{Z}_2$ furnished by each anyon. In a system with periodic boundary conditions, a single anyon is not a physical state; they always come in pairs. We see that while an endpoint individually represents the algebra $\mathrm{g}_e \mathrm{g}_o \sim -\mathrm{g}_o \mathrm{g}_e$, the symmetry generators act linearly on the entire many-body wavefunction as they must.

In summary, the structure of topological order (the quasiparticle labels and statistics) in this model is the same as the toric code, but the e particles form doublets. The argument for the robustness of the degeneracy given for the 1d model carries over directly to the snake monster. In §A.2 we study symmetric perturbations of this hamiltonian and show explicitly that the characteristic feature (the projective representation of g_e and g_o on the quasiparticles) is preserved.

It would be interesting to apply the methods of [56] to more precisely characterize the SET order of the cluster snake monster in the case of $d = 2$. It would also be interesting to gauge the $\mathbb{Z}_2 \times \mathbb{Z}_2$ symmetry; this can be done maintaining solvability and produces a model with topological order (and no global symmetry) whose spectrum is characteristic of the original SET.

2.4.3 Time-reversal-invariant cluster snake

The same model also produces a solvable representative of an SET protected by time-reversal symmetry [27]. Of course, the general $\mathscr{T}$-preserving perturbation will be different than that preserving the unitary symmetry described above.

In this case, the string endpoints are Kramers' doublets, a projective representation of the antiunitary symmetry $\mathscr{T}$, in the sense that $\mathscr{T}^2 = -1$ on the states of the endpoints. We can see this as follows, using $\mathscr{T} : \mathbf{CZ}_{12} \mapsto -Z_1 \mathbf{CZ}_{12} Z_2$. Consider a open string excitation with an endpoint labelled by 1,

$$W_0 |\mathrm{gs}\rangle = \prod_{j=1} \sigma^x_{j,j+1} \mathbf{CZ}_{j,j+1} |\mathrm{gs}\rangle. \tag{2.16}$$

This is an excited state which violates the star constraint at the end site, and is annihilated by the site term at the end site (whereas sites participating in closed strings are eigenstates with

eigenvalue -1). A degenerate and orthogonal state which is the Kramers' doublet partner is obtained by acting upon (2.16) with time-reversal:

$$W_1|\mathrm{gs}\rangle = \mathscr{T} W_0|\mathrm{gs}\rangle = (-1)^{L-1} Z_1 Z_f W_0|\mathrm{gs}\rangle.$$

where L is the length of the string. The states are orthogonal because

$$\langle \mathrm{gs}|W_1^\dagger W_0|\mathrm{gs}\rangle = (-1)^{L-1}\langle \mathrm{gs}|Z_1 Z_f|\mathrm{gs}\rangle$$

which vanishes by symmetry[9]. *Locally*, a second action of $\mathscr{T}$ on the endpoint $Z_1 W_0|\mathrm{gs}\rangle$ reproduces the original state with a phase of -1; in this sense the anyon represents time reversal projectively with $\mathscr{T}^2 = -1$. Of course the full hilbert space represents the symmetry linearly when we include the other endpoint of the string; this is the same situation as in the previous section. In §A.1 we generalize the construction to $\mathbb{Z}_N$ cluster states and describe the snake monster on a $\mathbb{Z}_N$ string net.

2.5 Exactly solvable models of topological paramagnets

Not all states which are equal-magnitude superpositions of closed string configurations have topological order. Finding a hamiltonian with such string-net groundstates which does *not* have topological order requires a local condition which prevents the strings from winding around noncontractible cycles. One way to do this is if the curves are all boundaries of a region. This is what happens in the quantum Ising paramagnet, where the groundstate of $h = -\sum_j X_j$ can be written in the z-basis as a uniform superposition of closed loops which are the boundaries of domain walls (A similar statement can be made about the groundstate of the Levin-Gu model [39], which involves an additional phase which counts the number of walls.)

For the case of 3d lattices, [36] provides a beautiful mechanism to accomplish this goal. As we review next (and elaborate in §A.4), it provides a mechanism for destroying the topological

[9] To see this more explicitly, recall that the groundstate is a uniform superposition of closed string configurations. **CZ** and Z commute, so the expectation value of Z in an arbitrary closed string configuration is

$$\langle \rightarrow_0 \rightarrow_1 \rightarrow_2 |\mathbf{CZ}_{01}^{-s_{01}} \mathbf{CZ}_{12}^{-s_{12}} Z_1 \mathbf{CZ}_{01}^{s_{01}} \mathbf{CZ}_{12}^{s_{12}}| \rightarrow_0 \rightarrow_1 \rightarrow_2 \rangle = \langle \rightarrow |Z_1| \rightarrow \rangle = 0.$$

order of a model with string condensation. In the appendix §A.4.1 we also generalize the construction from $\mathbb{Z}_2$ to $\mathbb{Z}_N$.

2.5.1 Pure loop model review

Following [36], consider two interpenetrating cubic lattices A and its dual lattice B. This means that the vertices of A are in the centers of the cubes of B (and vice versa) and each link of A pierces a plaquette of B (and vice versa). Put qbits on the links of both, and denote the associated Pauli operators for links of A, B by σ, τ respectively. Consider

$$\mathbf{H}_{\text{linking}} \equiv -J \left(\sum_{p \in A} \mathscr{F}_{Ap} + \sum_{p \in B} \mathscr{F}_{Bp} \right)$$

where

$$\mathscr{F}_{Ap} \equiv \tau_p^z \prod_{l \in p} \sigma_l^x, \qquad \mathscr{F}_{Bp} \equiv \sigma_p^z \prod_{l \in p} \tau_l^x,$$

Claims from [36]:

1. All the $\mathscr{F}$s commute with each other.

2. The condition $\mathscr{F}_{Ap} = 1$ says that if there is electric flux on the B-link p ($\tau_p^z = -1$) then there is magnetic flux on the A-plaquette p ($\prod_{l \in p} \sigma_l^x$). So this hamiltonian glues the electric flux lines of the A gauge field to the magnetic flux lines of the B gauge field. This is a lattice realization of the $B \wedge F$ term.

3. We don't need to add star operators to $\mathbf{H}_{\text{linking}}$ because they are products of the $\mathscr{F}$s. That is, if we have $\mathscr{F} = 1$ for all $p \in A, B$ then automatically $\prod_{l \in v} \sigma_l^z = 1$ for all vertices $v \in A$ and $\prod_{l \in v} \tau_l^z = 1$ for all vertices $v \in B$. More explicitly, the star operator for a site $v \in A$ (which is at the center of a cube $v \in B$) is

$$\prod_{l \in v} \sigma_l^z = \prod_{p \in \partial v} \mathscr{F}_p^B$$

where by ∂v we mean the six faces which bound the cube v.

4. The unique groundstate on any manifold is

$$
\begin{aligned}
|\mathrm{gs}\rangle &= \sum_{C_A, C_B} (-1)^{\ell(C_A, C_B)} |C_A\rangle \otimes |C_B\rangle \\
&= \sum_{C_A \text{ contractible mod 2}} \sum_{\mathscr{M} \subset \Omega_2(A) | \partial \mathscr{M} = C_A} |C_A\rangle |\mathscr{M}\rangle \ . \qquad (2.17)
\end{aligned}
$$

where $\ell(C_A, C_B)$ is the linking number of the two sets of loops. In the last expression $\Omega_2(A)$ denotes plaquettes of A, and

$$
|\mathscr{M}\rangle \equiv \left| \tau_p^x = \begin{cases} -1, \text{ if } p \in \mathscr{M}, \\ +1, \text{ else} \end{cases} \right\rangle
$$

The point of this last expression is that it makes clear that the loops C_A must be homologically trivial (mod two) since they are boundaries of the membranes $\mathscr{M}$ specifying the state of the B-lattice variables.

5. If the lattice has a boundary, this model has surface topological order, the same as the toric code. The e particles are the ends of the electric strings on the A lattice, and the m particles are the ends of the electric strings on the B lattice. These particles are deconfined bosons which are mutual semions. String operators which create them in pairs can be written as shown in fig 5 of [36]. More explicitly, for smooth boundary conditions on both A and B lattices, the e particle is created on the A sublattice by $\prod_{l \in L} \sigma_l^x$ where L lies on the boundary of A. $\prod_{l \perp \check{L}} \sigma_l^z \tau_{p_l}^x$ creates the magnetic excitations on the A sublattice boundary. We see that this involves an electric string on the boundary of the B sublattice.

6. This model does not have topological order and is actually adiabatically connected to a product state as shown explicitly in [36].

2.5.2 Cluster snake paramagnet

In order to build solvable three-dimensional SPTs starting from the pure loop construction, we will decorate the strings with extra degrees of freedom living on the sites. As we will explain, it is necessary to decorate both sublattices; adding qbits on one of the sublattices alone is not enough to generate a distinct phase. One way to see this is to use the membrane representation for the sublattice without the decorations. Then it is possible to adiabatically contract the membranes without breaking any symmetry of the site variables.

So, now add qbits on the sites of both lattices. We replace the magnetic flux operators $B_{Ap} \equiv \prod_{l \in p} \sigma_l^x$ with snake monster operators:

$$\mathscr{B}_{Ap} \equiv \prod_{l \in p} \sigma_l^x U_{\partial p}$$

where $U_{\partial p}$ is defined as in the previous sections on snake monsters. That is, consider instead:

$$\mathbf{H}_{\text{snake-linking}} \equiv -J \left(\sum_{p \in A} \mathscr{F}_{Ap} U_{\partial p} + \sum_{p \in B} \mathscr{F}_{Bp} U_{\partial p} \right) - \sum_v h_v$$

where

$$h_v \equiv X_v \prod_{\langle v|w \rangle} Z_w^{s_{vw}} \left(\frac{1 + A_v}{2} \right)$$

where $s_{vw} \equiv \frac{1}{2}(1 - \sigma_{vw}^z)$ if vw is an A-lattice link or $s_{vw} \equiv \frac{1}{2}(1 - \tau_{vw}^z)$ if vw is a B-lattice link.

These terms still commute. The star operators for the A and B sublattices are still products of the flip operators. This model still does not have topological order, since in the groundstate, the electric strings on each sublattice are boundaries of membranes in the dual lattice. The unique groundstate is

$$|\text{gs}\rangle = \sum_{\substack{C_A, C_B \\ \text{contractible mod 2}}} (-1)^{\ell(C_A, C_B)} |C_A\rangle \otimes |C_B\rangle \otimes U_{C_A \cup C_B} |\rightarrow\rangle^{\otimes v}.$$

With smooth boundary conditions on both A and B lattices, the surface is gapped and symmetric. The surface topological order is the same as for the pure loop model with the crucial difference that the anyons form doublets. Due to the binding of electric and magnetic flux, both e

and m now form projective representations of the global symmetry.

Other choices of boundary conditions are possible. However, the all-smooth boundary conditions are most convenient [57, 58, 59, 60, 41, 40, 61] because they produce a nondegenerate, gapped, symmetric groundstate (when the boundary is simply connected).

2.5.3 Nontriviality of the snake paramagnet

If we put cluster snakes on *only* the A sublattice the model is trivial: it can be shown to be adiabatically connected to a product state while preserving all symmetries by the string tension deformation described in [36]: Deform the flipper

$$\mathscr{F}_p^A \to \mathscr{F}_p^A(\gamma) \equiv \cosh^{-1}\gamma\left(\tau_p^z \prod_{l\in p}\sigma_l^x + \tau_p^x \sinh\gamma\right) \;;$$

these still commute, but interpolate to a product groundstate as $\gamma \to \infty$. If B were decorated as well, then this operator would break the B sublattice symmetry.

Cluster paramagnet with $\mathscr{T}$ symmetry.

Decorating both A and B lattice electric strings of the pure loop construction with time-reversal SPTs results in an 'anomalous' surface topological order, a characteristic feature of three dimensional bosonic SPTs. The spectrum of quasiparticles is shown in Table 2.2.

Table 2.2: Spectrum of anyons in the $eTmT$ model

quasiparticle	self-statistics	time-reversal property
e	B	1/2
m	B	1/2
ε	F	0

In this table, a $1/2$ denotes a Kramers' doublet. The crucial property here is that the fermionic quasiparticle is the only time-reversal singlet. This spectrum has the consequence that the surface topological order cannot be destroyed while preserving time-reversal symmetry.

To see this, recall that destroying topological order in 2d $\mathbb{Z}_2$ gauge theory requires

condensing some anyon. Condensing e is higgsing and condensing m is confinement; the resulting two phases are adiabatically connected [62]. In the model we've constructed, e cannot condense in a $\mathscr{T}$-symmetric way because it is a Kramers' doublet. That is, condensing any one e particle will break the time-reversal symmetry. This much can be realized (and we did realize it in §2.4.3 above) intrinsically in two dimensions. However, when we decorate the electric strings on *both* A and B lattices, the ends of the B-lattice electric strings behave as the m particles, which are therefore also Kramers' doublets. They can therefore also not condense in a $\mathscr{T}$-symmetric way. Finally, as usual, $\varepsilon = em$ can't condense because it's a fermion. Condensing pairs of these objects doesn't destroy the topological order.

This proves that the edge of our 3d model has no trivial gapped and symmetric edge, and therefore represents a nontrivial SPT protected by $\mathscr{T}$. Since the surface quasiparticles are Kramers' doublet bosons, this is the state labelled $eTmT$ in the classification reviewed in [38]. The surface theory with this spectrum is not 'edgeable'.

To summarize: the snake monster produces a model where the electric defects are doublets. In the topological paramagnet, the magnetic defects become doublets by binding to electric defect doublets on the other sublattice. If we don't decorate sublattice A then the m particle at a surface of sublattice B is a singlet under time reversal and can be symmetrically condensed, destroying the topological order. This further supports the previous assertion that it is necessary to decorate both sublattices to generate a distinct phase.

Cluster paramagnet with unitary symmetry. The cluster hamiltonian $\sum_v h_v$ also has a $\mathbb{Z}_2 \times \mathbb{Z}_2$ symmetry state on a bipartite lattice. This requires both A and B to be bipartite. If we put cluster snakes on both A and B sublattices (which are each bipartite) the solvable model actually has a $\mathbb{Z}_2^4$ symmetry. The spectrum of excitations is much as in the table above, if we interpret the $\frac{1}{2}$ to mean a projective doublet of the $\mathbb{Z}_2 \times \mathbb{Z}_2$ coming from the simultaneous spin flips on even and odd sublattices of both A and B.

It seems impossible to destroy this topological order symmetrically, since the only sym-

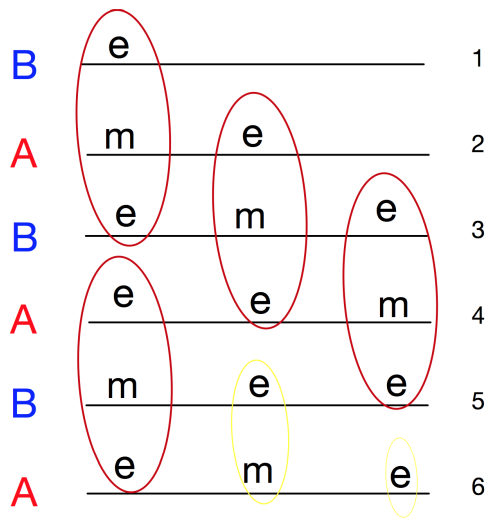

Figure 2.2: In the coupled layer construction, three anyons on neighboring surfaces are condensed, destroying topological order in the bulk.

metric particle is a fermion. However, in the absence of time-reversal symmetry, the statistics of the anyons can be changed by deforming the Hamiltonian, as in *e.g.* [48]. Indeed, in appendix A.3 we use methods of [40] to show that this model does not represent a nontrivial SPT for $\mathbb{Z}_2 \times \mathbb{Z}_2$[10].

2.5.4 Relation to coupled layer construction

It is instructive to ask about the relationship between the above solvable model for the $eTmT$ state and the coupled layer construction implied in [57, 58, 38]. A nice direct connection can be understood as follows; it uses the 2d cluster snake monster of §2.4.3 in a satisfying way.

Consider first a collection of layers of ordinary 2d toric code as in Figure 2.2. Condense the bosons $b_n \equiv e_n m_{n+1} e_{n+2}$ (circled in red in the figure). This higgses the gauge group of the layers of the same parity (n and $n+2$) to the diagonal $\mathbb{Z}_2$ subgroup, while at the same time confining the gauge group of the other-parity layer ($n+1$). The electric flux lines of the even layers are attached to the magnetic flux lines on the odd layers and vice versa. The bulk is trivial,

[10] We thank an anonymous referee for bringing this line of analysis to our attention

since every layer is confined by one of the b_n condensates. This is therefore (a coarse-grained version of) the pure-loop construction; the A sublattice arises from the even layers and the B sublattice from the odd layers. At the surface is a copy of the ordinary toric code where the excitations at the surface which are mutually local with all the condensates are the following (indicated in yellow in the figure). The effective e particle is the boson e_{last} and the effective m particle with which it is a mutual semion is the boson $m_{\text{last}} e_{\text{last}-1}$. This is perfectly ordinary and trivial, as expected.

Now take instead layers of the 2d cluster snake monster of §2.4.3: the 2d toric code where the electric flux lines are decorated by a SPT of time-reversal. This means that the e particles in any layer are Kramers' doublets, $e_{\alpha=\uparrow/\downarrow}$. Now we condense the Kramers' singlet bosons $b_n \equiv e_n^\alpha m_{n+1} e_{n+2}^\alpha$. The bulk is again trivial. The remaining surface excitations are now the Kramers' doublets $e_{\text{eff}}^\alpha = e_{\text{last}}^\alpha$ and $m_{\text{eff}}^\alpha = m_{\text{last}} e_{\text{last}-1}^\alpha$.

2.6 Discussion

The problem of finding circuit constructions of 1d SPTs meeting the demands listed in 2.2 is an interesting one. If such a circuit could be found for a single copy (or an odd number of copies) of the Kitaev chain [63], we would have a solvable gapped model in arbitrary dimension with deconfined *non-abelian* anyons, along similar lines to the suggestion of [64].

Although this is not a flat contradiction with the classification of particle statistics (since the information about the strings which end on these particles enhances the topology of the configuration space beyond that of particles [65]) many attempts at such a construction [64, 66, 67] have failed to produce deconfined, gapped non-abelian particles in $d > 2$, for interesting reasons. In particular, strong evidence against this possibility from a low-energy field theory viewpoint is given in [66].

Here the obstruction is the fact that a single copy of the Kitaev chain h_1 is a distinct

phase from the trivial chain h_0 even in the absence of symmetry. On the other hand, if one found the desired link unitaries which relate the two, one could then isospectrally interpolate between the two by $h_s = U^s h_0 U^{-s}, s \in [0,1]$. In other cases, this is prevented by the fact that U^s is not symmetric.

It would be interesting to find a sharp characterization of which 1d SPTs have such a description.

Here we have attached interesting 1d phases to 1d electric flux lines of 1-form discrete lattice gauge theory. In a future publication we will show how to attach in a similarly explicit manner p-dimensional topological phases to the p-dimensional electric flux sheets of p-form gauge theory.

Acknowledgements

We thank Dan Arovas and Shauna Kravec for many useful discussions. JM would like to thank Isaac Kim and Brian Swingle for discussions which inspired the construction described here, and Maissam Barkeshli and Ashvin Vishwanath for some very helpful comments. This work was supported in part by funds provided by the U.S. Department of Energy (D.O.E.) under cooperative research agreement DE-FG0205ER41360.

Chapter 2 is, in part, a reprint of material from published work done in collaboration with John McGreevy and Diptarka Das, as it appears in Physical Review B, as well as on the arXiv. D. Ben-Zion, D. Das, and J. McGreevy, "Exactly solvable models of spin liquids with spinons, and of three-dimensional topological paramagnets," *Phys. Rev. B* **93** 155147. The dissertation author was the primary investigator and author of this material.

Chapter 3

Strange metal from local quantum chaos

3.1 Introduction

How to make a model of a metal which is not a Fermi liquid, both in terms of the single-electron physics and in terms of its transport properties, is a long-standing problem in theoretical physics. A general field-theoretic strategy to make a non-Fermi liquid metal (NFL) is to couple a Fermi surface to some other gapless degrees of freedom. If those modes are bosonic (such as gauge fields or fluctuations of an order parameter)[1], the coupling must be (at least) trilinear, schematically $\psi^\dagger \psi \phi$, and the Landau quasiparticle decays predominantly by emission of soft ϕ modes. This process does not change the current much; in such models, therefore, the transport lifetime is much longer than the single-particle lifetime. On the other hand, there seem to exist NFLs where the two timescales are comparable, and have the same temperature dependence. This suggests that there should be other ways to make a NFL.

Not long ago, some people [69, 70, 71, 72, 73] were desperate enough to make progress on this problem that they tried to use gauge/gravity duality: an exotic large-N conformal field theory with a dual description in terms of Einstein gravity in one higher dimension was subjected

[1] For a review of the large literature, see [68].

to a chemical potential for a global $\mathsf{U}(1)$ symmetry.[2] The retarded Green's function of local fermionic operators in the resulting state revealed a Fermi surface in momentum space, near which the self-energy behaved as a power-law in frequency:

$$G_\psi(\omega,k) \overset{\text{small } \omega}{\sim} \frac{1}{\omega - v_F k_\perp - \mathscr{G}(\omega)}$$

with $\mathscr{G}(\omega) \sim \omega^{2\nu}$, indicative of a non-Fermi liquid metal. The special case of $\nu \to 1/2$, where $\mathscr{G} \sim \omega \log \omega$, is the marginal Fermi liquid Green's function of [75].

In [72], the power-law behavior was traced the region of the extra-dimensional geometry near the black-hole horizon. With the benefit of some hindsight [72, 76], the key feature of the near-horizon geometry of the black hole in this construction is that it describes a $z = \infty$ fixed point: its fluctuations are power-law in frequency, and essentially[3] independent of momentum – they are localized critical excitations. Hence, when coupled to a Fermi surface, they are able to render incoherent the propagation of the quasiparticles, and at the same time absorb arbitrary amounts of their momentum. Therefore, in a model where the quasiparticle decay is dominated by scattering off these excitations, the transport lifetime will equal the single-particle lifetime, and the power law in the conductivity $\rho(T)$ will match that of the fermion self-energy, as in the marginal Fermi liquid phenomenology [75].

The holographic construction summarized above, or even its 'semi-holographic' reduction [72, 76], have the drawback that the description of the $z = \infty$ fixed point is in terms of a mysterious gravitational system, whose dynamics is only under control in a limit $N \to \infty$ with infinitely many degrees of freedom at each point in space. Corrections to this limit require one to confront quantum gravity, or at least the back-reaction of quantum effects on the geometry [78, 79]. It would be useful to replace the near-horizon $AdS_2 \times \mathbb{R}^2$ region of the geometry with a more tractable locally critical system.

[2]For a more leisurely discussion of these issues, see also §5 of [74].

[3]In fact, as emphasized in [77], in the holographic construction described above, there is a weak, analytic dependence on the momentum. The authors of [77] call this 'semi-local criticality'. This is a feature of the holographic strange metal construction that we will not reproduce.

Such local quantum criticality is a fascinating idea, whose realization is desirable also as a justification of dynamical mean field theory [80, 81]. Such a fixed point is roughly a critical theory at each point in space, and hence requires the participation of many degrees of freedom. As explained in [82, 83, 84, 85], this intuition can be made precise by studying the dependence of the density of states on the energy. Dimensional analysis requires

$$\frac{dn}{dE}(E) = e^{S_0}\delta(E) + e^{S_1}\frac{1}{E}.$$

The first term represents a groundstate entropy S_0 and violates the Third Law of Thermodynamics. The second term is not integrable and requires the appearance of a new energy scale which violates the $z = \infty$ scaling and, as a consequence of this argument, cannot be disentangled from the low energy physics. The holographic construction is most naturally interpreted in the canonical ensemble, and at $T \ll \mu$ and leading order in N, gives an extensive entropy which remains nonzero at $T \to 0$, suggesting a violation of the Third Law and the associated instabilities. The low-energy fate of the construction is obscured since classical gravity requires $N \to \infty$ before $T/\mu \to 0$, and by the fact that the gravity construction involves many degrees of freedom besides the Fermi surface.

This discussion motivates the study of more accessible constructions of $z = \infty$ fixed points, to which one might couple a Fermi surface. With this in mind, we cannot avoid thinking about the SYK (Sachdev-Ye-Kitaev) model [86, 87, 15, 88], which is a solvable model of local quantum criticality, and which has many features in common with (dilaton) gravity in AdS_2 [89, 90, 15, 88]. For our purposes of destroying quasiparticles, we require a $z = \infty$ fixed point with fermion operators carrying a conserved $\mathsf{U}(1)$ charge. Such a generalization of the SYK model is provided in [88]:

$$H_{\text{SYK}} = \sum_{ijkl}^{N} J_{ijkl}\chi_i^\dagger\chi_j^\dagger\chi_k\chi_l \qquad \overline{J_{ijkl}} = 0,\ \overline{J_{ijkl}^2} = \frac{J^2}{2N^3} \quad . \tag{3.1}$$

Its low-energy physics should be similar to dilaton gravity plus electromagnetism in AdS_2.

A single SYK model has no notion of space, since each fermion talks to every other. Since we are interested in the effects of the $z = \infty$ fixed point on the physics of the Fermi surface,

we must introduce some notion of locality. Therefore, we consider a lattice of SYK clusters, decoupled from each other at the outset. Depicting a single 'cluster' of complex fermions as 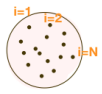

, a 1d implementation of the model can be illustrated as follows:

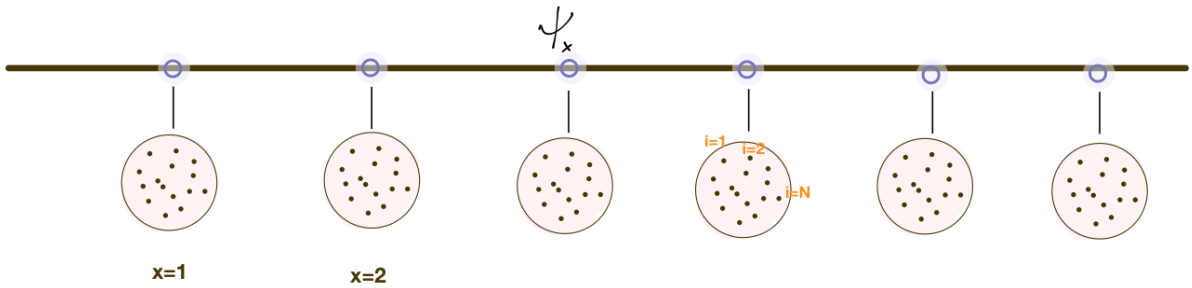

Figure 3.1: A cartoon of the model we study in this paper. Each blob represents an independent SYK model. The vertical edges represent the random couplings g_{ix}. The horizontal edges represent the translation-invariant hopping amplitudes t.

The model is a rather direct and crude discretization of the $AdS_2 \times \mathbb{R}^d$ near-horizon geometry of the extremal charged black hole in AdS_{d+2}. Nevertheless, we will see that it reproduces many of the features of interest of the holographic strange metal of [72, 73].

To be specific, the hamiltonian we will study is $H = H_0 + H_{\text{int}}$, with

$$H_0 = -t \sum_{\langle xy \rangle \in \text{lattice}} \psi_x^\dagger \psi_y + h.c. + \sum_{x \in \text{lattice}} H_{SYK}(\chi_{xi}, J^x_{ijkl}), \quad H_{\text{int}} = \sum_{x,i} g_{ix} \psi_x^\dagger \chi_{xi} + \text{h.c.}$$

where ψ_x, χ_{xi} are complex canonical fermion annihilation operators, with $\{\psi_x^\dagger, \psi_y\} = \delta_{xy}$. Since ψ form a Fermi surface under H_0, we refer to them as itinerant fermions. We occasionally refer to the χ modes as cluster fermions. The couplings g_{ix} are independently Gaussian:

$$\overline{g_{ix}} = 0, \; \overline{g_{ix} g_{jy}} = \delta_{ij} \delta_{xy} g^2 / N.$$

There are some precedents for our study. The result of hybridizing conduction electrons with the SY (as opposed to SYK) model, and its connection with holography, is studied in [89, 90]. The model studied in this paper is simpler in that no fractionalization is required to write down the Hamiltonian.

The system we study here has some similarities with models of heavy fermions, and in

particular those devoted to understanding NFL behavior in those systems, such as, for example, [91]. This paper solves a model of conduction electrons coupled to localized f-electrons by random hybridization terms. The f-electrons have random site energies and a uniform Hubbard U. The model is approximated using dynamical mean field theory. There is a large literature studying such heavy-fermion-like models using DMFT. One goal of this work is to understand better the local (momentum-independent) form of the self-energy assumed by the DMFT analysis.

Some related work has also appeared during the overly long gestation of our project. [92] makes lattices of SYK clusters, coupled by a less dangerous four-fermion coupling, and studies the propagation of information. [93] studies the coupling of a single SYK cluster to fermions which can hop (essentially in infinite dimensions) by the same kind of hybridization term we study; this model lacks a notion of locality, however. [94] couples non-locally several flavors of SYK clusters. [95] studies the phase diagram of two clusters by quadratic terms. Most recently and closest to our work, [96, 97, 98] study a chain of SYK clusters coupled by (random and non-random) quadratic links; although the starting point does not have a Fermi surface, the resulting states of matter may be closely related to ours. Studies of higher-dimensional generalizations of the SYK model, with various motivations, include [99, 100, 101, 102, 103, 104, 105, 106]. In particular, [106] realizes a bosonic analog of the semi-holographic construction using SYK chains.

In the next section, we analyze the model at large N, arriving at the same picture as in the semi-holographic models. The advantage of having an explicit model of the $z \to \infty$ fixed point is that we can analyze the extent to which the large-N and low-energy limits commute. In section §3.3, we analyze limits of the space of couplings and map out possible phase diagrams. In section §3.4, we attempt to make the fixed point perturbative by continuing in the number q of fermions participating in the SYK interactions. In section §3.5 we describe a DMRG study to decide between the possible phase diagrams proposed in §3.3.

Most of our work applies in any number of spatial dimensions, and only the discussion of

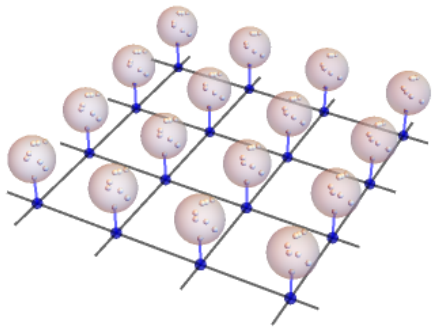

Figure 3.2: A diagram of the model in two spatial dimensions. The vertical (blue) bonds represent the random hybridization couplings g_{xi}. The black horizontal bonds are the uniform hoppings, t.

§3.5 is specific to one dimension. To emphasize this we include a diagram of the model in two dimensions in Fig. 3.2. In Fig. 3.3 we sketch our picture of the phase diagram of the model in the space of couplings $J/t, g/t$ studied here.

3.2 Large-N analysis

3.2.1 SYK review

We will use the complex fermion avatar of the SYK model described in [88], and here we provide a brief description of its relevant known properties. The degrees of freedom are a set of canonical fermions χ_i ($\{\chi_i, \chi_j^\dagger\} = \delta_{ij}, \{\chi_i, \chi_j\} = 0, i = 1..N$) governed by the Hamiltonian (3.1). The object of interest to us is the disorder averaged fermion green function $\mathscr{G}(\tau - \tau') = \overline{\langle \chi_a^\dagger(\tau)\chi_a(\tau')\rangle}$. This quantity can be calculated diagramatically by noticing that the only diagrams which survive disorder averaging are the ones in which interaction vertices can be grouped into pairs with identical indices.

The diagrams contributing at leading order in $1/N$ are those in which the vertices are

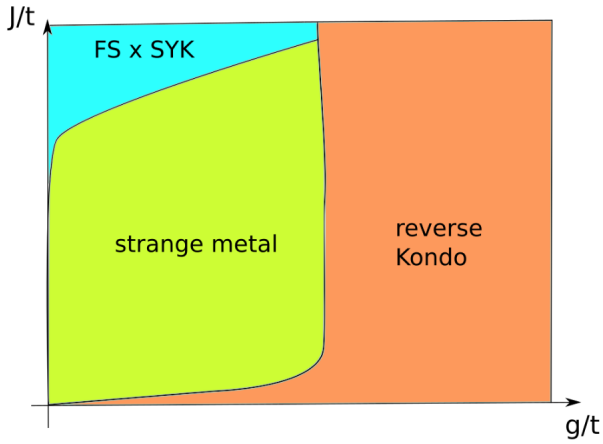

Figure 3.3: A (possibly optimistic) cartoon view of the proposed phase diagram. Orange: "reverse Kondo" refers to the regime where one linear combination of the fermions in each cluster hybridize with the mode of the Fermi surface at that site, leaving behind at low energies a chain of clusters with $N-1$ modes. Even for large J, we expect that the hybridization term is a relevant perturbation of the SYK hamiltonian, so we expect this phase to continue into the upper right corner where t is the smallest energy scale. Cyan: When g/J is too small (at fixed N), the hybridization is unable to mix the levels of the clusters, and in the infrared, the Fermi surface decouples; this phase is labelled FS $\times$ SYK. We estimate this phase boundary to occur where g is comparable to the single-cluster level spacing: $g \sim \Delta E \sim e^{-aN}J$. At infinite N, therefore, this phase does not persist.

paired as locally as possible starting from the interior of the diagram moving outwards: this leads to the series of so-called melon diagrams. This says that the one-particle irreducible part of $\mathscr{G}$, the self energy Σ, is itself a product of Green's functions: $\Sigma(\tau) = J^2\mathscr{G}^2(\tau)\mathscr{G}(-\tau)$. Since there are no quadratic terms in H, the free propagator is $\mathscr{G}_0 = (\mathbf{i}\omega)^{-1}$ in frequency space.

At small frequencies and strong coupling, the free $(\mathbf{i}\omega)^{-1}$ part of Schwinger-Dyson equation for the fermion propagator $\mathscr{G}^{-1}(\omega) = (\mathbf{i}\omega)^{-1} - \Sigma(\omega)$ becomes negligible compared to the self energy, resulting in the following closed set of integral equations for the Green's function:

$$\int ds\, \mathscr{G}(\tau - s)\Sigma(s) \approx -\delta(\tau), \quad \Sigma(\tau) = J^2\mathscr{G}(\tau)^2\mathscr{G}(-\tau) =$$

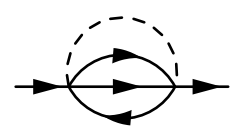

These equations allow a power law solution for the Green's funciton; here we quote the result

from [88]:

$$\mathcal{G}_{SYK}(\omega) = -\mathbf{i}\left(\frac{\pi}{J^2}\right)^{1/4}\sqrt{\frac{2\beta}{\pi}}\frac{\Gamma(\frac{1}{4}+\frac{\beta\omega}{2\pi})}{\Gamma(\frac{3}{4}+\frac{\beta\omega}{2\pi})},\quad \mathcal{G}_{SYK}(\omega) = -\mathbf{i}\left(\frac{\pi}{J^2}\right)^{1/4}\frac{\operatorname{sgn}\omega}{\sqrt{|\omega|}}$$

at finite and zero temperature respectively, and at half filling. Away from half filling, the Green's function has a phase which we discuss in section 3.4. Most significantly, we note that the mass dimension of the SYK field is $\Delta(\chi(\tau)) = -\frac{1}{4}$.

We can consider generalizing the $(q=4)$-fermion interactions of H_{SYK} to more general powers: $H(\chi) = J_{i_1\cdots i_q}\chi^\dagger_{i_1}\cdots\chi_{i_q}$. Redoing the above analysis gives $\nu(q) = \frac{2-q}{2q}$ and mass dimension $\Delta_q(\chi(\tau)) = -\frac{1}{q}$. We will take advantage of this parameter in §3.4.

It is also possible to define - and consider coupling to - the *bath field*

$$\tilde{\chi}_i \equiv \sum_{jkl} J_{ijkl}\chi^\dagger_j\chi_k\chi_l$$

which is the object multiplying χ_i in H_{SYK}. The bath field has correlator and scaling dimension

$$\langle\tilde{\chi}^\dagger(\omega)\tilde{\chi}(\omega)\rangle \propto (\mathbf{i}\omega)^{+\frac{1}{2}},\quad \Delta(\tilde{\chi}(t)) = \frac{3}{4}.$$

For general q, these are modified to $\langle\tilde{\chi}^\dagger(\omega)\tilde{\chi}(\omega)\rangle \propto (\mathbf{i}\omega)^{\frac{q-2}{q}}$ and $\Delta(\tilde{\chi}(t)) = \frac{q-1}{q}$.

3.2.2 Using SYK clusters to kill the quasiparticles and take their momentum

The system we will study for the rest of the paper has $H = H_{FS} + H_{SYK} + H_{\text{int}}$ with

$$H_{FS} = \sum_{\langle xy\rangle} t\psi^\dagger_x\psi_y + h.c. = \int d^dk\varepsilon(k)\psi^\dagger_k\psi_k,\quad H_{\text{int}} = \sum_{x,i} g_{ix}\psi^\dagger_x\chi_{xi} + \text{h.c.}$$

We denote respectively the unperturbed and full $\langle\psi\psi\rangle$ propagators with a thin and thick black line. The $\langle\chi\chi\rangle$ propagator, denoted by a red line, includes the full series of melon diagrams. Disorder contractions are drawn as a dashed line.

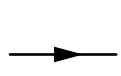 $= \dfrac{1}{\omega - v_F k_\perp}$, $= \langle\chi^\dagger_x\chi_y\rangle$, = disorder contraction

The itinerant-fermion Green's function is given by a series of alternating ψ and χ propagators. The only choice to make is how to contract the various interaction vertices in doing the Gaussian disorder averages. Any pattern other than the one shown below constrains an index sum over

SYK flavors and is therefore suppressed by powers of $1/N$:

Thus, the ψ self-energy is $\Sigma(\omega,k) = g^2\mathscr{G}(\omega)$ (just as in the holographic model). If we are interested in low energy physics near the Fermi surface, the SYK clusters are in the conformal limit and the Green's function behaves as

$$G_\psi(\omega,k) \overset{\text{small } \omega}{=} \frac{1}{\omega - v_F k_\perp - g^2\mathscr{G}_{SYK}(\omega)}$$

This is of the same form as found in the charged black hole calculation. In that context, various ν arise, but all have $\nu \geq 0$. In contrast, our model has $\nu = -\frac{1}{4}$, that is, $\mathscr{G}(\omega) \sim \omega^{-\frac{1}{2}}$. This self-energy is not only non-analytic, but also *infinite* at $\omega \to 0$. As a consequence, the Green's function *vanishes* at the Fermi surface. The spectral density $A(k,\omega) = \frac{1}{\pi}\mathrm{Im}\,G(k,\omega)$ near the Fermi surface is illustrated in Fig. 3.4. For general q, the exponent is $2\nu = \frac{2}{q} - 1$, still negative for all $q > 2$.

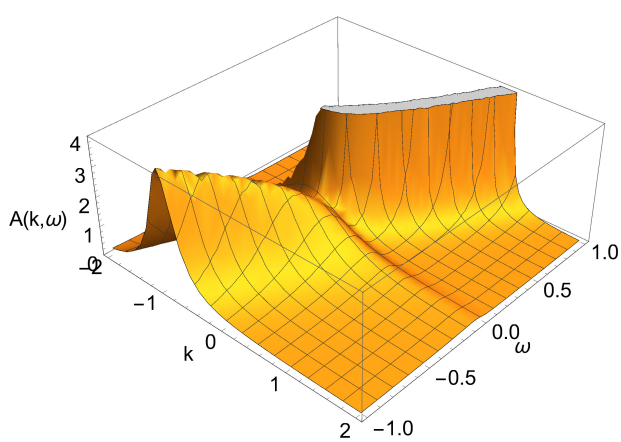

Figure 3.4: The self-energy diverges at $\omega = 0$, leading to a *zero* of the Green's function, and of the spectral density $A(k,\omega)$, exactly at the Fermi surface.

Coupling to the bath field $\tilde{\chi}$ would seem to give a more-familiar positive value of $\nu = +\frac{1}{4}$. For general q, it would give $\nu = \frac{q-2}{2q}$, which approaches a marginal fermi liquid as $q \to \infty$. We

will see below, however, that this is a place where the $N \to \infty$ and low energy limits do not commute.

The conductivity from the itinerant fermions can be calculated using the Kubo formula. In the large N limit, the transport analysis of [107, 108] (and related semi-holographic analyses [109, 110]) can largely be carried over. The temperature dependence of the DC conductivity is a power-law determined by the localized-fermion Green's function exponent as $\sigma \propto T^{-2\nu}$. In particular, coupling to the SYK fermion and coupling to the bath field yield, at large N, a resistance which is proportional to $T^{-1/2}$ and $T^{1/2}$ respectively.

The divergence of the resistance as $T \to 0$ is related to the fact that the hybridization coupling is a relevant perturbation; this is a similar phenomenon to the resistance minimum in the Kondo problem [111]. In the Kondo case, the interaction is only marginally relevant, and hence the resistance minimum occurs at an exponentially low scale; here, for $q > 2$ the interaction is relevant by a finite amount. In the limit $q \to 2$, the interaction becomes marginal, suppressing the temperature at which the resistance rise sets in. We study this limit further in §3.4.

Does the Fermi surface delocalize the clusters?

Contributions to the cluster fermion Green's function $\mathscr{G}$ are again of the form shown in Figure 3.5, where the only decision to be made is the manner of disorder contraction. Here is a place where the randomness of the hybridization couplings g_{ix} is crucial: the processes by which $\mathscr{G}_{xy}$ would develop off-diagonal terms vanish by the disorder average over g_{ix}. The cluster fermions therefore stay localized, on average (however $\overline{\mathscr{G}_{xy}\mathscr{G}_{xy}}$ will not be zero).

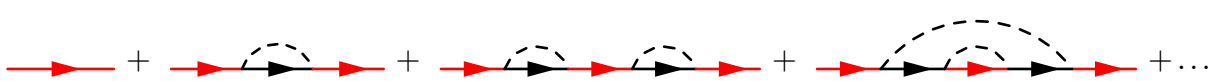

Figure 3.5: Diagrams contributing to cluster fermion green's function

Futhermore, the onsite corrections to the SYK Green's function are small; they are of order $1/N$. The leading order correction is obtained by summing the 'turtle' diagrams in Fig. 3.6.

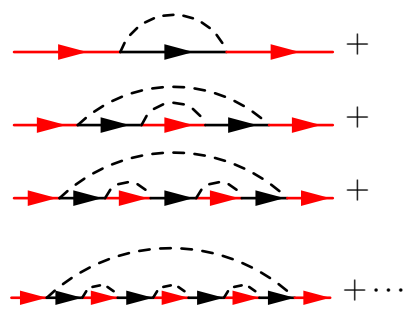

Figure 3.6: The corrections to the localized-fermion propagator $\mathscr{G}$ at order $1/N$.

Taken together, this series of diagrams combines into the object $\frac{g^2}{N}\mathscr{G}_0^2(\omega)\int d^d k\, G(k\omega)$, as we show in Appendix B.1. Thus there is the possibility that the SYK-ness of the cluster fermion will be disrupted at parametrically low energies. In Appendix B.1, we show that this correction in fact does not modify the leading low frequency behavior, even at frequencies small compared to $1/N$.

Now consider the effects of $\delta\mathscr{G}$ on the itinerant propagator. The leading-in-N self-energy $\mathscr{G}(\omega)$ itself diverges like $\omega^{-1/2}$ at low frequency. It therefore dominates over $\delta\mathscr{G}$, which vanishes at asymptotically small ω, as we show in Appendix B.1.

3.2.3 Replica analysis

The leading-order diagrammatic calculation above can be reproduced by a replica calculation. It suffices to consider a single cluster impurity. The replicated action before any disorder averaging is

$$S[\psi,c] = \sum_a \int d\tau \sum_i \bar{c}_{ia\tau}\partial_\tau c_{ia\tau} + \bar{f}_{xa\tau}\left(\partial_\tau - \xi(\partial_x)\right) f_{xa\tau}$$
$$+ \sum_{ijkl} J_{ijkl}\bar{c}_{ia\tau}\bar{c}_{ja\tau}c_{ka\tau}c_{la\tau} + \sum_i g_i \bar{c}_{ia\tau} f_{a\tau}(r_{imp}) + h.c.$$

Here $\xi(k)$ is the band dispersion. In what follows, we will occasionally drop the time arguments for compactness of writing. In that case the argument τ is always accompanies the replica index

a and τ' with b. Averaging over gs with a gaussian weight of width g produces a term

$$\mathscr{I} \equiv \exp\left(\frac{g^2}{2N}\int d\tau d\tau' \bar{f}_a(r_{imp},\tau) f_b(r_{imp},\tau')\sum_i c_{a\tau i}\bar{c}_{b\tau' i}\right).$$

This is decoupled with two hermitian Hubbard Stratonovich (HS) fields $\rho_{ab}(\tau,\tau')$ and $\sigma_{ab}(\tau,\tau')$. By 'hermitian', we mean $\rho_{ab}(\tau,\tau') = \rho^{\star}_{ba}(\tau',\tau)$.

$$\mathscr{I} = \int D\rho_{ab} D\sigma_{ab}\, \exp\left[-\frac{1}{2}\int d\tau d\tau'\, N\sum_{ab}\rho^2_{ab}(\tau,\tau') + \sigma^2_{ab}(\tau,\tau') \right.$$
$$\left. + \frac{1}{2}\int d\tau d\tau' g\left(\sum_{ab}\rho_{ab}F^-_{ab} + \mathbf{i}\sigma_{ab}F^+_{ab}\right)\right]$$

where $F^{\pm}_{ab} = \bar{\psi}_a(\tau)\psi_b(\tau') \pm \sum_i \bar{c}_{ia}(\tau)c_{ib}(\tau')$.

Introducing two sets of Hubbard-Stratonovich fields following Bray-Moore [112] and Sachdev [88], we can factorize the contribution from the average over J as

$$\int \prod_{ijkl} dJ_{ijkl}\, e^{-N^3\frac{J^2_{ijkl}}{J^2}} e^{\int dt J_{ijkl}\bar{c}_i c_j \bar{c}_k c_l} = e^{\frac{J^2}{4N}\sum_{ab}\int dt \int dt' |\sum_i \bar{c}_{iat} c_{ibt'}|^4}$$
$$= \int [dQdP] \exp\left(\int d\tau d\tau' \sum_{ab}\left(-\frac{N}{4J^2}Q_{ab}(\tau,\tau')^2 - \frac{N}{2}Q_{ab}|P_{ab}(\tau,\tau')|^2 + Q_{ab}P_{ba}\sum_i \bar{c}_{ia}c_{ib}\right)\right) \tag{3.2}$$

where Q and P are real and complex symmetric and hermitian fields, respectively. Dropping the "site" index on the cluster fermions, the replicated disorder averaged action takes the form $\sum_{ab} S_0[\psi] + NS_1[c] + NS_2(\rho,\sigma,Q,P)$ with

$$\begin{aligned}
S_0[\psi] &= \int d\tau d\tau' d^d x\, \bar{\psi}_{ax\tau}\left(\delta_{ab}\partial_\tau - \delta_{ab}\xi(\partial_x) - \frac{g}{2}\delta^d(x-r_{imp})(\rho_{ab} + \mathbf{i}\sigma_{ab})\right)\psi_{bx\tau'}, \\
S_1[c] &= \int d\tau d\tau'\, \bar{c}_{a\tau}\left(\delta_{ab}\partial_\tau + \frac{g}{2}(\rho_{ab} - \mathbf{i}\sigma_{ab}) - Q_{ab}P_{ba}\right)c_{b\tau'}, \\
S_2(\rho,\sigma,Q,P) &= \frac{1}{2}\int d\tau d\tau'\left(\rho^2_{ab} + \sigma^2_{ab} + \frac{1}{2J^2}Q^2_{ab} + Q_{ab}|P_{ab}|^2\right).
\end{aligned}$$

The saddle point equations for Q, P, ρ, and σ resulting from this effective action give us the standard SYK saddle point results

$$P_{ab} = \langle \bar{c}_{a\tau} c_{b\tau'}\rangle, \;\; Q_{ab} = J^2|P_{ab}|^2$$

supplemented by two additional relations for the fields $\rho \pm \mathbf{i}\sigma$.

$$\rho + \mathbf{i}\sigma = -g\langle \bar{c}_{a\tau} c_{b\tau'} \rangle, \;\; \rho - \mathbf{i}\sigma = \frac{g}{N}\langle \bar{\psi}_{a\tau,x=0}\psi_{b\tau,x=0}\rangle.$$

Upon integrating out ψ and c degrees of freedom, and assuming no replica symmetry breaking (and setting the position of the cluster at the origin $r_{imp} = 0$) one finds the effective action ($e^{-NS_{eff}} \equiv \int [DcD\psi] e^{-S}$),

$$S_{eff} = S_2(\rho,\sigma,Q,P) - \ln\det\left(\partial_\tau - QP + \frac{g}{2}(\rho - \mathbf{i}\sigma)\right) - \frac{1}{N}\ln\det\left(\partial_\tau - \xi(\partial_x) - \frac{g}{2}\delta^d(x)(\rho + \mathbf{i}\sigma)\right).$$

We can identify

$$\Sigma_{SYK} = J^2\mathscr{G}|\mathscr{G}|^2 + \frac{g^2}{N}G_\psi(x,x), \;\; \Sigma_\psi = g^2\mathscr{G}_{syk}$$

which reproduces the previous result. In fact the replica analysis goes a step beyond the analysis of the previous section: it sums the series of corrections to the SYK propagator in powers of g^2/N, of which we only explicitly analyzed the first term. The $\delta(x)$ in these equations appears because we studied a single impurity, and yields a momentum-independent self energy upon Fourier transforming.

3.3 Towards finite N

3.3.1 Renormalization group analysis of impurity problem

Consider a single SYK cluster coupled to the itinerant mode. There is quite a bit of physics in this impurity problem, and it will be an extremely useful starting point. As we noted in §3.2.3, the large-N analysis is basically identical.

Weak coupling. First consider the regime where $g \ll t, J$. In this case, the correlation length of ψ is large compared to the lattice spacing, and we can treat the itinerant fermions in the continuum. Following the literature on the Kondo problem [111], only the s-wave mode of the Fermi surface $\psi_0(k) \sim k\int d\hat{\Omega}\psi(\Omega k)$ couples. Linearizing the s wave mode near the fermi surface with a bandwidth cutoff Λ the Hamiltonian for the left/right moving fields $\psi_{L/R} =$

$\int_{-\Lambda}^{\Lambda} dk\, e^{\pm \mathbf{i}kr} \psi_0(k+k_f)$ is [111]

$$H_{FS} = \frac{v_F}{2\pi} \int_0^\infty dr \left(\psi_L^\dagger \partial_r \psi_L - \psi_R^\dagger \partial_r \psi_R \right)$$

This implies that the free fields under consideration have mass dimension $[\psi_{L/R}] = \frac{1}{2}$. The scaling dimension of the SYK fields was determined in the low energy analysis in the previous section and found to be $1/4$ for the fermion field and $3/4$ for the bath field. The perturbation we are considering are of the forms

$$\Delta H = g \psi_L^\dagger(0) \chi, \qquad \Delta \tilde{H} = \tilde{g} \psi_L^\dagger(0) \tilde{\chi}.$$

The scaling dimension of the coupling constant g determines whether the hybridization becomes more or less important at low energies. Demanding that the action is dimensionless, the coupling to the bath field has mass dimension $-[\int dt\ \psi^\dagger \tilde{\chi}] = -\left(-1 + \frac{1}{2} + \frac{3}{4}\right) = -\frac{1}{4}$ and is therefore irrelevant. The coupling to the fundamental field χ has dimension $-[\int dt\ \psi^\dagger \chi] = -\left(-1 + \frac{1}{2} + \frac{1}{4}\right) = +\frac{1}{4}$, and is therefore relevant. Here again we depart from the holographic construction, where $\mathscr{G} \sim \omega^{2\nu}$ with positive ν – according to the above analysis the construction studied here, only $\mathscr{G}$ with negative ν can dominate the infrared physics.

Strong coupling. Now consider the regime where $g \gg t, J$. This is a highly-underscreened Anderson model. At each site, the itinerant fermion $\psi(x)$ is coupled to a particular linear combination $\frac{1}{N}\sum_i g_i \chi_i(x) \equiv \tilde{\chi}_N(x)$ of the SYK fermions at site x. Take linear combinations of the χ_i to orthogonalize the first $N-1$ with $\tilde{\chi}_N$. Then in the limit where $|g \gg J|$ (where g is the average of the g_i), we can simply neglect the four-fermion interactions involving $\tilde{c}_N$ and the result of the hybridization is simply to pair up $\psi(x)$ and $\tilde{\chi}_N(x)$ at each site, leaving behind at low energy only $N-1$ decoupled SYK clusters. This can be called a reverse Kondo phase: whereas the Kondo effect describes the absorption of an impurity into the Fermi sea of conduction electrons, here the situation is reversed: the impurities absorb the conduction electrons!

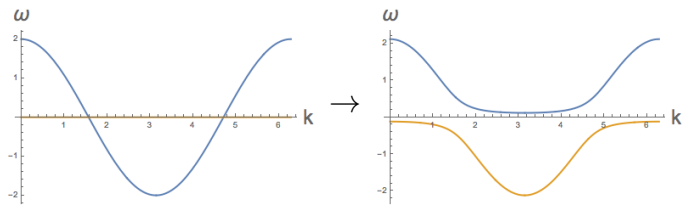

Figure 3.7: When $g \gg J$, we can neglect the SYK interactions, and our problem becomes quadratic. Hybridizing a localized fermion (flat band) with an itinerant fermion produces this bandstructure.

3.3.2 Possibilities for the phase diagram

Considerations of the topology of coupling space constrain the possibilities for the low-energy behavior of our system. Given that g is a relevant perturbation of the decoupled fixed point with $g = 0$, and given that at large g, it produces a mass gap, the possible RG flow diagrams are as follows:

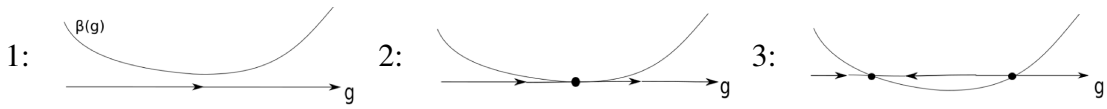

Figure 3.8: Possible behaviors of the beta function for g, given the known asymptotics. Arrows point toward the infrared.

The middle case (2) is nongeneric[4]. Therefore, if we find a fixed point, it is stable. In the following section, we will study the half-chain entanglement entropy. The above scenarios for the beta function would imply the following rough consequences for this quantity, respectively:

The respective scenarios *would* imply these behaviors of the half-chain entropy *if* the system were translation invariant. Although there are examples of highly-disordered fixed points which exhibit logarithmic area-law violation [113, 114], it is not clear whether this is inevitable.

We note that the behavior in scenario 3 does not violate RG monotonicity [115] of the 'central charge', because the UV fixed point is tensored with decoupled, localized clusters and is

[4] A well-known example where the beta function has a double zero is in the BCS phase diagram, where $\beta(V) \propto V^2 + \ldots$. Here the double zero occurs at the free theory, and is therefore protected by dimensional analysis.

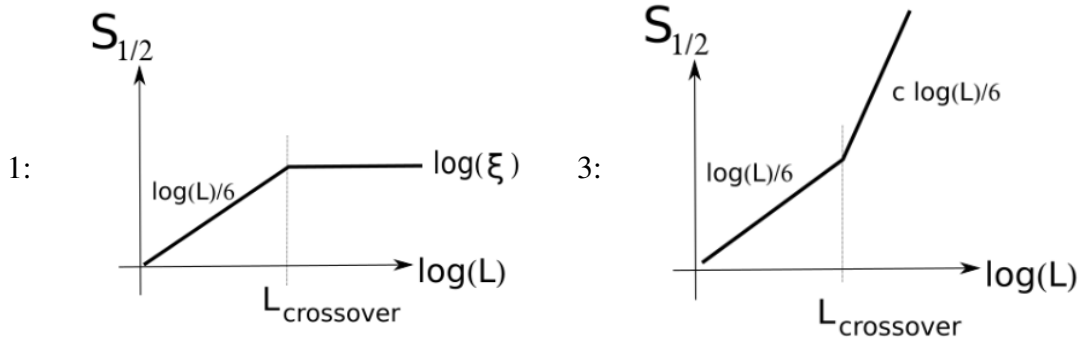

Figure 3.9: Behavior of the half-chain entanglement entropy in scenarios 1 and 3 of Fig. 3.8.

not a field theory. More generally, in a system without Lorentz symmetry, $\left(\frac{d}{d\log L}\right)^2 S_{\frac{1}{2}}$ may be positive. There are indeed known examples of disordered [116] and otherwise non-relativistic systems [117] where the 'central charge' (coefficient of $\log L$) increases towards the infrared. Note further that the condition we are violating, $\left(\frac{d}{d\log L}\right)^2 S_{\frac{1}{2}} < 0$, is a stronger condition than $\frac{d^2}{dL^2} S_{\frac{1}{2}} < 0$. In any case, the quantity $S_{\frac{1}{2}}(L)$ does not obey a known convexity theorem analogous to that of [118], which applies instead to the entanglement entropy as a function of subsystem of size ℓ of a *fixed* total system[5].

3.4 Coupling a Fermi surface to $\mathbf{SYK}_{2.0001}$ clusters

In the limit $q \to 2$, the coupling $\int \psi\chi^\dagger$ becomes marginal. Therefore, in this limit, there is a hope that the NFL fixed point we're after can be accessed perturbatively in g. Indeed, as we sketch here, this seems to be the case.

[5]Thanks to Tarun Grover for helpful discussions of these constraints on the behavior of $S(\ell, L)$.

Consider the replicated and disorder-averaged euclidean partition function[6] at $T=0$

$$Z^n = \int [d\psi d\chi] e^{-S_0 - g^2 a^{2-2\Delta(q)} \int d\tau \int d\tau' \sum_{x,i} \psi_x(\tau)\chi_{xi}(\tau)^\dagger \chi_{xi}(\tau')\psi_x(\tau')^\dagger}.$$

Replica indices accompany the time labels and are suppressed. Here S_0 is the action for the fixed point described by a Fermi surface

$$\langle \psi^\dagger(\omega,k)\psi(\omega,k)\rangle_0 = \frac{1}{\mathbf{i}\omega - v_F|k-k_F|}$$

times decoupled SYK$_q$ clusters at each site *in their conformal limit*,

$$\langle \chi^\dagger(\tau)\chi(0)\rangle_0 = C(J)\mathrm{sign}(\tau)|\tau|^{-2/q}.$$

Here $C(J) = CJ^{-2/q}$ with $C>0$ [88, 119]. The factor of $a^{2-2\Delta(q)}$ (where $2-2\Delta(q) = \frac{q-2}{q}$ is the scaling dimension of $\chi\psi^\dagger$)) has been pulled out of g to make g dimensionless.

We implement the RG as in [120], by expanding

$$\begin{aligned} Z^n = Z^n_\star \Bigg(1 - g^2 \langle \int d\tau \int d\tau' \psi(\tau)\chi(\tau)^\dagger \chi(\tau')\psi(\tau')^\dagger \rangle_0 \\ + g^4 \langle \int d\tau \int d\tau' \psi(\tau)\chi(\tau)^\dagger \chi(\tau')\psi(\tau')^\dagger \int d\tau'' \int d\tau''' \psi(\tau'')\chi(\tau'')^\dagger \chi(\tau''')\psi(\tau''')^\dagger \rangle_0 + \cdots \Bigg). \end{aligned} \tag{3.3}$$

We wish to let $g = g(a)$ run with the UV cutoff a in such a way as to cancel the dependence of Z on a, perturbatively in g. The cutoff dependence appears explicitly in the perturbation term and implicitly in the need to regulate collisions of the integrations $|\tau - \tau''| > a$.

The contractions in the $\mathscr{O}(g^2)$ term produce corrections to the renormalized action of the form

$$\delta S = g^2 \int d\tau \left(\psi^\dagger(\tau)\psi(\tau)A + \chi^\dagger(\tau)\chi(\tau)B \right)$$

where

$$\begin{aligned} B &= \int_a d\tau \langle \psi^\dagger(\tau,x)\psi(0,x)\rangle_0 = \int_a d\tau \int đ\omega e^{-\mathbf{i}\omega\tau} \int \frac{đ^d p}{\mathbf{i}\omega - v_F|p-k_F|} \\ &= \int_a d\tau \int đ^d p e^{-v_F p_\perp \tau} \end{aligned}$$

[6] In many disordered systems, one must consider the RG evolution of the probability distribution for the disorder. The renormalization group strategy pursued here, of studying the flow of the disorder-averaged action, *assumes* that the Gaussian disorder-distribution for g_{ix} is self-similar under an RG transformation – we are allowing only its variance g to evolve.

$$\simeq \frac{1}{2}\int_{-\beta}^{\beta} d\tau \underbrace{\frac{\Omega_{d-1}}{(2\pi)^d}}_{\equiv K_d} k_F^{d-1} \underbrace{\int dp_\perp e^{-\mathbf{i}v_F p_\perp \tau}}_{=\frac{1}{v_F\tau}} = -\frac{K_d k_F^{d-1}}{v_F}\left(\int_{-\beta}^{a}+\int_{a}^{\beta}\right)\frac{d\tau}{\tau} = 0 \qquad (3.4)$$

and

$$A = \int_a d\tau \langle \chi^\dagger(\tau)\chi(0)\rangle_0 = C(J)\int_a d\tau \mathrm{sign}(\tau)|\tau|^{-2/q} = 0.$$

In (3.4), β was introduced as an IR regulator[7]. A, were it nonzero, would be an innocuous correction to the ψ chemical potential. Away from half-filled clusters, where $|\mathscr{G}(\tau)| \neq |\mathscr{G}(-\tau)|$, we find $A \sim a^{1-2/q}$. Similarly, B would be a correction to the chemical potential for χ. In [88, 119], such a chemical potential is included in the analysis; the phase of $\mathscr{G}$ depends on it, but it is otherwise innocuous as well.

The interesting term for us is the (connected) contraction of the g^4 term which renormalizes g^2. This is

$\delta g^2 \;=\; -\frac{1}{2}$ 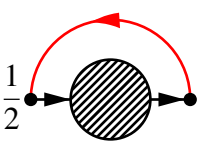

$$= (-1)^2\frac{1}{2}\int_a d\tau \langle \chi^\dagger(\tau)\chi(0)\rangle_0 \langle \psi^\dagger(\tau,x)\psi(0,x)\rangle_0 + h.c.$$

$$\simeq \frac{1}{2}C(J)\frac{K_d k_F^{d-1}}{v_F}\int_a d\tau \tau^{-2/q}\tau^{-1} \simeq \frac{1}{2}C(J)\frac{K_d k_F^{d-1}}{v_F}a^{-2/q}\,. \qquad (3.5)$$

The minus sign in the first line is from the relative sign between the $\mathscr{O}(g^4)$ term and the $\mathscr{O}(g^2)$ term in (3.3). The minus sign in the second line is from the fermion loop – we are contracting non-adjacent fermion operators. Crucially, $C(J)$ is *positive* for all values of the parameter θ (which is determined by the filling).

Therefore,

$$\beta_{g^2} \equiv \frac{d}{d\log a}g^2 = (2-2\Delta(q))g^2 + \frac{1}{2}C(J)\frac{K_d k_F^{d-1}}{v_F}\left(-\frac{2}{q}\right)g^4 + \mathscr{O}(g^6).$$

Here

$$2-2\Delta(q) = \frac{q-2}{q} = 1-\frac{2}{2+\varepsilon} = \varepsilon + \mathscr{O}(\varepsilon^2), \quad -\frac{2}{q} = -\frac{2}{2+\varepsilon} = -1+\varepsilon+\mathscr{O}(\varepsilon^2).$$

[7]Note that since zero is a bosonic matsubara frequency, it is important that we integrate from $-\beta$ to β (and divide by two), rather than just a to β. The latter would give $B \overset{?}{\sim} \log aT$. Thanks to Aavishkar Patel for patient explanations of this point.

Besides the trivial fixed point at $g = 0$, this indicates a fixed point $0 = \beta_{g^2}(g = g_\star)$ at

$$g_\star^2 = \frac{2v_F}{C(J)K_d k_F^{d-1}}\varepsilon + \mathscr{O}(\varepsilon^2),$$

which is indeed at weak coupling, parametrically in ε. We note that it is also parametrically small in the area of the Fermi surface, k_F^{d-1}, suggesting that perhaps the physics at $q = 4$ can be captured by this analysis. The fixed point depends on J like $g_\star^2 \sim C(J)^{-1} \sim J^{2/q}$.

3.5 Numerical analysis

We have attempted to perform some quantitative studies of the model considered in this paper, in the special case of a one-dimensional chain. We use the standard technique for numerical studies of one dimensional systems, the density matrix renormalization group (DMRG) [121]. Specifically, we use a single site matrix product state sweeping algorithm [122]. There are several factors which make it difficult to study this system numerically.

The unusually large size of the local Hilbert space at each site (which is $2^{N_{syk}+1}$, as opposed to 2 for a spin 1/2 chain or 4 for spinful fermions) means that the computational resources required at a given bond dimension are significantly larger than what is needed for studying spin chains. Furthermore, as is the case in most studies of systems with quenched disorder, we are interested in correlation functions averaged over many disorder realizations. Therefore, at each set of coupling constants, we must perform enough trials to achieve convergence. In some cases the number of trials required is relatively small (~ 50) and in other cases it is larger (~ 500).

We use two different methods for our DMRG study. One is a completely standard MPS based DMRG sweeping algorithm in which we take $N_{syk} = 6$ on each site. This number is not very large, but is perhaps comparable to the numbers one might hope for in material realizations of such a model.

The other method, which we'll refer to as the truncation method, begins with $N_{syk} = 12$ on each site. The size of the local Hilbert space here is too large to work with in our DMRG

algorithm, so we form an isometry which projects the Hamiltonian into the subspace spanned by the $128 = 64 * 2$ lowest energy eigenstates. That is, we exactly diagonalize $\mathbf{H}_{syk}$ with 12 modes in the presence of one extra fermionic mode which the Hamiltonian doesn't act on. So we truncate a Hilbert space of the form $2^{12} \otimes 2 \to 64_{syk} \otimes 2$. The entire Hamiltonian, as well as the hybridization and hopping terms, are projected into this truncated space.

The idea behind the truncation approach is that the properties of interest (in particular, the singular self-energy) arise due to the special low energy physics of the SYK cluster. The expressions given for the Green's functions of the large N theory considered in section 3.2.2 were all valid at low energies and at momenta near the Fermi surface. The relevant energy scales to compare are the hybridization coupling g and the bandwidth D of the states that are retained. This is found to be $D \sim 0.26J$ at $N_{syk} = 12$.

To help map out the phase diagram, one of the most convenient and easily accessible quantities we can measure is the entanglement entropy of subregions of the chain (EE). In particular, (a review is [123]) a one dimensional conformal field theory (CFT) in the thermodynamic limit has an entanglement entropy which grows with the size L of the subregion as $\frac{c}{3}\log L$, where c is the central charge of the CFT[8]. Similarly, for a CFT on a space of length L, the half-chain entanglement entropy scales with the system size as $\frac{c}{6}\log L$. Thus, measuring the growth of the half-chain entanglement entropy with the system size allows us to access some universal information about the phase and its low-energy excitations, from just the groundstate wavefunction. We note that the emergence of Lorentz symmetry, much less conformal symmetry, is unlikely in our disordered system, so the measured behavior of the entanglement entropy is a proxy for the number of low-energy degrees of freedom.

Considering fixed J, we know the behaviour of the half-chain EE at both small g and very large g. At zero g, the SYK clusters are decoupled from the free fermion chain. The latter is responsible for all of the spatial entanglement, and has $c = 1$ for spinless fermions. That is what

[8]For simplicity, we assume a non-chiral spectrum.

we observe from the slope of the half chain EE. At large g, the hybridization term dominates and we expect the itinerant fermions to bind into a local singlet. This phase has a finite correlation length which becomes very small at large g. Hence the EE satisfies an area law and $c = 0$. We observe this behaviour in our simulations.

As g increases from zero, there are two possibilities, as we discussed in §3.3. Although finite size effects are hard to overcome in our particular model, measuring the slope of the half chain EE at different values of g provides some evidence for either scenario 1 or 3 above.

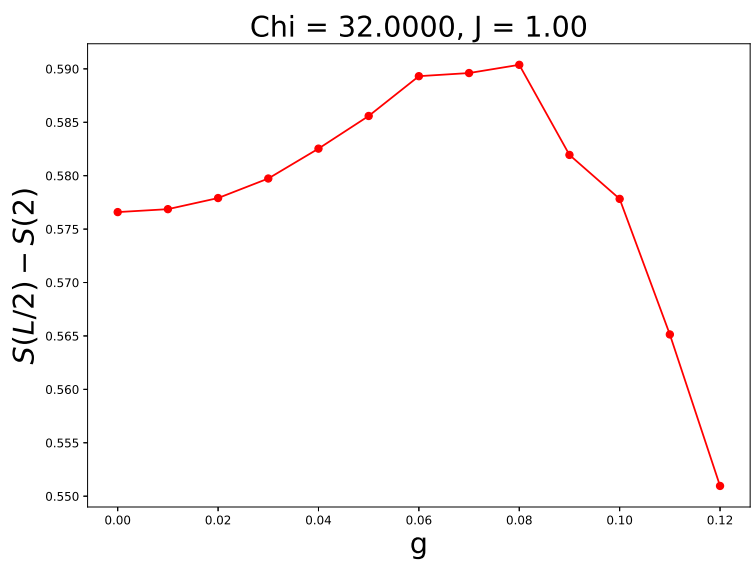

Figure 3.10: The half-chain entanglement $S(L/2) - S(2)$ at fixed $L = 52$, as a function of g, averaged over up to 600 samples.

Half-chain entropies. In Fig. 3.10 we plot $S(L/2) - S(2)$ at fixed L for various g, and observe smooth growth to a maximum value, suggestive of scenario 3 with an intermediate-coupling fixed point. $S(2)$ is subtracted to remove a g-dependent constant shift. Beyond the maximum, all the entanglement is destroyed; this is the reverse Kondo phase.

The right panel of Fig. 3.11 illustrates the fact that the coupling to bath field $\tilde{g}\psi\tilde{\chi}$ is irrelevant – it is identical to the free fermion answer for all $\tilde{g}$.

The left panel of Fig. 3.11 shows the half-chain entanglement entropy as a function of

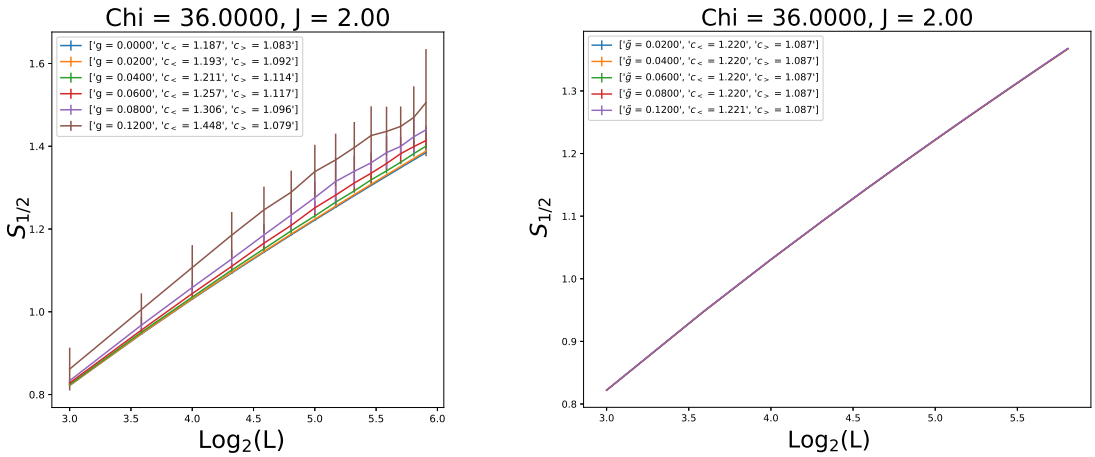

Figure 3.11: Left: half-chain entanglement entropy versus log of system size for $J = 2, t = 1$, and various values of g, the coupling to the fermion field, computed in the truncated scheme. $c_<$ and $c_>$ are six times the slope calculated at $\log_2 L < 5$ and $\log_2 L \geq 5$ respectively. Right: half-chain entanglement entropy versus log of system size, for various values of $\tilde{g}$, the coupling to bath field. In the latter case, the curves all lie on top of the free fermion curve. The inset gives fits to the slope (times 6).

$\log(L)$ for $J = 2, t = 1$, and various values of g, computed using the truncation scheme. We expect these choices of J and g are in the regime of validity of the truncation especially for the smaller values of $g \lesssim D/10$. For comparison, the results obtained using the standard DMRG are shown in Appendix B.2.

There is a regime at small g where the entanglement grows faster with L than the free-fermion answer at small system sizes At larger L, the curve levels off to approximately the same slope as the free-fermion curve. One possibility is that this is due to some extra finite-range correlation between the cluster degrees of freedom on top of the extended contribution from the itinerant degree of freedom, and that the true area law violating term has the same coefficient as a decoupled spinless fermion.

Another possiblity is that the apparent rejoining with the free fermion value is related to a previously-observed difficulty in the use of DMRG algorithms for disordered critical systems

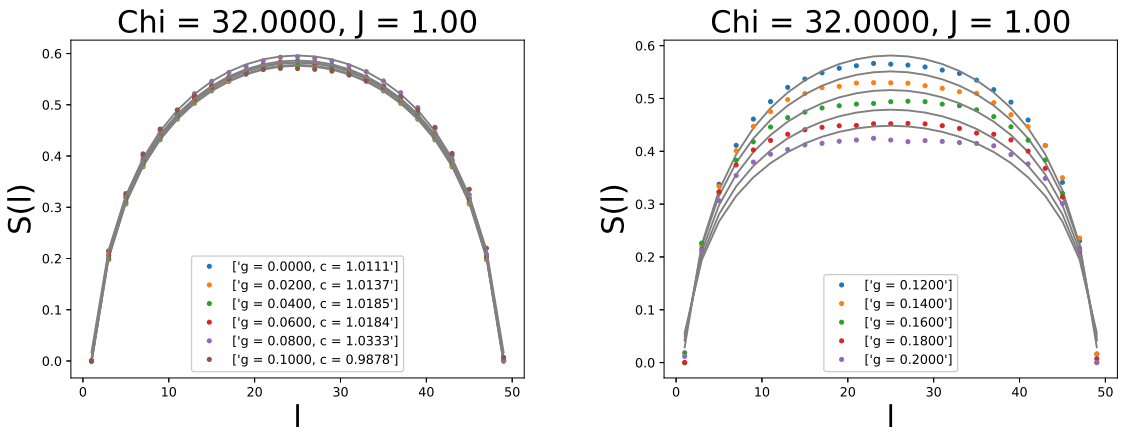

Figure 3.12: The finite size entanglement as a function of the position of the entanglement cut at a fixed system size $L = 52$. We plot only the even sites in order to remove even-odd oscillations. At small values of g, the data is well fit by the expression $S(x) = \frac{c}{6}\log_2\left(\frac{2L}{\pi}\sin(\pi x/L)\right) + a$. At larger values of g the fit fails. Data are averaged over $200-400$ disorder realizations.

[124]. If we parametrize the EE as

$$S_{1/2}(L) = \frac{1}{6}\log_2 L + \frac{\delta c_{dis}}{6} g(L) + const,$$

where $g(x) = \log_2(x)$ at $x < l_{crossover} \sim 2^5$ and saturates to a constant at $x \gtrsim l_{crossover}$, this reproduces our observed results. A more conservative explanation is that $c \sim 1$ throughout the extended phase.

In addition to the scaling of the EE with the system size, we can also look at the dependence on the size of the bipartition at fixed system size. Fitting our data to known expressions for the finite size entanglement in critical systems [125, 126, 127] provides another method to extract the 'central charge'. The quality of the fit is also a useful diagnostic of whether the system is approximately critical or has a finite correlation length. Our results are shown in Figure 3.12; at small g we observe a small rise in the entanglement but cannot draw a strong conclusion. At larger values of g we observe the onset of a finite correlation length.

Correlation functions. Fig. 3.13 shows the fermion equal-time correlation functions in the DMRG approximation to the groundstate. The absolute value is averaged over 50 instances.

The result fits well to

$$\left|\langle \psi_x^\dagger \psi_{L/2}\rangle\right| \sim \frac{|\sin 2k_F(x-L/2)|}{|x-L/2|^\alpha} \tag{3.6}$$

with $\alpha < 1$. The free fermion answer is of the form (3.6) with $\alpha = 1$. For $g > 0$, the exponent is larger than the free fermion value. It would be interesting to try to reproduce this change in the exponent using the $q-2$ expansion. The right column of Fig. 3.13 shows that at the same values of g, the so-called localized fermions χ are indeed still localized. The bottom row of Fig. 3.13 shows that at large g, everybody is localized – this is the reverse Kondo phase.

Lesion studies. To what extent is the use of the SYK model as the cluster Hamiltonian crucial? We can attempt to address this question by perturbing the cluster Hamiltonian by (relevant) quadratic terms. In the case of purely quadratic clusters, the entire Hamiltonian is quadratic, and we can study larger system sizes, calculating the entropy by the Peschel formula [128]. The result is shown in Fig. 3.14.

Another reason to study the case of quadratic clusters is to identify the length scale at which localization sets in. In one dimension, to which our numerical work is sadly limited, localization is likely the inevitable long-distance fate. We see in Fig. 3.14 that at $g \lesssim 0.3$ localization sets in at system sizes which are too large for us to accurately study using DMRG. Therefore we cannot rule out the possibility that the quartic model would show a finite correlation length as well at larger system sizes. However, whereas localization is guaranteed for the disordered quadratic system in one dimension [129], it is possible that the interacting system remains extended.

3.6 Conclusions

In this paper we have studied what happens when we couple a Fermi surface to a lattice of locally critical clusters. We have provided evidence from various approaches for the existence of a novel strange metal fixed point at intermediate values of the root-mean-square hybridization coupling g. This fixed point is stable to perturbations of g. Intra-cluster quadratic terms are likely

to be relevant. We note that the proposed new strange metal fixed point is not Lorentz invariant.

A comment about the role of large N is in order. The power-law in the SYK fermion Green's function is a crucial ingredient in the construction. Such critical behavior in a (0+1)-dimensional system requires a large number of degrees of freedom: if one takes $\omega \to 0$ before $N \to \infty$, the low-lying level spacing of the clusters will be discrete. The effects of this phenomenon are visible in the top left of Fig. 3.3: if the level spacing of the SYK clusters is large compared to t and g, the hybridization coupling has no effect. At leading order in large-N, the power-law in the cluster-fermion Green's function is directly carried over into the itinerant fermion self-energy, as in the holographic calculation. In contrast, at finite N, only power-laws corresponding to relevant perturbations (in the sense of §3.3) affect the low-energy behavior of the itinerant fermions. The bath field $\tilde{\chi}$, for example, is irrelevant for all q. This restricts the resulting states to have self-energy exponent $2\nu < 0$.

We should emphasize that the stability of the putative strange metal fixed point is predicated on not adding other (quadratic) operators to the SYK cluster hamiltonian. (Such relevant deformations are also visible in the semi-holographic description [76].) So inevitably, the physics we have discussed should only be realized at intermediate temperatures.

The title of the paper merits a comment. Its maximal chaos is a signature property of the SYK model, and this justifies our use of the term 'local quantum chaos' for the behavior of the clusters. This maximal quantum chaos is a property of the states in the middle of the spectrum. In contrast, the essential ingredient for our construction is the power-law behavior in frequency of the groundstate and low-temperature Green's functions. The absence of quasiparticles certainly requires breaking of integrability, as borne out by the data show in Fig. 3.14. But whether there is indeed an intimate connection between these different facets of the physics of SYK is an interesting open question.

We conclude with a suggestion for a direction for progress towards corroborating the existence of this fixed point and studying its properties. The matrix product ansatz used in the

DMRG study of §3.5 does not take advantage of all of the structure of the problem. In particular, the fact that the clusters do not couple directly to each other represents a kind of 'entanglement bottleneck' – any long-ranged entanglement along the chain necessarily passes through the itinerant fermion sites. To take advantage of this, it would be useful to construct a variational tensor product state with the structure of our interaction graph shown in Fig. 3.1. It would also be interesting to try to apply an adaptation of the dMera of [124] to answer the question regarding the scaling of the EE in our disordered system.

3.7 Acknowledgements

We thank Sid Parameswaran for collaboration at the initial stage of this work, and Dan Arovas, Tarun Grover, Aavishkar Patel and Shenglong Xu for helpful input. This work was supported in part by funds provided by the U.S. Department of Energy (D.O.E.) under cooperative research agreement DE-SC0009919. This research was done using resources provided by the Open Science Grid [130, 131], which is supported by the National Science Foundation award 1148698, and the U.S. Department of Energy's Office of Science.

Chapter 3 is, in part, a reprint of material from published work done in collaboration with John McGreevy, as it appears on Physical Review B. D. Ben-Zion and J. McGreevy, "Strange Metal from Local Quantum Chaos," *Phys. Rev. B* **97** 155117 . The dissertation author was the primary investigator and author of this material.

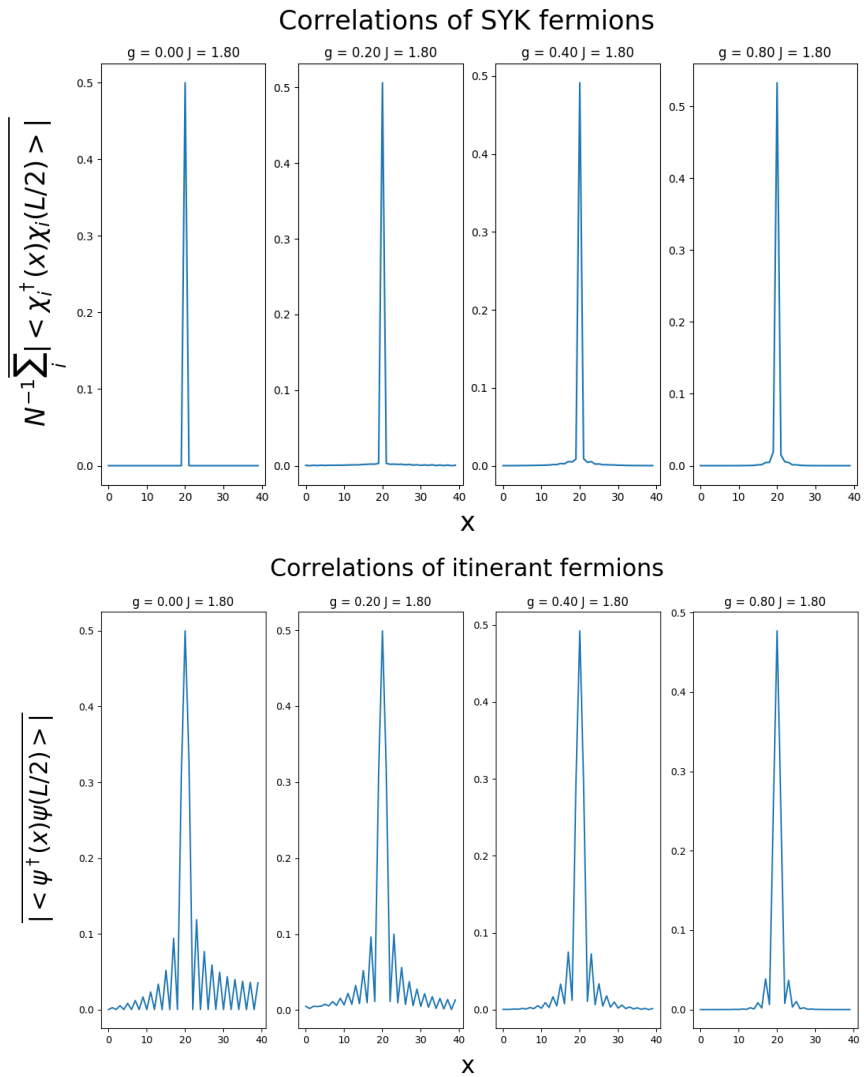

Figure 3.13: Top: The averaged absolute value of correlation functions of the localized χ fermions between the middle site and the site x, for various g. Bottom: The absolute value of correlation functions of the itinerant ψ fermions between the middle site and the site x, for various g.

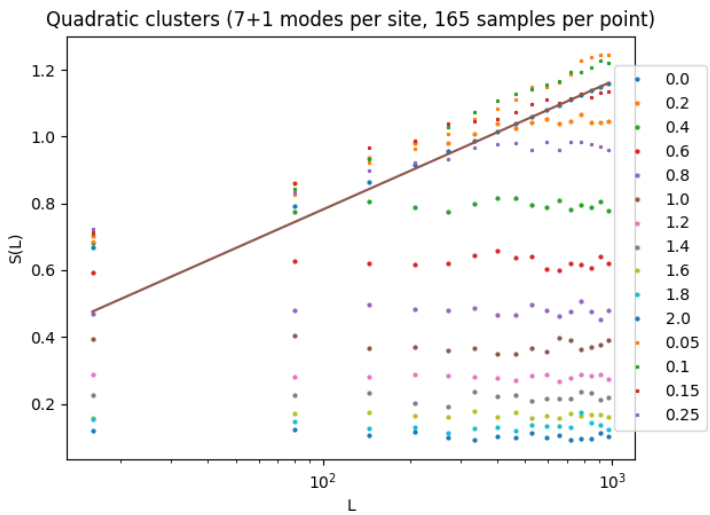

Figure 3.14: Half-chain entropy as a function of chain length for a free-fermion chain (uniform hopping $t = 1$) hybridized with local *quadratic* clusters, with random quadratic intra-cluster interactions of mean 1. Different curves are different values of the root-mean-square hybridization coupling g, which varies from 0 to 2.0. The solid line is the asymptotic behavior in the clean limit, $S(L) = \frac{1}{6}\log(L) + a$.

Chapter 4

Disentangling quantum matter: Applications to scars, heavy fermions, and gapless topological phases

4.1 Context

Understanding the pattern of entanglement in a quantum state often leads to deep insights about the nature of the phase that wavefunction belongs to. Topologically ordered phases provide one class of dramatic examples of this, where the entanglement entropy of the ground state(s) reveals nonlocal correlations and contains information about the anyon spectrum of the phase [132, 133, 134, 135]. Entanglement entropy has also been used to address questions concerning thermalization of quantum systems; many-body-localized systems are partially characterized by an area law at finite energy density, and logarithmic entanglement growth after a quench [136, 137].

One relatively unexplored area concerns the distribution of entanglement in multi-component systems. In [22], the authors introduced the notion of a quantum disentangled state to describe a

scenario in which the eigenstate thermalization hypothesis (ETH) partially breaks down. In this work we extend the scope of QDL and show that quantum disentangling has applications beyond questions regarding thermalization. Specifically, we consider QDL type measurements on ground states . In section 4.2 we study a model where gapless charge modes are proposed to coexist with a symmetry protected topological phase of spins. In section **??** we apply similar ideas to models of heavy fermion systems in order to find a gauge-invariant order parameter for the heavy Fermi liquid.

We also establish a correspondence between the QDL measure and the mutual information. Based on this correspondence we derive a constraint on the distribution of entanglement in ergodic wavefunctions, and show that the QDL measure must be slightly modified in order to distinguish between states which satisfy ETH and those which do not.

4.2 SPT physics in the presence of gaplessness

We consider a model of spin 1 hardcore bosons governed by the Hamiltonian

$$\mathbf{H} = -t\sum_{i\sigma} b^{\dagger}_{i\sigma} b_{i+i\sigma} + h.c. + J\sum_{i} \vec{S}_i \cdot S_{i+1} + D\sum (S^z_i)^2. \tag{4.1}$$

The hopping amplitude t determines an overall energy scale and we set it equal to 1. This model was originally considered in [138] as a strong coupling limit of a particular two leg fermionic ladder; the spinful hardcore boson represents two fermions bound into a triplet state across a rung of the ladder.

In addition to a trivial paramagnet phase, a spin-1 chain also posseses a nontrivial SPT phase known as the Haldane phase [139, 140, 141]. The model described by 4.1 is argued to exhibit spin charge separation in the sense that the ground state wavefunction factorizes into a charge wave function times a spin wave function on the squeezed lattice (the lattice obtained by deleting the unoccupied sites). As a result of this spin-charge separation, it is possible for the spin degrees of freedom to form an SPT phase, despite the presence of the gapless charge degrees of

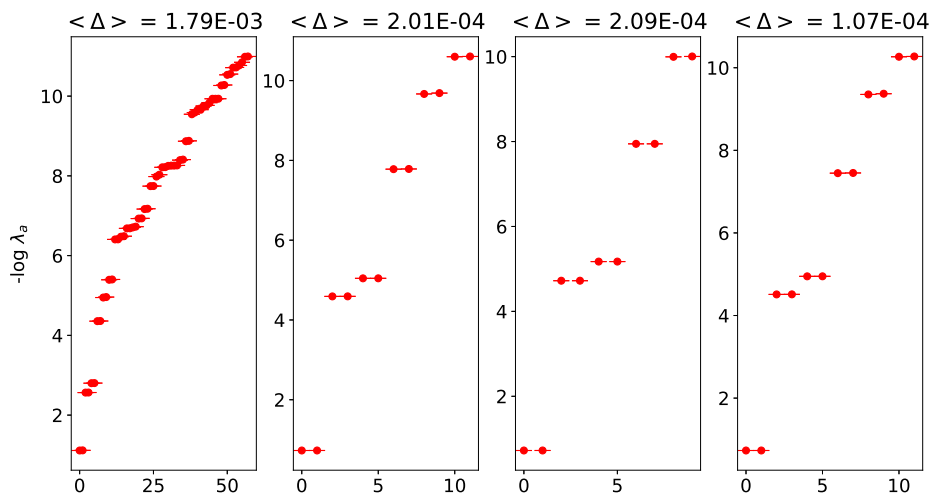

Figure 4.1: Leftmost: Entanglement spectrum across the center bond of the full wave function. Right plots: Entanglement spectrum across the center bond for the projected wave function $|\Psi_s\rangle$ for three randomly chosen hole configurations. The system size is $L = 96$, with couplings $J = 0.1$ and $D = 0.01$. Also shown is the mean spacing between pair levels in the entanglement spectrum $\langle\Delta\rangle$.

freedom.

We apply the QDL protocol to freeze the charge degrees of freedom and study the entanglement properties of the leftover spins. For a conventional spin wavefunction, one signature of an SPT phase is a degeneracy in the entanglement spectrum due to the edge modes [142]. We therefore propose to use the entanglement spectrum of the post-projection wavefunction to access the topological properties of the state.

The ground state of (4.1) was obtained for both open and periodic boundary conditions using DMRG, with bond dimensions up to $\chi = 3000$. Figure 4.1 shows the post-projection entanglement spectra in the topological phase ($J \gg D$). It is very easy to see the systematic double degeneracy throughout the entire entanglement spectrum. As we increase D and go over to the trivial phase, the degeneracy disappears as expected.

Other than the entanglement spectrum, we can also look at the entanglement entropy of the post-projection wavefunction. To keep the discussion self contained, we recall some of the

definitions from Ref [22]. They considered multi-component systems [1] and the main object they studied was the entanglement entropy of one set of degrees of freedom s after fixing the other

$$S^{s/c} = \mathrm{tr}_{\{R_c\}} p(\{R_c\}) \left(\mathrm{tr}_s \rho_s^{(\{R_c\})} \log \rho_s^{(\{R_c\})} \right). \tag{4.2}$$

The reduced density matrix $\rho_s^{(\{R_c\})}$ is a density matrix for spins in a fixed configuration of charges (holes). Specifically, if $\hat{\rho}$ is the full density matrix constructed from the ground state wave function, then

$$\rho_s^{(\{R_c\})} = \langle \{R_c\} | \hat{\rho} | \{R_c\} \rangle.$$

Finally, the weighting factor in the trace over charge configurations is the probability to observe the charge in the particular configuration $\{R_c\}$:

$$p(\{R_c\}) = \mathrm{tr}_s \rho_s^{(\{R_c\})}.$$

We studied (4.1) at system size $L = 64$ with periodic boundary conditions. It is somewhat impractical (and in general impossible) to perform the full trace over charge configurations in 4.2, so we calculated $S^{s/c}$ via Monte Carlo sampling with the distribution $p(\{R_c\})$. The results in the topological phase, in the trivial phase, and directly at the critical point are shown in Figure 4.2. In all cases, the full wavefunction has the form

$$S(l) \sim \frac{c}{3} \log \left(\frac{L}{\pi} \sin \left(\frac{\pi l}{L} \right) \right) + b$$

with $c = 1$ away from the critical point, and $c = 2$ at the critical point. Away from the critical point, the spins are essentially in a gapped phase which mixes very weakly with the gapless charge degrees of freedom, so we see $c = 1$ worth of gapless charge.

Applying the QDL projection freezes the charge degrees of freedom, and the entanglement entropy of the post-projection wavefunction collapses into an area law behaviour characteristic of a gappled phase in one dimension. At the critical point, both spin and charge are gapless, so we see $c = 2$. In this case, the post-projection wavefunction retains the entanglement entropy of a critical wavefunction with precisely $c = 1$.

[1] We refer to the two components as s and c for spin and charge, although in general the two components need not be spin and charge

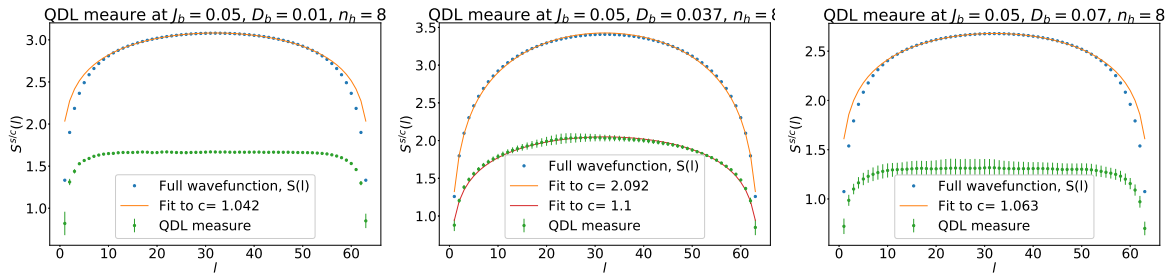

Figure 4.2: QDL Measure $S^{s/c}$ across the phase diagram. Left) Topological phase: entanglement entropy of post-projection spin wavefunction collapses to an area law. Middle) Critical point: entanglement entropy of post-projection spin wavefunction shows critical behaviour with $c = 1$. Right) Trivial phase: entanglement entropy of post-projection spin wavefunction collapses to an area law.

As far as we are aware, performing partial projections and studying properties of the 'leftover' wavefunction has not been generally explored. The distinction between an SPT and a trivial phase is typically predicated on the existence of a finite energy gap in both phases [7]. However there appear to be a few examples where features usually associated with SPT phases persist in the presence of gapless modes, including the model studied in this section as well as the models described in [143]. Quantum disentangling is likely to provide a useful method for studying such systems.

4.3 An operator-agnostic QDL measurement

We now discuss some general aspects of the QDL diagnostic. Consider a Hilbert space $\mathscr{H} = A \otimes B \otimes C$ with three parts. The QDL protocol takes as input a state ρ_{ACB} and a choice of operator $\mathscr{O}_C$ on C. The protocol is: (1) measure $\mathscr{O}_C$ and obtain outcome C with probability $p(C) = \mathrm{tr}_{AB}\langle C|\rho_{ACB}|C\rangle$. (2) In the resulting state $\rho_{AB|C}$ find the entanglement entropy of A, $S(A|C)$. (3) Average over the distribution $p(C)$ to obtain the QDL diagnostic

$$\overline{S(A|\mathscr{O}_C)} \equiv \sum_C p(C) S(A|C).$$

An alternate protocol replaces the von Neumann entropy with the mutual information.

(2) In the resulting state $\rho_{AB|o_C}$ find the mutual information between A and B: $I_{\rho^C_{AB}}(A:B)$. (3) Average over the distribution $p(o_C)$ to obtain an alternate QDL diagnostic

$$\overline{I_{\mathscr{O}_C}(A|C)} \equiv \sum_C p(C) I_{\rho^C_{AB}}(A:B).$$

When ABC is the full system, and measuring c completely fixes the state of C, then $\rho_{AB}|c$ is a pure state. To see this explicitly, write the initial state $|\psi_{ABC}\rangle$ in the basis of eigenstates of the operator $\mathscr{O}_C$:

$$|\psi_{ABC}\rangle = \sum_c |\psi_{AB}(c)\rangle \otimes |c\rangle.$$

Then by the axioms of quantum mechanics, when we measure $\mathscr{O}_C$ and get the outcome c, the resulting state (up to normalization) is

$$|\psi_{ABC}\rangle \overset{\text{measure } \mathscr{O}_C, \text{ get } c}{\rightarrow} |\psi_{AB}(c)\rangle \otimes |c\rangle$$

a product state between AB and C, $\rho_{AB}|c = |\psi_{AB}(c)\rangle\langle\psi_{AB}(c)|$. In such a state the vN entropy of AB vanishes, $S(AB|c) = 0$ and hence

$$I(A:B|c) = S(A|c) + S(B|c) - S(AB|c) = 2S(A|c). \tag{4.3}$$

Averaging (4.3) over the distribution of outcomes $p(c)$ says that under these conditions, the mutual information version of the QDL diagnostic is twice the original QDL diagnostic

$$\overline{I_{\mathscr{O}_C}(A|C)} = 2\overline{S(A|\mathscr{O}_C)}.$$

A related quantity which depends on a state ρ_{ACB} but not a choice of operator is the conditional mutual information

$$I(A:B|C) \equiv S_{AC} + S_{BC} - S_{ACB} - S_C = I(A:BC) - I(A:C) \tag{4.4}$$

$$= D(\rho_{ACB}||\rho_A \otimes \rho_{BC}) - D(\rho_{AC}||\rho_A \otimes \rho_C) \tag{4.5}$$

where $D(\rho||\sigma) \equiv \mathrm{tr}\rho\log\rho - \mathrm{tr}\rho\log\sigma \geq 0$ is the relative entropy. We will show that the conditional mutual information bounds above the alternate QDL diagnostic:

$$I(A:B|C) \geq \overline{I_{\mathscr{O}_C}(A|C)}. \tag{4.6}$$

Proof: The relative entropy is monotonic under the action of any quantum channel $\mathscr{E}$: $D(\rho||\sigma) \geq D(\mathscr{E}(\rho)||\mathscr{E}(\sigma))$. Consider the diagonal-part channel on C in the basis of eigenstates

of $\mathscr{O}_C$, defined as:

$$\rho_{ABC} \mapsto \mathscr{E}(\rho_{ABC}) \equiv \sum_C \langle C|\rho_{ABC}|C\rangle \otimes |C\rangle\langle C| \equiv \sum_C p_C \rho_{AB}^C \otimes |C\rangle\langle C|. \tag{4.7}$$

Because $\mathscr{E}$ acts only on C, (4.5) shows that $I(A:B|C)$ is also monotonic under $\mathscr{E}$. Therefore:

$$I_\rho(A:B|C) \geq I_{\mathscr{E}(\rho)}(A:B|C) \tag{4.8}$$

In terms of the spectral decomposition of $\rho_{AC}^C = \sum_i \lambda_i^{(C)} |\lambda_i^{(C)}\rangle\langle\lambda_i^{(C)}|$ in the state (4.7) we have

$$S_{\mathscr{E}(\rho)}(ACB) = \sum_C p_C \sum_i \lambda_i^{(C)} \log p_C \lambda_i^{(C)} = H(p) + \sum_C p_C S(\rho_{AC}^C)$$

and similarly for $S_{\mathscr{E}(\rho)}(CB)$ and $S_{\mathscr{E}(\rho)}(AB)$, giving

$$\begin{aligned} I_\rho(A:B|C) &\geq I_{\mathscr{E}(\rho)}(A:B|C) = S_{\mathscr{E}(\rho)}(AC) + S_{\mathscr{E}(\rho)}(CB) - S_{\mathscr{E}(\rho)}(ACB) - S_{\mathscr{E}(\rho)}(C) \\ &= H(p) + \sum_C p_C S(\rho_A^C) + H(p) + \sum_C p_C S(\rho_B^C) - \left(H(p) + \sum_C p_C S(\rho_{AB}^C) \right) - H(p) \\ &= \sum_C p_C \left(I_{\rho_{AB}^C}(A:B) \right) = \overline{I_{\mathscr{O}_C}(A|C)}. \end{aligned}$$

To establish the usefullnes of this alternative measurement, we first use the conditional mutual information to carry out the same study as in [144]. We perform exact diagonalization of the one dimensional Hubbard model with a repulsive nearest neighbor interaction added to break integrability

$$\mathbf{H} = -t \sum_{i\sigma} c_{i\sigma}^\dagger c_{i\sigma} + U \sum_i n_{i\uparrow} n_{i\downarrow} + V \sum_i n_i n_{i+1}. \tag{4.9}$$

First we compute the entanglement entropy after a bipartition into left and right halves as usual. We then use the CMI as a diagnostic of QDL behavior. Specifically, we bipartition the chain into two halves A and B and calculate the CMI between spins (charge) in A and B conditioned on all charge (spin). For simplicity of notation, we refer to this quantity as $S^{s/c}$ ($S^{c/s}$) despite the fact that it is not exactly the same thing as the originally defined QDL measure.

The CMI between regions A and B conditioned on C is

$$I(A:B|C) = S(AC) + S(BC) - S(ABC) - S(C).$$

When ABC is the entire system, this expression simplifies to the mutual information between A and B: $I(A:B) = S(A) + S(B) - S(AB)$. In this expression, $S(A)$ refers to the entanglement entropy of spins (or charge) *only* in region A, and $S(AB)$ is the total entanglement between spins

and charge.

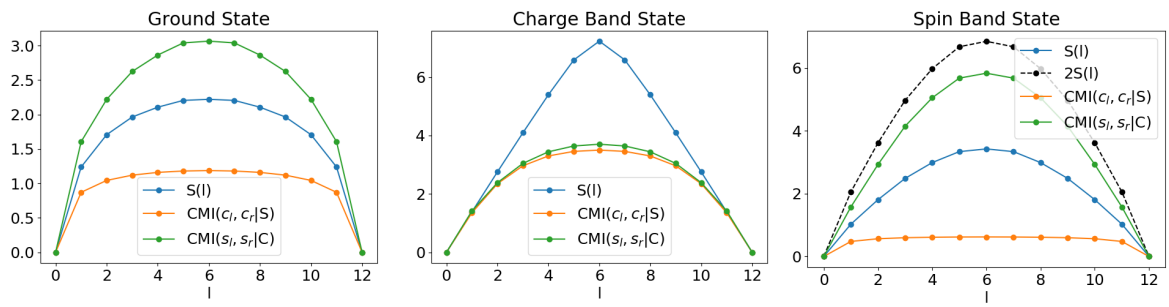

Figure 4.3: Entanglement entropy and CMI measurements on one dimensional Hubbard model as a function of bipartioning cut at couplings $U = 4$, $V = 3/4$. Left: Ground state. Middle: A generic state in the charge band. Right: A state in the spin band. Colors corresonpond to the same legend as the other two plots.

The results are presented in Figure 4.3. We calculate entanglement entropy after a normal bipartition, $S^{s/c}$ and $S^{c/s}$ for three states obtained by exact diagonalization of 4.9. We study the ground state, a generic state taken from the middle of the spectrum, and a state belonging to the 'spin band'. Our results are in agreement with those of [144], confirming the validity of the use of CMI as a proxy for observing QDL behavior.

In the ground state, all three quantities S, $S^{s/c}$, and $S^{c/s}$ exhibit sub-thermal scaling. For an excited state in the charge band the entanglement entropy follows a volume law, as expected. One area where the mutual information measurement seems to differ from the QDL measure is with regards to the behavior of $S^{s/c}$ and $S^{c/s}$ for a generic state. For an excited state from the spin band, both the entanglement entropy and $S^{s/c}$ exhibit a volume law. However $S^{c/s}$ saturates to an area law, in agreement with the measurement from Garrison *et. al.*.

Some evidence that the spin band states actually exhibit 'complete' disentanglement between spin and charge in the sense that

$$|\psi\rangle \approx |\psi_{charge}\rangle \otimes |\psi_{spin}\rangle \tag{4.10}$$

is provided by comparing the mutual information of spins and the entanglement entropy of the full wavefunction. If 4.10 holds, then it is possible to consider a scenario in which $|\psi_{charge}\rangle$ is

an area law state and $|\psi_{spin}\rangle$ is a volume law state. In this case, the entanglement entropy of the full wavefunction will be dominated by contributions from the spin wavefunction, so that $S(l) \approx S(\rho^{spin}(l))$.

Given the factorization 4.10, the mutual information of spins is then approximately twice the entanglement of the spin wavefunction: $I(s_l, s_r) \approx 2S(\rho^{spin}(l)) \approx 2S(l)$. Comparing the two quantities in the right plot of Figure 4.3, we see that the mutual information of spins indeed comes close to twice the entanglement entropy, indicating that 4.10 may hold for the spin band states.

A comment is in order regarding the behaviors of $I(A:B|C)$ for generic finite energy states. It appears that both $S^{s/c}$ and $S^{c/s}$ calculated with a state from the charge band exhibit sub-thermal growth in Figure 4.3. This result is at odds with the results of [144] who find a volume law for the QDL measure, albeit at similarly small system sizes. The apparent inevitable violation of the bound $I(\text{spins } \in A, \text{spins } \in A) \geq S^{s/c}(A)$ (and similarly for charge) requires a reexamination of the QDL measure applied to ergodic wavefunctions.

In [145], Vidmar *et. al.*showed that the entanglement entropy of high energy eigenstates of chaotic Hamiltonians is given by volume law, plus a correction which grows as $\sqrt{L_A}$ when $L_A = L/2$. For $L_A < L/2$, they showed that $S(A)$ is given by a volume law plus a correction which decreases exponentially fast with L_A. As it relates to the mutual information and the QDL measure, there are thus three scenarios to consider in terms of the relative sizes of the Hilbert spaces of the different degrees of freedom.

Given a Hilbert space of the form $\mathscr{H}_s \otimes \mathscr{H}_c$ (here we continue to use generic labels s and c to refer to the two different sets of degrees of freedom), we further partition the Hilbert space into $\mathscr{H}_{s\in A} \otimes \mathscr{H}_{s\notin A} \otimes \mathscr{H}_c$. For simplicity of notation, we refer to $s \in A$ as A, $s \notin A$ as B, and c and C. When $\dim \mathscr{H}_c > \dim \mathscr{H}_{s\in A} \otimes \mathscr{H}_{s\notin A}$, the entropy of both subregions of spins scales as a volume law with exponentially small corrections: $S(A) \sim A,\ S(B) \sim B$. This predicts that the mutual information between spins in region A and spins in region B is essentially zero.

This result has a rather striking consequence, when interpreted from the point of view

of the QDL measure. For a tripartite Hilbert space $\mathscr{H}_{ABC}$, we previously showed that $I(A,B) \geq S^{QDL}(A|C)$, where the right hand side involves measuring region C, calculating the post-measurement entanglement entropy of region A, and then averaging over outcomes of the measurement of C. The vanishing of the mutual information thus implies that measuring slightly more than half of an ergodic wavefunction collapses the remaining wavefunction into an area law. This reflects the highly nonlocal nature of entanglement in a volume law state.

Given a partition of a Hilbert space ABC where $\mathscr{H}_{AB}$ is the same size as $\mathscr{H}_C$, a finite energy density eigenstate of a chaotic Hamiltonian will have $I(A,B) \sim \sqrt{A \cup B}$ after cancellation of the volume law terms. This represents an area law as a function of the L_A, while keeping $L_A + L_B$ fixed. It is therefore tempting to argue that the results of [144] regarding the QDL measure applied to a charge band state would saturate to an area law in the thermodynamic limit.

It is worth noting however that it is not entirely clear whether the results from [145], who studied local bipartitions of a hardcore boson chain, are directly applicable to the nonlocal bipartition across spin and charge considered here, so these arguments do not constitute a proof by any means. However there are very early results on entanglement entropy of random pure states by Page, which found essentially a volume law everywhere [146]. As these random pure states have no notion of descending from a local Hamiltonian, we expect that a nonlocal bipartition across spin and charge does not raise any exceptions in Page's derivation. Using Page's results in place of Vidmar and Rigol's leads to the same conclusion. The situation considered here falls somewhere in between the two in that we have an eigenstate arising from a local Hamiltonian bipartitioned in a nonlocal way. It is therefore possible to imagine that there might be some loophole out of the conclusion that the QDL measure saturates to an area law when each set of degrees of freedom constitutes half the system.

Finally, let us consider the case where $\mathscr{H}_{AB} > \mathscr{H}_C$, and specifically let us take $\mathscr{H}_A > \mathscr{H}_C > \mathscr{H}_B$ with $\mathscr{H}_A$ larger than half the system. In this case, $S(B) \sim B$ while $S(A)$ is given by the entanglement entropy of the complement of A: $S(A) = S(BC)$. The entanglement of AB is

similarly given by the entanglement of the complement C. All of these entanglement entropies scale, at leading order, as a volume law. The mutual information can therefore be schematically written as

$$I(A,B) \sim BC + B - C \sim B,$$

which is a volume law. More generally, when $AB > C$ with A (or B) small compared to AB, we find $I(A,B) \sim \min(A,B)$, which is a volume law.

These considerations allow us to 'repair' the QDL measure such that when applied to a state which does satisfy ETH, both $S^{s/c}$ and $S^{c/s}$ are volume law. The original QDL protocol consists of measuring *all* of one set of degrees of freedom - say, the heavy particles - and then computing the entanglement of light particles. The problem is that measuring all of the heavy particles is too much, and disentangles the light particles regardless of whether the state is ergodic or not.

Rather than measuring all heavy particles, a refinement of the QDL protocol measures the heavy particles only in a region Γ which is small compared to the total system. Within Γ, we then measure entanglement entropy of the light particles in a subregion $A \ll \Gamma$. This captures the same physics as the original QDL diagnostic in the sense that it identifies when the light particles in Γ/A fail to act as a bath which thermalizes A. On the other hand for an ergodic state lacking any of the special structure of the QDL state, we generically expect that even after fixing the heavy particles the light particles are still able to thermalize. In this case, we will obtain volume law for both $S^{s/c}$ and $S^{c/s}$, whereas a QDL state will have volume law for one and area law for the other.

To check the validity of these arguments, we applied this measurement to the same eigenstates of the Hubbard model. From a chain of length $L = 12$, we first choose a subregion Γ corresponding to six sites. We then bipartition Γ into Γ_l and Γ_r and measure the mutual information between spins (or charge) in Γ_l with spins (or charge) in Γ_r. The results are shown in Figure 4.4, and fully agree with our expectations for how the QDL measurement distinguishes between ergodic and ETH-violating states.

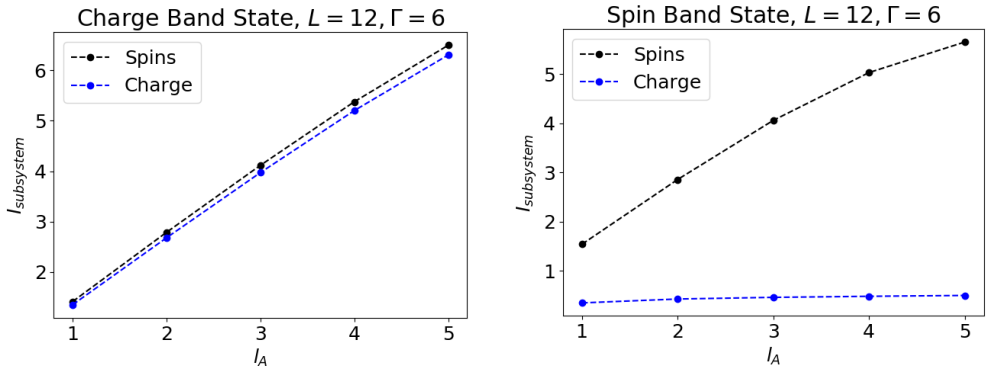

Figure 4.4: Subsystem mutual information calculated based on the refined QDL protocol. Left) Subsystem mutual information of charge and spins in a charge band state. Both exhibit a volume law, as we expect of a generic ergodic state. Right) Subsystem mutual information of charge and spins in a spin band state. Spin mutual informations follows a volume law whereas charge mutual information is sharply decreased to an area law, identifying the spin band states as quantum disentangled states.

4.4 Disentangling heavy Fermi liquids

We now turn to the applications to heavy-fermion physics. An elementary model for heavy fermion materials consists of a lattice of localized moments $\vec{S}$ coupled to a sea of conduction electrons by spin exchange.

$$\mathbf{H}_K = \sum_k \varepsilon(k) c_k^\dagger c_k + J_K \sum_i \vec{S}_i \cdot \vec{s}_i + J_H \sum_{\langle ij \rangle} \vec{S}_i \cdot \vec{S}_j$$

where $\vec{s} = \frac{1}{2} c_\alpha^\dagger \vec{\sigma}_{\alpha\beta} c_\beta$ is the electron spin. We have also included the possibility of antiferromagnetic exchange interactions between the local spins. This model has been extensively studied and exhibits a few exotic phases. In addition to the Heavy Fermi Liquid (HFL) phase which has a large FS, it is possible that the spins decouple from the conduction electrons. In the absence of magnetic order, the Lieb-Shultz-Mattis-Hastings-Oshikawa theorem then requires the spins to enter a spin liquid phase. This is the FL* phase characterized by a fractionalized spin liquid coexisting with a small FS of conduction electrons.

We propose to use conditional mutual information as a tool to study the nature of the Fermi

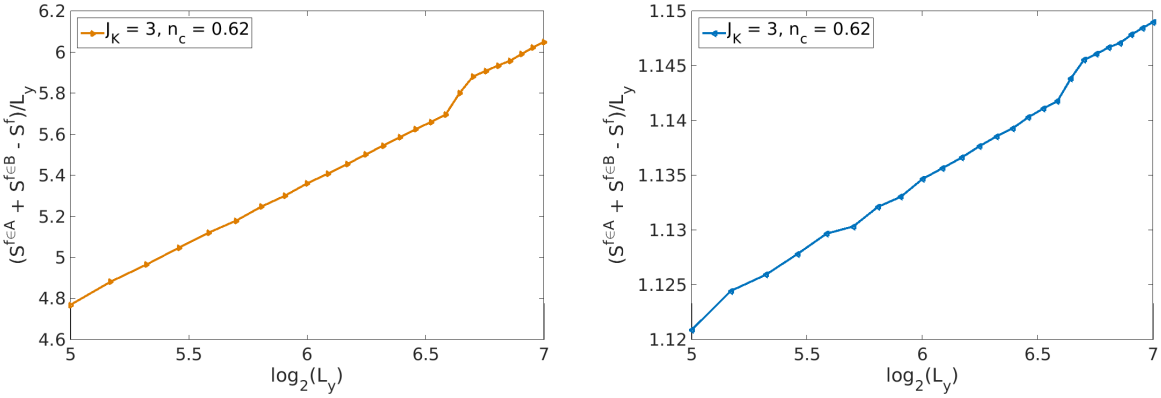

Figure 4.5: Conditional mutual information calculated in the paramagnetic HFL phase. Left: Conditional mutual information of f electrons as a function of linear size of region A. Right: Conditional mutual information of c electrons. The system is bipartitioned into left and right halves.

surface. Specifically, we consider calculating the conditional mutual information between two non-overlapping sets of *local moments only*. Due to the Kondo hybridization, the entanglement entropy of local moments will be dominated by a volume law. Schematically, we expect the entanglement of spins in a region of size l to be described by

$$S^{\text{local moments}}(l) \sim a_1 l^d + a_2 l^{d-1} \log l + a_3 l^{d-1} + a_4.$$

In the HFL phase, spins participate in the Fermi surface and we expect the area law violating coefficient a_2 to be nonzero. Consider bipartitioning the system into two regions A and B. The mutual information between spins in A and spins in B conditioned on all itinerant electron degrees of freedom provides a subtraction scheme for exposing the coefficient a_2.

A approximate description of the KLM is possible in terms of a mean field theory where the local moments are represented by slave fermions $\vec{S}_i = f^\dagger_{i\alpha}\vec{\sigma}_{\alpha\beta} f_{i\beta}$. The phase diagram is determined by a competition between an RKKY effect which favors a magnetically ordered state, and the Kondo interaction. The HFL phase is characterized by a mean field parameter $V = \langle c^\dagger f \rangle$ representing the hybridization between c and f electrons. When the Kondo coupling is large enough, the system forms a paramagnetic metal with finite hybridization between c and f

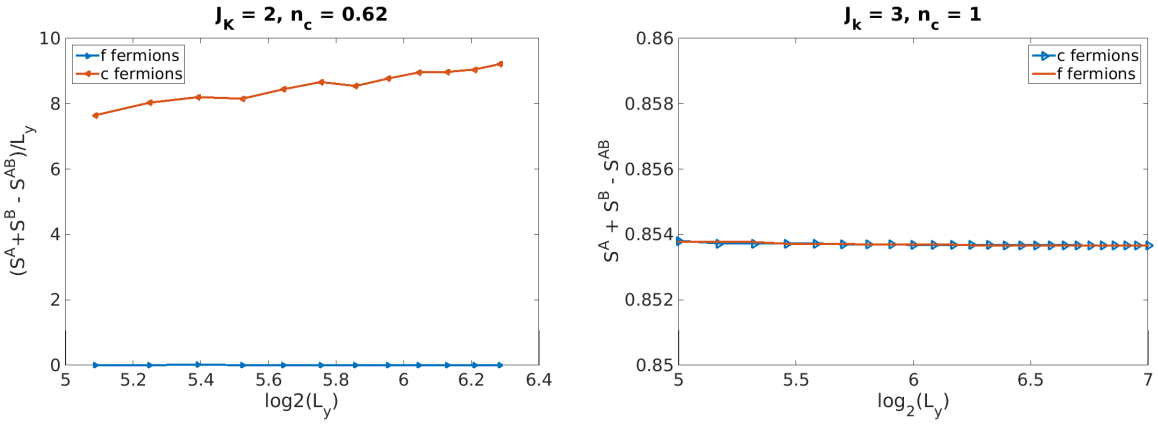

Figure 4.6: Left: Conditional mutual information calculated in the AFs phase. Right: Conditional mutual information at $n_c = 1$ in the HFL phase.

electrons.

We can calculate the entanglement entropy of subsets of degrees of freedom using the correlation matrix technique [128]. Specifically, we consider a rectangular system of size $2L_y \times L_y$, and measure the mutual information between spins (or charge) in the left and right halves of the system. The results in the HFL phase are shown in Figure 4.5. Entanglement entropy of f or c electrons alone follows a volume law their mutual information follow $I(A:B) \sim l \log l$, providing evidence that both f and c participate in the Fermi surface.

When the Kondo screening is not operative, the mean field description of the system has $V = 0$ and antiferromagnetic order. In this case, a decoupled small Fermi surface of c electrons coexists with antiferromagnetically ordered local moments. The left panel of Figure 4.6 shows that as expected, the mutual information of c fermions is Fermi-surface like while the f fermions are in a product state with no entanglement. The right panel of Figure 4.6 shows that at the Kondo insulator point at $n_c = 1$, mutual information of both f and c saturates to an area law.

The mean field parameter V is not gauge invariant, so it vanishes if the constraint $n_f = 1$ is implemented exactly and it cannot be measured experimentally. Therefore, we propose that the mutual information provides a gauge invariant order parameter for the HFL phase. Although it

is difficult to imagine measuring the mutual information experimentally, it would be extremely interesting to repeat these measurements using a projected wavefunction where $n_f = 1$ on each site. We leave this for future work.

4.5 Acknowledgements

We thank Tsung Lu for helpful discussions, and for sharing some of his unpublished results on entanglement negativity in chaotic wavefunctions with us.

Chapter 4 is, in part, a reprint of material from work done in collaboration with Tarun Grover and John McGreevy, as it will appear on the arXiv. The dissertation author was the primary investigator and author of this material.

Appendix A

A.1 Cluster states for $\mathbb{Z}_N$

Consider now an N-dimensional Hilbert spaces at the sites. We will use the conventions

$$XZ = \omega ZX, \;\; X = \sum_n |n\rangle\langle n+1|, \;\; Z = \sum_n \omega^n |n\rangle\langle n|.$$

A $\mathbb{Z}_N$ generalization of control-Z is

$$\mathbf{CZ}_{12} = \sum_{mn} |mn\rangle\langle mn|\omega^{mn} \;,$$

which satisfies

$$\mathbf{CZ}_{12}^k X_2 = X_2 \mathbf{CZ}_{12}^k Z_1^{-k}, \; \mathbf{CZ}^N = 1. \tag{A.1}$$

Consider also a $\mathbb{Z}_N$ (bipartite) string net: that is, assign to the edges $\langle ij\rangle$ of a (bipartite) graph a configuration of integers s_{ij} mod N, satisfying

$$s_{ij} = -s_{ji}$$

and

$$\sum_{\langle i|j\rangle} s_{ij} = 0, \;\; \forall i \tag{A.2}$$

– the net flux into each site is zero, so the strings are closed. (The notation $\sum_{\langle i|j\rangle}$ means sum over neighbors j of a fixed site i.) On a bipartite lattice, a canonical orientation for the links is pointing from the A sublattice to the B sublattice.

For each site, let

$$H_j = u_j^\dagger h_j^0 u_j = -u_j^\dagger (X_j + X_j^\dagger) u_j = -X_j \left(\prod_{\langle j|k \rangle} Z_k^{s_{jk}} \right)^{\text{sgn }(j)} + \text{h.c}$$

where $u_j = \prod_{\vec{l} \in v(j)} \mathbf{CZ}_l^{s_l}$ is a product of unitary operators on the oriented links in the vicinity of j and sgn (j) is $+1(-1)$ for j on the A(B) sublattice. These terms commute in the same way as the terms in the $\mathbb{Z}_2$ cluster Hamiltonian.

The plaquette term in a $\mathbb{Z}_N$ toric code is a product of alternating operators σ^x and $(\sigma^x)^\dagger$ on the links bounding the plaquette. For example, on a square lattice we have $B_p = \sigma_N^x (\sigma_E^x)^\dagger \sigma_S^x (\sigma_W^x)^\dagger$. Under snake monsterification, this becomes $\mathscr{B}_p = B_p \mathbf{CZ}_N \mathbf{CZ}_E^\dagger \mathbf{CZ}_S \mathbf{CZ}_W^\dagger$. The full Hamiltonian for the $\mathbb{Z}_N$ theory is then

$$\mathbf{H} = \sum_j \mathscr{V}\left(A_j\right) + \sum_p \mathscr{V}\left(\mathscr{B}_p\right) + \sum_j H_j P_j$$

where $\mathscr{V}(z)$ is a real-valued function of a phase $|z|^2 = 1$ which is minimized when $z = 1$.

The groundstate of this model is

$$|\text{gs}\rangle = \mathscr{N}^{-1/2} \sum_C (W_C + W_C^\dagger) |0\rangle \otimes \prod_j |0_j\rangle.$$

where C is a closed $\mathbb{Z}_N$ string-net and $W_C = \prod_{l \in C} (\sigma_l^x \mathbf{CZ}_l)^{n_l} (\sigma_{l+1}^x \mathbf{CZ}_{l+1})^{-n_{l+1}} \ldots$ is the $\mathbb{Z}_N$ dimensional analog of the string creation operator. The exponent n_l is the multiplicity of link l in the string-net C, $|0\rangle$ is the empty link configuration, and $|0_j\rangle$ is the groundstate of h_j^0.

When the graph is bipartite, this model has a $\mathbb{Z}_N \times \mathbb{Z}_N$ symmetry which is generated by

$$\text{g}^{o/e} \equiv \prod_{j \in o/e} X_j.$$

A quasiparticle is obtained by acting on $|\text{gs}\rangle$ by W_L where L is an open curve. Thus using (A.1) we see that the successive action of $\text{g}^{o/e}$ generates a set of degenerate, orthogonal quasiparticle states. For an endpoint labelled by 1, there is a N-dimensional Hilbert space spanned by $\{Z_1^k W_L |\text{gs}\rangle; k \in [0, N-1]\}$. These furnish a projective representation of the symmetry in that $\text{g}^e \text{g}^o = \omega \text{g}^o \text{g}^e$ when acting on a single anyon.

This model also possesses a nontrivial anti-unitary symmetry, which acts by complex conjugation.

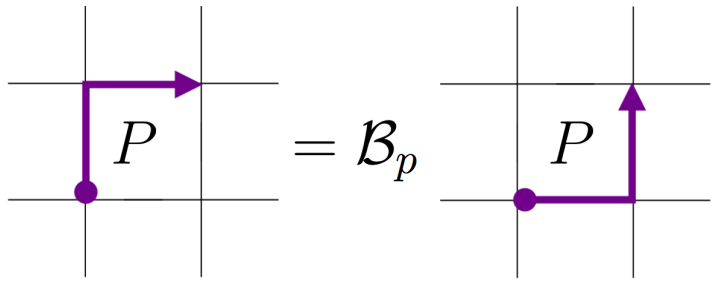

Figure A.1: As the quasiparticles hop around, they acquire phases dependent on the flux through the plaquettes.

Generalizations of the cluster state (or *graph state*) to other groups, on bipartite graphs, are described here [147]. However, only a stabilizer construction (and not the circuit construction that we require) is provided. It would be very interesting to generalize this construction to attach locally 1-dimensional SPTs to the string nets of arbitrary quantum double models.

A.2 Stability of the physics of the snake monster

Here we study the stability of the physics the cluster snake monster of §2.4 with respect to symmetric perturbations. We show that the degenerate doublet is stable to small perturbations which preserve the $\mathbb{Z}_2 \times \mathbb{Z}_2$ symmetry. The basic claim is that the argument for stability §2.3.1 of the 1d SPT carries over to the 3d model.

Observe first that a naive hopping term for the electric defects $\mathbf{T}_{ij} = \mathbf{CZ}_{ij}\sigma^x_{ij}$ is not symmetric under either $\mathbb{Z}_2 \times \mathbb{Z}_2$ or $\mathscr{T}$. We can construct a symmetric hopping term if the anyon stays on the same sublattice: $\mathbf{T}_{ac} = (1 + Z_a Z_c)\mathbf{CZ}_{ab}\mathbf{CZ}_{bc}\sigma^x_{ab}\sigma^x_{bc}$, where b is a neighbor of both a and c. This acts as a kinetic energy for the anyons and leads to identical dispersion relations $\varepsilon(k) \sim \cos(k)$ for the two states comprising the doublet; they are degenerate at all momenta.

As an aside, we note that this realizes an Aharonov-Bohm effect. On the square lattice, there are two direct paths from one site to a same-sublattice-nearest-neighbor, illustrated in Figure A.1. The difference between these two paths is a factor of $\mathscr{B}_p$. Thus we see that the phase

difference between the two paths is the flux through the plaquette.

Another possibility is to just add to the hamiltonian $\sum_l \sigma_l^x$, the kinetic term for the site defects in the 'normal' toric code. In our case we need to check that the state obtained by acting with σ_l^x on an anyon state actually produces another anyon state. To do so, we calculate the overlap of the states $\sigma_{bc}^x|+/-\rangle_b$ with the states $|+/-\rangle_c$. This calculation is illustrated for one of the four cases:

$$\begin{aligned}\sigma_{bc}^x|+\rangle &= \sigma_{bc}^x W^{ab}|\text{gs}\rangle \\ &= \sigma_{bc}^x \prod_{a\to b} \mathbf{CZ}_l \sigma_l^x \left(\frac{1}{\sqrt{\mathcal{N}_c}} \sum_C \prod_{l\in C} \mathbf{CZ}_l |\Rightarrow\rangle \prod_{l\in C} \sigma_l^x \otimes_l |\sigma_l^z = +1\rangle \right) .\end{aligned} \tag{A.3}$$

We find the overlap of this state with an anyon state at the neighboring site $|+\rangle_c$

$$\begin{aligned}&\frac{1}{\mathcal{N}_c} \sum_{C,C'} \left(\langle \Rightarrow | \prod_{l'\in C'} \mathbf{CZ}_{l'} \prod_{l'\in C} \otimes_{l'} \langle \sigma_{l'}^z = +1 | \sigma_{l'}^x \prod_{a\to c} \mathbf{CZ}_l \sigma_l^x \right) \sigma_{bc}^x \times \\ &\qquad \left(\prod_{a\to b} \mathbf{CZ}_l \sigma_l^x \prod_{l\in C} \mathbf{CZ}_l |\Rightarrow\rangle \prod_{l\in C} \sigma_l^x \otimes_l |\sigma_l^z = +1\rangle \right) \\ &= \frac{1}{\mathcal{N}_C} \sum_{C,C'} \delta_{C,C'} \left(\langle \Rightarrow | \prod_{l'\in C'} \mathbf{CZ}_{l'} \prod_{a\to c} \mathbf{CZ}_l \sigma_l^x \right) \sigma_{bc}^x \left(\prod_{a\to b} \mathbf{CZ}_l \sigma_l^x \prod_{l\in C} \mathbf{CZ}_l |\Rightarrow\rangle \right) \\ &= \frac{1}{\mathcal{N}_C} \sum_C \langle \Rightarrow | \mathbf{CZ}_{bc} | \Rightarrow\rangle = {}_{bc}\langle \to\to | \mathbf{CZ}_{bc} | \to\to\rangle_{bc}.\end{aligned} \tag{A.4}$$

The overlap reduces to calculating the expectation value of the link operator in the ground state. The overlap of the other anyon states can be found by inserting factors of Z_b or Z_c, yielding

$$\begin{aligned} {}_c\langle + | \sigma_{bc}^x | + \rangle_b &= 1/2 \\ {}_c\langle - | \sigma_{bc}^x | + \rangle_b &= 1/2 \\ {}_c\langle + | \sigma_{bc}^x | - \rangle_b &= 1/2 \\ {}_c\langle - | \sigma_{bc}^x | - \rangle_b &= -1/2. \end{aligned} \tag{A.5}$$

There are two other states produced by acting with σ^x on an anyon state which have a defect in the site hamiltonian at the previous location of the anyon. In principle we should therefore assess the effect of this term through both degenerate and non-degenerate perturbation theory. However as we are interested in the dynamics of the anyons, degenerate perturbation theory leads to the relevant effect. Using the results given in A.5 we obtain the first order effective

Hamiltonian

$$\mathbf{H}_{\text{eff}} \approx \sum_{ij,\sigma\sigma'} t_{\sigma\sigma'} c^{\dagger}_{i\sigma} c_{j\sigma'} + \text{h.c.}$$

with

$$t_{\sigma\sigma'} = \begin{pmatrix} 1 & 1 \\ 1 & -1 \end{pmatrix}.$$

Diagonalizing this Hamiltonian leads to two hopping bands with energies proptional to $\pm\cos(ka)$. In this case the two bands are not identical; they are related by a π phase shift. Every energy level at momentum k has a degenerate mode in the other band at momentum $k+\pi$. The anyons still form doublets, albeit under an extended symmetry $\mathsf{G}\times\mathsf{S}$ where S denotes the sublattice exchange operation.

A.3 Triviality of the cluster paramagnet with unitary symmetry

In this appendix we apply the methods of [40, 148] to decide whether the snake-monster paramagnet can be protected by the unitary symmetry $\mathbb{Z}_2^{E,AB} \times \mathbb{Z}_2^{O,AB}$ generated by the action on even and odd sites of both intercalated sublattices. The idea is to look at the symmetry action on a symmetric topologically-ordered surface termination, and ask whether gauging the global symmetry can lead to a consistent larger topologically ordered theory.

From the coupled-layer picture, e transforms under the symmetry acting at the surface, and m transforms due to the bound e on the layer below. In this picture, the way the particle transforms also depends on whether the e particle, either directly on the surface, or, bound on the layer below, sits on the even or odd sub-lattice. Depending on the sub-lattice on which the the e particles sits, we have the following charge assignment:

where g_z represents $\mathbb{Z}_2^E$ and g_x represents $\mathbb{Z}_2^O$ (and g_y represents the diagonal subgroup). *If* we could gauge the global $\mathbb{Z}_2 \times \mathbb{Z}_2$ symmetry to make a larger topological field theory, we would

Table A.1: Sublattice-dependent symmetry action on anyons

	even		odd	
	e	m	e	m
g_x	σ^x	σ^x	σ^z	σ^z
g_y	$\mathbf{i}\sigma^y$	$\mathbf{i}\sigma^y$	$\mathbf{i}\sigma^y$	$\mathbf{i}\sigma^y$
g_z	σ^z	σ^z	σ^x	σ^x

introduce gauge fluxes Ω_x, Ω_y, Ω_z and gauge charges. The projective action of the $\mathbb{Z}_2 \times \mathbb{Z}_2$ symmetry on the anyons has the consequence that the gauge fluxes obey *projective fusion* rules: they satisfy the group algebra up to the creation of an anyon, specifically an ε particle in our case.

Consider braiding a flux Ω_y of g_y around an e particle. This has the effect of acting locally with the symmetry operator corresponding to g_y in the area encircled by the path, so acting with the symmetry on the e particle. If we do this twice, it is like acting with the symmetry generated by g_y twice which, due to the half-integral charge of e under g_y results in an overall sign of -1. But we may just as well have fused the two fluxes before braiding them around the e particle; this tells us that two fluxes of Ω_y fuse into something which has mutual semion statistics with e, so an ε or m. Similarly, we have $\Omega_x \times \Omega_y = -\Omega_y \times \Omega_x$ due to the projective nature of the representation, so we find that the two orders of fusing the fluxes differs by an anyon. We can repeat the argument for all cases to build the following table for flux fusion in the presence of various quasiparticles.

The fusion rules are operator equations, which must hold for any state. This implies that the consistent choice is

$$\begin{aligned}
&\Omega_x \times \Omega_x = 1 && \Omega_x \times \Omega_y = \varepsilon\Omega_z && \Omega_x \times \Omega_z = \varepsilon\Omega_y \\
&\Omega_y \times \Omega_y = \varepsilon && \Omega_y \times \Omega_x = \Omega_z && \Omega_y \times \Omega_z = \varepsilon\Omega_x \\
&\Omega_z \times \Omega_z = 1 && \Omega_z \times \Omega_x = \Omega_y && \Omega_z \times \Omega_y = \Omega_x\ .
\end{aligned}$$

These relations determine the 'factor set', the collection of coefficients denoted by $\omega(g_i, g_j)$ in

Table A.2: Flux fusion table for gauged cluster paramagnet

	even		odd	
	e	m	e	m
$\Omega_x \times \Omega_x$	1	1	1	1
$\Omega_x \times \Omega_y$	$\Omega_z(\varepsilon \text{ or } m)$	$\Omega_z(\varepsilon \text{ or } e)$	$\Omega_z(\varepsilon \text{ or } m)$	$\Omega_z(\varepsilon \text{ or } e)$
$\Omega_x \times \Omega_z$	$\Omega_y(\varepsilon \text{ or } m)$	$\Omega_y(\varepsilon \text{ or } e)$	$\Omega_y(\varepsilon \text{ or } m)$	$\Omega_y(\varepsilon \text{ or } e)$
$\Omega_y \times \Omega_y$	$\varepsilon \text{ or } m$	$\varepsilon \text{ or } e$	$\varepsilon \text{ or } m$	$\varepsilon \text{ or } e$
$\Omega_y \times \Omega_x$	Ω_z	Ω_z	Ω_z	Ω_z
$\Omega_y \times \Omega_z$	$\Omega_x(\varepsilon \text{ or } m)$	$\Omega_x(\varepsilon \text{ or } e)$	$\Omega_x(\varepsilon \text{ or } m)$	$\Omega_x(\varepsilon \text{ or } e)$
$\Omega_z \times \Omega_z$	1	1	1	1
$\Omega_z \times \Omega_x$	Ω_y	Ω_y	Ω_y	Ω_y
$\Omega_z \times \Omega_y$	Ω_x	Ω_x	Ω_x	Ω_x

the projective fusion rules $\Omega_{g_i} \times \Omega_{g_j} = \omega(g_i, g_j)\Omega_{g_i g_j}$ to be

$$\omega(g_x, g_x) = 1 \qquad \omega(g_x, g_y) = \varepsilon \qquad \omega(g_x, g_z) = \varepsilon$$

$$\omega(g_y, g_y) = \varepsilon \qquad \omega(g_y, g_x) = 1 \qquad \omega(g_y, g_z) = \varepsilon$$

$$\omega(g_z, g_z) = 1 \qquad \omega(g_z, g_x) = 1 \qquad \omega(g_z, g_y) = 1\ .$$

These factors participate in the pentagon equation, which is a consistency condition for a proposed set of braiding and fusion rules (characterized by matrices R and F respectively) that a topological quantum field theory must satisfy. If the pentagon equation is violated (and cannot be repaired by re-phasing the F-tensor), then this inability to gauge the model and promote it to a full TQFT is an obstruction to realizing this spectrum of quasiparticles inherently in two dimensions. Quite beautifully, [40] identifies this obstruction with an element of $H^4(\mathbb{Z}_2 \times \mathbb{Z}_2, \mathsf{U}(1))$, the cohomology group expected to classify 3d bosonic SPTs for a unitary $\mathbb{Z}_2 \times \mathbb{Z}_2$ symmetry [29].

In the toric code, all of the F tensors are equal to 1. Appendix B of [40] shows that in such a case the three nontrivial obstruction classes in $H^4(\mathbb{Z}_2 \times \mathbb{Z}_2, \mathsf{U}(1))$ are encoded entirely in the full braiding statistics matrix of the anyons in the factor set of the candidate projective fusion rules. Because the ε particle is a fermion, the full braid of two ε particles gives 1 (in contrast to -1 for the case of two semions). This means that this obstruction to realizing this topological

order intrinsically in two dimensions vanishes. [40] argue further that this is a necessary condition for nontriviality, so in fact the bulk theory described in §2.5 is trivial as an SPT with respect to the *unitary* symmetry $\mathbb{Z}_2 \times \mathbb{Z}_2$.

A.4 Self-dual models of confinement

In this appendix we provide some context for the workings of the pure loop construction of [36], and generalize it to $\mathbb{Z}_N$ strings.

The basic idea is to take a model of fluctuating string nets and add an energetic penalty term which forbids nontrivial winding of the strings. How do we impose a local condition which forces the strings to be contractible?

Here is a classical implementation which is well-known in certain corners of the statistical mechanics literature (*e.g.* [149]): Consider a model with $\mathbb{Z}_k$ variables $E_p = 0..k-1$ on the $d-1$-cells p of a d-dimensional cell complex Δ. A configuration of such variables specifies by duality a string net (an assignment of $\mathbb{Z}_k$ variables to the links of the dual cell complex $\check{\Delta}$) $\check{C}$. We will show that a sum over closed surfaces can produce the desired constraint that this string net is contractible – that is, it is the boundary of a collection of plaquettes.

A sum over $\mathbb{Z}_N$ closed surfaces S can be written as

$$\sum_{S,\text{closed}} \ldots = \sum_{\{\mu_p\}} \prod_l \delta\left(\sum_{q\in v(l)} \mu_q\right) \ldots = \sum_{\{\mu_p\}} \sum_{\{\alpha_l\}} \omega^{\sum_l \sum_{q\in v(l)} \mu_q \alpha_l} \ldots$$

Consider the sum

$$\sum_{S,\text{closed}} \omega^{\oint_S \vec{E}\cdot d\vec{a}} = \sum_{\{\mu_p\}} \sum_{\{\alpha_l\}} \omega^{\sum_l \sum_{q\in v(l)} \mu_q \alpha_l} \omega^{\sum_p \mu_p E_p}$$

By definition of the vicinity operator,

$$\sum_l \alpha_l \sum_{q\in v(l)} \mu_q = \sum_p \mu_p \sum_{l\in\partial p} \alpha_l \tag{A.6}$$

Using this identity (A.6), we have

$$\sum_{S,\text{closed}} \omega^{\oint_S \vec{E}\cdot d\vec{a}} = \sum_{\{\alpha_l\}} \sum_{\{\mu_p\}} \omega^{\sum_p \mu_p \left(E_p - \sum_{l\in\partial p} \alpha_l\right)} = \sum_{\{\alpha_l\}} \prod_p \delta\left(E_p - \sum_{l\in\partial p} \alpha_l\right)$$

This sum exactly imposes that E_p is exact.

A.4.1 $\mathbb{Z}_N$ self-dual models of confinement

Consider two interpenetrating lattices A and its dual lattice B in three dimensions (generalizations to other dimensions are interesting and will be discussed elsewhere). Place $\mathbb{Z}_N$ rotors on the links of the A lattice (with operators σ_l^x, σ_l^z), and independent $\mathbb{Z}_N$ rotors on the links of the B lattice (with operators $\tau_p^{x,z}$); these are in 1-to-1 correspondence with $d-1$-cells of the A lattice and we will label a link of B by the $d-1$ cell of A which it penetrates. We try not to speak of cells of the B lattice at all from now on.

$$H = -\sum_{l\in\Delta_1(A)} V(\mathscr{F}_l^A) - \sum_{p\in\Delta_{d-1}} V(\mathscr{F}_p^B)$$

where V is a real-valued function of a $\mathbb{Z}_N$ variable with maximum when its argument is 1, and

$$\mathscr{F}_l^A \equiv \left(\sigma_l^z\right)^\dagger \prod_{p\in v(l)} \tau_p^x \quad \mathscr{F}_p^B \equiv \tau_p^z \prod_{l\in\partial p} \left(\sigma_l^x\right)^\dagger \quad .$$

Here all the links are counted with orientation, and v is the vicinity operator, the oriented setwise inverse of the boundary map.

These operators all commute. Their simultaneous unique eigenstate with eigenvalue 1 has various useful representations:

$$|\psi\rangle = \sum_{\check{\mathscr{M}}} |\partial \check{\mathscr{M}}_z\rangle_A \otimes |\check{\mathscr{M}}_x\rangle_B \tag{A.7}$$

$$|\psi\rangle = \sum_{\mathscr{M}} |\mathscr{M}_x\rangle_A \otimes |\partial \mathscr{M}_z\rangle_B \tag{A.8}$$

$$|\psi\rangle = \sum_{C,\check{C},\text{contractible}} |C_z\rangle_A \otimes |\check{C}_z\rangle_B \tag{A.9}$$

More explicitly, (A.7) is

$$|\psi\rangle = N^{-N_p/2} \sum_{\{\mu_p\}} |\mu_p\rangle_B \otimes |s_l = \sum_{q\in v(l)} \mu_q\rangle_A \tag{A.10}$$

where N_p is the number of links of the B lattice, $|\mu_p\rangle$ are τ_p^x eigenstates and $|s_l\rangle$ are σ_l^z eigenstates.

To see (A.7), apply the flip operators in the basis

$$|\psi\rangle = \sum_{\{\mu_p\}} \sum_{\{s_l\}} \Phi(\mu, s) |\mu_p\rangle_B \otimes |s_l\rangle_A;$$

$\mathscr{F}_l^A = 1$ requires s to be a total divergence: $s_l = \sum_{q\in v(l)} \mu_q$, while $\mathscr{F}_p^B = 1$ requires a uniform superposition of such states, by making the sheets hop.

Now let's discuss how to get from (A.7) to (A.9). On a given link p, the z-basis and x-basis are related by

$$|\mu_p\rangle = \frac{1}{\sqrt{N}} \sum_{\sigma_p} \omega^{-\sigma_p \mu_p} |\sigma_p\rangle$$

Therefore

$$|\psi\rangle = \sum_{\sigma_p} |\sigma\rangle_B \, N^{-N_p} \sum_{\{\mu_p\}} \omega^{-\sum_p \sigma_p \mu_p} |s_l = \sum_{q\in v(l)} \mu_q\rangle_A \tag{A.11}$$

Here

$$\sigma_l^z |s, \sigma\rangle = \omega^{s_l} |s, \sigma\rangle, \;\; \tau_p^z |s, \sigma\rangle = \omega^{\sigma_p} |s, \sigma\rangle.$$

We rewrite the sum over μ_p in two parts: a membrane configuration μ on $\Delta_{d-1}(A)$ (the plaquettes p) can be decomposed as

$$\mu = \partial^{-1}(C) + S$$

where S is a closed membrane, $\partial S = 0$. $C = \partial\mu$ is the boundary of the membrane μ, a closed curve in $\Omega_1(A) = \ker(\partial) \subset \Delta_0(A)$. $\partial^{-1}(C)$ is a *particular* fiducial membrane whose boundary is C. S represents the deviation of μ from that choice.

Therefore

$$|\psi\rangle = \sum_{\sigma_p} |\sigma\rangle_B \, N^{-N_p} \sum_{\{\mu_p = \mu_p^0 + \hat{\mu}_p\}} \omega^{-\sum_p \sigma_p \mu_p^0} \omega^{-\sum_p \sigma_p \hat{\mu}_p} |s_l = \sum_{q\in v(l)} \mu_q^0\rangle_A \tag{A.12}$$

Here we have represented the plaquette sum as

$$\sum_{\{\mu_p = \mu_p^0 + \hat{\mu}_p\}} .. = \sum_{\{\mu_p^0\}} \sum_{\{\hat{\mu}_p\}} .. \equiv \sum_C \sum_S ..$$

and used the fact that the closed bit $\hat{\mu}_p$ satisfies by definition $\sum_{q\in v(l)} \hat{\mu}_q = 0$ and therefore does

not contribute to s_l. Therefore:

$$|\psi\rangle = \sum_{\sigma_p} |\sigma\rangle_B \, N^{-N_p} \sum_C \omega^{-\sum_p \sigma_p \mu_p^0} |C\rangle_A \cdot \underbrace{\sum_{\{\hat{\mu}_p\}} \omega^{-\sum_p \sigma_p \hat{\mu}_p}}_{\equiv \sum_S \omega^{\oint_S \vec{\sigma} \cdot d\vec{a}}} . \tag{A.13}$$

The underbraced factor is a (classical, *i.e.* no kets involved) sum over all closed $\mathbb{Z}_N$ valued surfaces weighted by the flux of a vector field through those surfaces. The result of this sum is to constrain $\{\sigma_p\}$ to only have support on contractible curves, $\check{C}$ *i.e.* $\sigma_p = \sum_{l \in \partial p} \alpha_l$ for some set of link variables α_l.

The remaining factor from the fiducial membrane is then the linking number of these two sets of curves

$$\omega^{-\sum_p \sigma_p \mu_p^0} = \omega^{l(C,\check{C})}.$$

Using the classical formulae around (A.6), we can see explicitly that the fluctuating magnetic flux leads to confinement. The sum over $\hat{\mu}_p$ imposes that σ_p is made of contractible curves $\check{C}$ and we get (A.9)

$$|\Psi\rangle = \mathscr{N} \sum_C |C\rangle_A \sum_{\check{C}} |\check{C}\rangle_B \; \omega^{l(C,\check{C})}$$

where $\mathscr{N}$ is a normalization factor.

Some comments:

1. Consider the z-basis representation (which will be (A.9)).

$$|\psi\rangle = \sum_{\{s_l\},\{\sigma_p\}} \Psi(s,\sigma)|s,\sigma\rangle \; . \tag{A.14}$$

By combining $\mathscr{F}$s we can make star operators on both sublattices:

$$\prod_{l \in v(j)} \mathscr{F}_l^A = \prod_{l \in v(j)} (\sigma_l^x)^\dagger, \forall j \in \Delta_0(A) \quad \prod_{p \in \partial V} \mathscr{F}_p^B = \prod_{p \in \partial V} \tau_p^z, \; \forall V \in \Delta_d(A).$$

This means that $\Psi(s,\sigma)$ only has support on closed string configurations.

2. Directly applying the flip operators to the z-basis representation (A.14) we learn that

$$\begin{aligned} \Psi(s,\sigma) &= \omega^{\sigma_p} \Psi(s + \partial p, \sigma_p), \;\; \forall p \in \Delta_{d-1}(A) \\ \Psi(s,\sigma) &= \omega^{-s_l} \Psi(s, \sigma_p + v(l)), \;\; \forall l \in \Delta_1(A) \end{aligned} \tag{A.15}$$

3. By comparing to (A.8) and (A.7) we see that these closed strings must furthermore be contractible, since they are boundaries of membranes. This means that their linking number is well-defined.

4. The conditions (A.15) are solved (up to normalization) by

$$\Psi(s,\sigma) = \omega^{l(s,\sigma)}$$

where l is the linking number of the two configurations of closed surfaces. A lattice formula for the linking number (from which we should be able to directly check (A.15)) is

$$\omega^{l(s,\sigma)} = \omega^{\sum_p \sigma_p \sum \mu_p}\big|_{s_l = \sum_{p\in v(l)} \mu_p}$$

The expression for μ_p which solves $s_l = \sum_{p\in v(l)} \mu_p$ is a lattice version of the Chern-Simons propagator.

Appendix B

B.1 $1/N$ corrections to the cluster-fermion propagator

As promised in §3.2, here we analyze the $1/N$ correction to the propagator of the localized fermions. Starting from the conformal SYK propagator as $\mathscr{G}_0$, and denoting convolution over the intermediate variable by $*$, we have

$$\mathscr{G}(\omega, x-y) - \mathscr{G}_0(\omega)\delta_{xy} = \frac{g^2}{N}\mathscr{G}_0(\omega)^2 G^0_{xy}\delta_{xy} + \frac{g^4}{N}\mathscr{G}_0(\omega)^3\delta_{xy}G^0_{xz} * G^0_{zy} + \dots$$

Fourier transforming and using results from §3.2, we find

$$\delta\mathscr{G}(k\omega) = N^{-1}\left(g^2\mathscr{G}_0^2(\omega)\int đk\, G^0(k\omega) + g^4\mathscr{G}_0^3\int đk\, G^0(k\omega)^2 + \dots\right)$$

$$= \frac{g^2}{N}\int đk\mathscr{G}_0^2\frac{1}{G_0(k)^{-1} - g^2\mathscr{G}_0} = \frac{g^2}{N}\mathscr{G}_0^2\int đk G(k).$$

$$= \frac{g^2}{N}\mathscr{G}_0^2(\omega)\int đ^d k\,\frac{1}{\mathbf{i}\omega - \xi(k) + \mathbf{i}g^2(\pi/J^2)^{1/4}|\omega|^{-1/2}\mathrm{sgn}\,\omega}$$

Analysis of the integral. Thus the $1/N$ correction to the localized fermion propagator is proportional to

$$D(\omega) \equiv \int đ^d k G(k,\omega) = G(\omega; xx), \tag{A.1}$$

the local density of states of the itinerant fermions, the quantity which determines the dI/dV curve measured by scanning-tunneling microscopy.

Some difficulty arises from the UV-sensitivity of this integral: the answer is not a property

of only the physics at the Fermi surface, but depends also on short-distance details. Here we will show that, given the form of the SYK propagator $\mathscr{G}_0(\omega)$, the resulting $D(\omega)$ *vanishes* at small frequency, independent of those short-distance details. Therefore, this $1/N$ correction does not modify the leading low-frequency scaling behavior of $\mathscr{G}$, even at frequencies very small compared to N.

Let us parametrize G as follows:

$$G(k,\omega) = \frac{1}{\omega - \xi(k) - \Sigma(\omega)}. \tag{A.2}$$

(Note that we assume k-independent self-energy.) To learn something about integrals of the form (A.1), consider free fermions with bandstructure $\xi(k)$, in which case we have the Schwinger-Dyson equation

$$(-\mathbf{i}\partial_t + \xi(\mathbf{i}\partial_x))\, G_{x,0}(t) = \delta^d(x)\delta(t)$$

and hence by Fourier transform

$$G(k,\omega) = \int dt d^d x e^{-\mathbf{i}(kx-\omega t)} G_{x,0}(t),$$

(A.2) obtains with $\Sigma(\omega) = 0$. On the other hand, we also have

$$G_{x,0}(t) \equiv \langle \mathrm{gs}|c_x^\dagger(t)c_0(0)|\mathrm{gs}\rangle = \int \mathrm{d}^d k \int \mathrm{d}^d q \langle \mathrm{gs}|e^{-\mathbf{i}\omega_k t + \mathbf{i}kx} c_k^\dagger c_q|gs\rangle = \int_{q\in FS} \mathrm{d}^d q e^{-\mathbf{i}\omega_q t + \mathbf{i}qx}.$$

Therefore

$$D(\omega) = \int \mathrm{d}^d k \int dt d^d x e^{-\mathbf{i}(kx-\omega t)} \frac{1}{V} \sum_{q\in FS} e^{-\mathbf{i}\omega_q t + \mathbf{i}qx} \tag{A.3}$$

$$= \int dt e^{\mathbf{i}\omega t} \int_{q\in FS} \mathrm{d}^d q e^{-\mathbf{i}\omega_q t} \tag{A.4}$$

$$= \int_{q\in FS} \mathrm{d}^d q \delta(\omega - \omega_q) \tag{A.5}$$

$$= \int_{q\in FS} \mathrm{d}^d q \frac{\delta(q - q(\omega))}{\partial_q \omega} = \theta(\mu - \omega)\rho(\omega) \tag{A.6}$$

which is the density of filled levels. Notice that (A.6) correctly reproduces

$$\int d\omega D(\omega) = \int \mathrm{d}^d q G_q(t=0) = \int \mathrm{d}^d q \langle gs|c_q^\dagger c_q|\mathrm{gs}\rangle = \int_{q\in FS} N_q = N$$

the total number of fermions.

For example, consider the case when the Fermi level is near the edge of a 1d band, so that

$\rho(\omega) = \frac{1}{\sqrt{\omega - 2t}}\theta(2t-\omega)$. Let us reproduce this answer using (A.6) starting from the Green's function (A.2). Linearizing about the Fermi surface $k_\perp = k - k_F$,

$$\xi(k) = -\mu + v_F k_\perp + \mathscr{O}(k_\perp)^2 \tag{A.7}$$

would give

$$D(\omega) \stackrel{?}{=} \Omega_d k_F^{d-1} \int_{-\Lambda}^{\Lambda} dk_\perp \frac{1}{f(\omega) - v_F k_\perp} = \Omega_d k_F^{d-1} \log\left(\frac{f(\omega) - v_F\Lambda}{f(\omega) + v_F\Lambda}\right)$$

which depends on Λ at large Λ – this is the UV sensitivity we advertised above. The answer will be different if we include the next term in the expansion (A.7) about the Fermi surface:

$$\xi(k) = -\mu + v_F k_\perp + t k_\perp^2 + \ldots$$

since then the integral $\sim \int^\Lambda \frac{dk_\perp}{k_\perp^2}$ would be finite as $\Lambda \to \infty$. For definiteness, focus on the 1d band edge example: that is, suppose $d = 1$ and μ is near the bottom of the band so $v_F = 0$. Then

$$D(\omega) = \int_{-\infty}^{\infty} \text{đ}k \frac{1}{\omega - tk^2} = \frac{1}{\sqrt{\omega t}}$$

(the contour can be closed in either half-plane). The imaginary part is only nonzero for $\omega < 0$, and reproduces the divergence at the 1d band edge.

Armed with this intuition, we return to the case of interest, where at low frequency the singular self-energy dominates, and $f(\omega) \sim \omega^{-1/2}$. In that case (still in $d = 1$ for now),

$$D(\omega) = \int \text{đ}k \frac{1}{C\omega^{-1/2} - \mu - \xi(k)} = \int \text{đ}k \frac{\omega^{1/2}}{C - (\mu - \xi(k))\,\omega^{1/2}}.$$

Assume that ξ is a polynomial of degree D in k, $\xi = a_0 k^D + a_1 k^{D-1} + \cdots$; then letting $u \equiv \omega^{\frac{1}{2D}} k$, this integral at small ω is

$$D(\omega) = \omega^{\frac{1}{2}-\frac{1}{D}} \int \text{đ}k \frac{1}{C - a_0 u^D + a_1 u^{D-1}\omega^{\frac{1}{2D}} + \cdots} \stackrel{\omega\to 0}{\sim} \omega^{\frac{1}{2}-\frac{1}{D}}$$

Alternatively, suppose the we are working in a lattice model, so that the momentum integral $\int \text{đ}^d k$ is over a finite Brillouin zone; in that case, $D(\omega) \stackrel{\omega\to 0}{\sim} \omega^{1/2}$. In either case, we find $D(\omega) \stackrel{\omega\to 0}{\to} 0$.

In general d, the same analysis gives

$$D(\omega) = \omega^{1/2} \int \frac{\text{đ}^d k}{\omega^{\frac{1}{2}} k^D + \ldots} = \omega^{\frac{1}{2}-\frac{d}{2D}} K_d \int \frac{u^{d-1} du}{u^D + \cdots}$$

where $K_d = \frac{\Omega_{d-1}}{(2\pi)^d}$. The integral converges when $D > d$, in which case the power of omega is $\frac{1}{2} - \frac{d}{2D} > 0$, and the integral vanishes as $\omega \to 0$. Alternatively, we can appeal to the lattice

regulator: compactness of the Brillouin zone guarantees that $D(\omega) \overset{\omega\to 0}{\to} \omega^{\frac{1}{2}} \int d^d k \frac{1}{C}$ is $\omega^{\frac{1}{2}}$ times a finite integral.

B.2 Other numerical results

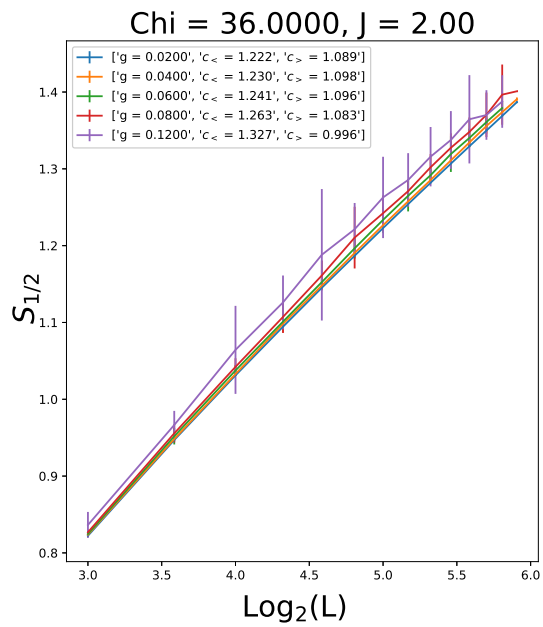

Figure B.1: $S_{1/2}$ vs Log(L) calculating using standard DMRG at small g.

The standard vMPS algorithm with only six cluster fermions is an especially poor representative of the large N model at very small g; if g is smaller than the finite size energy gap between the SYK ground state and the excited states then the hybridization interaction is essentially frozen out. The truncated version of the algorithm starting with a larger Hilbert space does a better job in representing the large N model.

A benchmark of the truncation method. The truncation method outlined above is an uncontrolled approximation for the sizes of local Hilbert spaces available to us. As a test of the method, in Fig. B.2 we show the spectrum of an SYK impurity coupled to a single extra

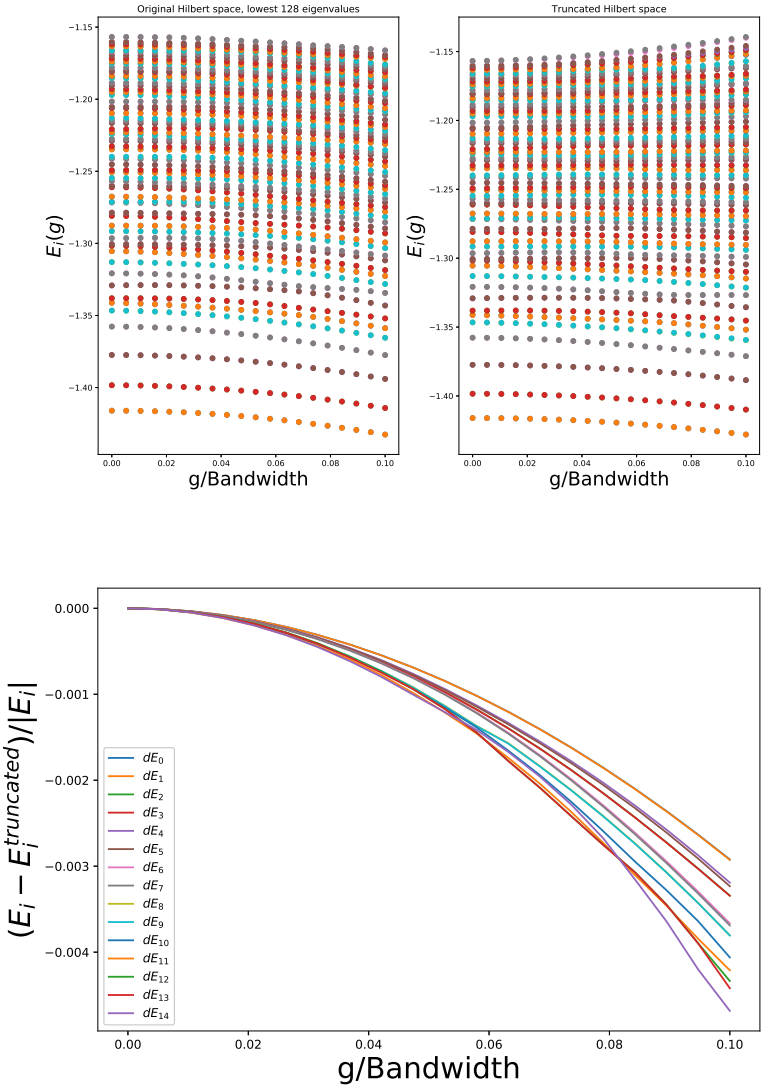

Figure B.2: A check on the validity of the truncation method. Top Left: first 128 levels of an SYK cluster with $N_{syk} = 12$ hybridized with a single extra fermion mode. Top Right: the spectrum of the truncated SYK hamiltonian (truncated to 64 levels) coupled to an extra fermion mode. Bottom: Fractional error in the energy eigenvalues of the lowest fifteen states.

fermionic mode (one site of the chain). The bottom part of the truncated spectrum matches quite well with the correct spectrum. The top of the truncated spectrum is wrong: the level repulsion from the levels above is missing. We used this method in studying the growth of the half-chain entanglement entropy in addition to the standard MPS algorithm.

Bibliography

[1] L. Bonsall and A. Maradudin, "Some static and dynamical properties of a two-dimensional wigner crystal," *Physical Review B* **15** no. 4, (1977) 1959.

[2] M. I. Katsnelson and V. Y. Irkhin, "Metal-insulator transition and antiferromagnetism in the ground state of the hubbard model," *Journal of Physics C: Solid State Physics* **17** no. 24, (Aug, 1984) 4291–4308.

[3] L. Balents, "Spin liquids in frustrated magnets," *Nature* **464** no. 7286, (2010) 199.

[4] R. J. Baxter, *Exactly solved models in statistical mechanics*. Elsevier, 2016.

[5] L. Landau and E. Lifshitz, "Statistical physics, part 1: Volume 5 (course of theoretical physics, volume 5)," *Publisher: Butterworth-Heinemann* **3** (1980) .

[6] X. G. Wen, "Mean-field theory of spin-liquid states with finite energy gap and topological orders," *Phys. Rev. B* **44** (Aug, 1991) 2664–2672.

[7] T. Senthil, "Symmetry-protected topological phases of quantum matter," *Annu. Rev. Condens. Matter Phys.* **6** no. 1, (2015) 299–324.

[8] A. Y. Kitaev, "Fault-tolerant quantum computation by anyons," *Annals of Physics* **303** no. 1, (2003) 2–30.

[9] G. Baym and C. Pethick, *Landau Fermi-liquid theory: concepts and applications*. John Wiley & Sons, 2008.

[10] R. Shankar, "Renormalization-group approach to interacting fermions," *Rev. Mod. Phys.* **66** (Jan, 1994) 129–192.

[11] J. Polchinski, "Effective Field Theory and the Fermi Surface," *ArXiv High Energy Physics - Theory e-prints* (Oct., 1992) , hep-th/9210046.

[12] T. Timusk and B. Statt, "The pseudogap in high-temperature superconductors: an experimental survey," *Reports on Progress in Physics* **62** no. 1, (1999) 61.

[13] N. Hussey, K. Takenaka, and H. Takagi, "Universality of the mott–ioffe–regel limit in metals," *Philosophical Magazine* **84** no. 27, (2004) 2847–2864.

[14] S.-S. Lee, "Recent developments in non-fermi liquid theory," *Annual Review of Condensed Matter Physics* **9** (2018) 227–244.

[15] A. Kitaev, "A simple model of quantum holography," *unpublished* (2015) .

[16] J. Maldacena and D. Stanford, "Comments on the Sachdev-Ye-Kitaev model," arXiv:1604.07818 [hep-th].

[17] A. C. Hewson, *The Kondo problem to heavy fermions*, vol. 2. Cambridge university press, 1997.

[18] E. Lieb, T. Schultz, and D. Mattis, "Two soluble models of an antiferromagnetic chain," *Annals of Physics* **16** no. 3, (1961) 407–466.

[19] M. Oshikawa, "Commensurability, excitation gap, and topology in quantum many-particle systems on a periodic lattice," *Physical review letters* **84** no. 7, (2000) 1535.

[20] M. Oshikawa, "Topological approach to luttinger's theorem and the fermi surface of a kondo lattice," *Physical Review Letters* **84** no. 15, (2000) 3370.

[21] M. B. Hastings, "Lieb-schultz-mattis in higher dimensions," *Physical review b* **69** no. 10, (2004) 104431.

[22] T. Grover and M. P. Fisher, "Quantum disentangled liquids," *Journal of Statistical Mechanics: Theory and Experiment* **2014** no. 10, (2014) P10010.

[23] J. Polchinski, "String theory. Vol. 2: Superstring theory and beyond,". Cambridge, UK: Univ. Pr. (1998) 531 p.

[24] A. M. Polyakov, "Two-dimensional quantum gravity: Superconductivity at high T/c,".

[25] X. Chen, Y.-M. Lu, and A. Vishwanath, "Symmetry-protected topological phases from decorated domain walls," *Nature Communications* **5** (Mar., 2014) 3507, arXiv:1303.4301 [cond-mat.str-el].

[26] A. C. Potter and A. Vishwanath, "Protection of topological order by symmetry and many-body localization," *ArXiv e-prints* (June, 2015) , arXiv:1506.00592 [cond-mat.dis-nn].

[27] L. H. Santos, "Rokhsar-Kivelson models of bosonic symmetry-protected topological states," *Physical Review B* **91** no. 15, (2015) 1–10, arXiv:1502.0066.

[28] X.-G. Wen, *Quantum Field Theory of Many-Body Systems*. Oxford Univ. Press, Oxford, 2004.

[29] X. Chen, Z.-C. Gu, Z.-X. Liu, and X.-G. Wen, "Symmetry protected topological orders and the group cohomology of their symmetry group," *Phys. Rev. B* **87** (Apr, 2013) 155114.

[30] Y.-M. Lu and A. Vishwanath, "Theory and classification of interacting integer topological phases in two dimensions: A Chern-Simons approach," *Phys. Rev. B* **86** no. 12, (Sept., 2012) 125119, arXiv:1205.3156 [cond-mat.str-el].

[31] A. Vishwanath and T. Senthil, "Physics of three-dimensional bosonic topological insulators: Surface-deconfined criticality and quantized magnetoelectric effect," *Phys. Rev. X* **3** (Feb, 2013) 011016.

[32] C. Xu and S. Sachdev, "Global phase diagrams of frustrated quantum antiferromagnets in two dimensions: Doubled Chern-Simons theory," *Phys.Rev.* **B79** (2009) 064405, arXiv:0811.1220 [cond-mat.str-el].

[33] K. Walker and Z. Wang, "(3+ 1)-tqfts and topological insulators," *Frontiers of Physics* **7** no. 2, (2012) 150–159.

[34] A. M. Essin and M. Hermele, "Classifying fractionalization: Symmetry classification of gapped Z_2 spin liquids in two dimensions," *Phys. Rev. B* **87** no. 10, (Mar., 2013) 104406, arXiv:1212.0593 [cond-mat.str-el].

[35] A. Mesaros and Y. Ran, "Classification of symmetry enriched topological phases with exactly solvable models," *Phys. Rev. B* **87** no. 15, (Apr., 2013) 155115, arXiv:1212.0835 [cond-mat.str-el].

[36] C. Wang, A. Nahum, and T. Senthil, "Topological Paramagnetism in Frustrated Spin-One Mott Insulators," *ArXiv e-prints* (2015) , arXiv:1501.01047.

[37] A. M. Turner and A. Vishwanath, "Beyond Band Insulators: Topology of Semi-metals and Interacting Phases," arXiv:1301.0330 [cond-mat.str-el].

[38] T. Senthil, "Symmetry Protected Topological phases of Quantum Matter," *Ann.Rev.Condensed Matter Phys.* **6** (2015) 299, arXiv:1405.4015 [cond-mat.str-el].

[39] M. Levin and Z.-C. Gu, "Braiding statistics approach to symmetry-protected topological phases," *Phys. Rev. B* **86** no. 11, (Sept., 2012) 115109, arXiv:1202.3120 [cond-mat.str-el].

[40] X. Chen, F. J. Burnell, A. Vishwanath, and L. Fidkowski, "Anomalous Symmetry Fractionalization and Surface Topological Order," *ArXiv e-prints* (Mar., 2014) , arXiv:1403.6491 [cond-mat.str-el].

[41] L. Fidkowski, X. Chen, and A. Vishwanath, "Non-Abelian Topological Order on the Surface of a 3D Topological Superconductor from an Exactly Solved Model," *Physical Review X* **3** no. 4, (Oct., 2013) 041016, arXiv:1305.5851 [cond-mat.str-el].

[42] B. Yoshida, "Topological phases with generalized global symmetries," *ArXiv e-prints* (Aug., 2015) , arXiv:1508.03468 [cond-mat.str-el].

[43] Y.-Z. You, Z. Bi, A. Rasmussen, M. Cheng, and C. Xu, "Bridging Fermionic and Bosonic Short Range Entangled States," *ArXiv e-prints* (Apr., 2014) , arXiv:1404.6256 [cond-mat.str-el].

[44] A. Y. Kitaev, "Fault tolerant quantum computation by anyons," *Annals Phys.* **303** (2003) 2–30, arXiv:quant-ph/9707021 [quant-ph].

[45] M. D. Schulz, S. Dusuel, R. Orus, J. Vidal, and K. P. Schmidt, "Breakdown of a perturbed Z_N topological phase," *New J. Phys.* **14** (2012) 025005, arXiv:1110.3632 [cond-mat.stat-mech].

[46] E. Rieffel and W. Polak, *Quantum Computing: A Gentle Introduction*. MIT Press, Cambridge, MA, 2011.

[47] Y. Bahri, R. Vosk, E. Altman, and A. Vishwanath, "Localization and topology protected quantum coherence at the edge of 'hot' matter," *ArXiv e-prints* (July, 2013) , arXiv:1307.4092 [cond-mat.dis-nn].

[48] A. Kitaev, "Anyons in an exactly solved model and beyond," *Annals of Physics* **321** (Jan., 2006) 2–111, cond-mat/0506438.

[49] T. Grover, Y. Zhang, and A. Vishwanath, "Entanglement entropy as a portal to the physics of quantum spin liquids," *New Journal of Physics* **15** no. 2, (Feb., 2013) 025002, arXiv:1302.0899 [cond-mat.str-el].

[50] D. S. Rokhsar and S. A. Kivelson, "Superconductivity and the Quantum Hard-Core Dimer Gas," *Phys.Rev.Lett.* **61** (1988) 2376–2379.

[51] R. Moessner and S. L. Sondhi, "Resonating Valence Bond Phase in the Triangular Lattice Quantum Dimer Model," *Physical Review Letters* **86** (Feb., 2001) 1881, cond-mat/0007378.

[52] H. Yao, L. Fu, and X.-L. Qi, "Symmetry fractional quantization in two dimensions," *ArXiv e-prints* (Dec., 2010) , arXiv:1012.4470 [cond-mat.str-el].

[53] C.-Y. Huang, X. Chen, and F. Pollmann, "Detection of symmetry-enriched topological phases," *Phys. Rev. B* **90** no. 4, (July, 2014) 045142, arXiv:1312.3093 [cond-mat.str-el].

[54] W. Li, S. Yang, M. Cheng, Z.-X. Liu, and H.-H. Tu, "Topology and criticality in the resonating Affleck-Kennedy-Lieb-Tasaki loop spin liquid states," *Phys. Rev. B* **89** no. 17, (May, 2014) 174411, arXiv:1312.3922 [cond-mat.str-el].

[55] K. S. Raman, R. Moessner, and S. L. Sondhi, "SU(2)-invariant spin- (1)/(2) Hamiltonians with resonating and other valence bond phases," *Phys. Rev. B* **72** no. 6, (Aug., 2005) 064413, cond-mat/0502146.

[56] M. Barkeshli, P. Bonderson, M. Cheng, and Z. Wang, "Symmetry, Defects, and Gauging of Topological Phases," *ArXiv e-prints* (Oct., 2014) , arXiv:1410.4540 [cond-mat.str-el].

[57] C. Wang, A. C. Potter, and T. Senthil, "Classification of Interacting Electronic Topological Insulators in Three Dimensions," *Science* **343** (Feb., 2014) 629–631, arXiv:1306.3238 [cond-mat.str-el].

[58] C. Wang, A. C. Potter, and T. Senthil, "Gapped symmetry preserving surface state for the electron topological insulator," *Phys. Rev. B* **88** (Sep, 2013) 115137.

[59] M. A. Metlitski, C. Kane, and M. P. A. Fisher, "Bosonic topological insulator in three dimensions and the statistical Witten effect," arXiv:1302.6535 [cond-mat.str-el].

[60] P. Bonderson, C. Nayak, and X.-L. Qi, "A time-reversal invariant topological phase at the surface of a 3D topological insulator," *J.Stat.Mech.* **2013** (2013) P09016.

[61] M. A. Metlitski, C. L. Kane, and M. P. A. Fisher, "A symmetry-respecting topologically-ordered surface phase of 3d electron topological insulators," *ArXiv e-prints* (June, 2013) , arXiv:1306.3286 [cond-mat.str-el].

[62] E. Fradkin and S. H. Shenker, "Phase diagrams of lattice gauge theories with higgs fields," *Phys. Rev. D* **19** (1979) 3682.

[63] A. Y. Kitaev, "Unpaired majorana fermions in quantum wires," *Physics-Uspekhi* **44** no. 10S, (2001) 131, cond-mat/0010440v2.

[64] J. C. Y. Teo and C. L. Kane, "Majorana Fermions and Non-Abelian Statistics in Three Dimensions," arXiv:0909.4741 [cond-mat.mes-hall].

[65] M. Freedman, M. B. Hastings, C. Nayak, X.-L. Qi, K. Walker, and Z. Wang, "Projective ribbon permutation statistics: A remnant of non-abelian braiding in higher dimensions," *Physical Review B* **83** no. 11, (2011) 115132.

[66] J. McGreevy and B. Swingle, "Non-Abelian statistics versus the Witten anomaly," *Phys.Rev.* **D84** (2011) 065019, arXiv:1106.0004 [hep-th].

[67] M. Freedman, M. B. Hastings, C. Nayak, and X.-L. Qi, "Weakly coupled non-Abelian anyons in three dimensions," *Phys. Rev. B* **84** no. 24, (Dec., 2011) 245119, arXiv:1107.2731 [cond-mat.str-el].

[68] S.-S. Lee, "Recent developments in non-fermi liquid theory," *arXiv preprint* (2017) , 1703.08172.

[69] S.-S. Lee, "A Non-Fermi Liquid from a Charged Black Hole: A Critical Fermi Ball," *Phys. Rev.* **D79** (2009) 086006, arXiv:0809.3402 [hep-th].

[70] H. Liu, J. McGreevy, and D. Vegh, "Non-Fermi liquids from holography," *Phys.Rev.* **D83** (2011) 065029, arXiv:0903.2477 [hep-th].

[71] M. Cubrovic, J. Zaanen, and K. Schalm, "String Theory, Quantum Phase Transitions and the Emergent Fermi-Liquid," *Science* **325** (2009) 439–444, arXiv:0904.1993 [hep-th].

[72] T. Faulkner, H. Liu, J. McGreevy, and D. Vegh, "Emergent quantum criticality, Fermi surfaces, and AdS(2)," *Phys.Rev.* **D83** (2011) 125002, arXiv:0907.2694 [hep-th].

[73] T. Faulkner, N. Iqbal, H. Liu, J. McGreevy, and D. Vegh, "Strange metal transport realized by gauge/gravity duality," *Science* **329** (2010) 1043–1047, arXiv:1003.1728 [hep-th].

[74] J. McGreevy, "TASI lectures on quantum matter (with a view toward holographic duality)," arXiv:1606.08953 [hep-th].

[75] C. M. Varma, P. B. Littlewood, S. Schmitt-Rink, E. Abrahams, and A. E. Ruckenstein, "Phenomenology of the normal state of cu-o high-temperature superconductors," *Phys. Rev. Lett.* **63** (Oct, 1989) 1996–1999.

[76] T. Faulkner and J. Polchinski, "Semi-Holographic Fermi Liquids," arXiv:1001.5049 [hep-th].

[77] N. Iqbal, H. Liu, and M. Mezei, "Semi-local quantum liquids," *JHEP* **04** (2012) 086, arXiv:1105.4621 [hep-th].

[78] A. Allais, J. McGreevy, and S. J. Suh, "A quantum electron star," *Phys. Rev. Lett.* **108** (2012) 231602, arXiv:1202.5308 [hep-th].

[79] A. Allais and J. McGreevy, "How to construct a gravitating quantum electron star," *Phys. Rev.* **D88** no. 6, (2013) 066006, arXiv:1306.6075 [hep-th].

[80] A. Georges, G. Kotliar, W. Krauth, and M. J. Rozenberg, "Dynamical mean-field theory of strongly correlated fermion systems and the limit of infinite dimensions," *Rev. Mod. Phys.* **68** (1996) 13–125.

[81] G. Kotliar, S. Y. Savrasov, K. Haule, V. S. Oudovenko, O. Parcollet, and C. A. Marianetti, "Electronic structure calculations with dynamical mean-field theory," *Rev. Mod. Phys.* **78** (2006) 865–951.

[82] K. Jensen, S. Kachru, A. Karch, J. Polchinski, and E. Silverstein, "Towards a holographic marginal Fermi liquid," *Phys. Rev.* **D84** (2011) 126002, arXiv:1105.1772 [hep-th].

[83] K. Jensen, "Chaos and hydrodynamics near AdS_2," arXiv:1605.06098 [hep-th].

[84] J. Maldacena, D. Stanford, and Z. Yang, "Conformal symmetry and its breaking in two dimensional Nearly Anti-de-Sitter space," arXiv:1606.01857 [hep-th].

[85] A. Almheiri and B. Kang, "Conformal Symmetry Breaking and Thermodynamics of Near-Extremal Black Holes," arXiv:1606.04108 [hep-th].

[86] S. Sachdev and J. Ye, "Gapless spin-fluid ground state in a random quantum Heisenberg magnet," *Physical Review Letters* **70** (May, 1993) 3339–3342, cond-mat/9212030.

[87] A. Georges, O. Parcollet, and S. Sachdev, "Mean Field Theory of a Quantum Heisenberg Spin Glass," *Physical Review Letters* **85** (July, 2000) 840–843, cond-mat/9909239.

[88] S. Sachdev, "Bekenstein-Hawking Entropy and Strange Metals," *Phys. Rev.* **X5** no. 4, (2015) 041025, arXiv:1506.05111 [hep-th].

[89] S. Sachdev, "Strange metals and the AdS/CFT correspondence," *Journal of Statistical Mechanics: Theory and Experiment* **11** (Nov., 2010) 22, arXiv:1010.0682 [cond-mat.str-el].

[90] S. Sachdev, "Holographic metals and the fractionalized Fermi liquid," *Phys.Rev.Lett.* **105** (2010) 151602, arXiv:1006.3794 [hep-th].

[91] E. Miranda, V. Dobrosavljevic, and G. Kotliar, "Kondo disorder: a possible route towards non-fermi-liquid behaviour," *Journal of Physics: Condensed Matter* **8** no. 48, (1996) 9871.

[92] Y. Gu, X.-L. Qi, and D. Stanford, "Local criticality, diffusion and chaos in generalized sachdev-ye-kitaev models," *Journal of High Energy Physics* **2017** no. 5, (2017) 125.

[93] S. Banerjee and E. Altman, "Solvable model for a dynamical quantum phase transition from fast to slow scrambling," *Physical Review B* **95** no. 13, (2017) 134302.

[94] A. Haldar and V. B. Shenoy, "Strange Half Metals and Mott Insulators in SYK Models," *ArXiv e-prints* (Mar., 2017) , arXiv:1703.05111 [cond-mat.str-el].

[95] X. Chen, R. Fan, Y. Chen, H. Zhai, and P. Zhang, "Competition between Chaotic and Non-Chaotic Phases in a Quadratically Coupled Sachdev-Ye-Kitaev Model," arXiv:1705.03406 [cond-mat.str-el].

[96] X.-Y. Song, C.-M. Jian, and L. Balents, "A strongly correlated metal built from sachdev-ye-kitaev models," *arXiv preprint* (2017) , 1705.00117.

[97] P. Zhang, "Dispersive SYK model: band structure and quantum chaos," arXiv:1707.09589 [cond-mat.str-el].

[98] A. Haldar, S. Banerjee, and V. B. Shenoy, "Higher-dimensional SYK Non-Fermi Liquids at Lifshitz transitions," *ArXiv e-prints* (Oct., 2017) , arXiv:1710.00842 [cond-mat.str-el].

[99] M. Berkooz, P. Narayan, M. Rozali, and J. Simón, "Higher dimensional generalizations of the syk model," *Journal of High Energy Physics* **2017** no. 1, (2017) 138.

[100] G. J. Turiaci and H. Verlinde, "Towards a 2d qft analog of the syk model," *Journal of High Energy Physics* **2017** no. 10, (2017) 167.

[101] M. Berkooz, P. Narayan, M. Rozali, and J. Simón, "Comments on the random thirring model," *Journal of High Energy Physics* **2017** no. 9, (2017) 57.

[102] C.-M. Jian, Z. Bi, and C. Xu, "Model for continuous thermal metal to insulator transition," *Physical Review B* **96** no. 11, (2017) 115122.

[103] Y. Gu, A. Lucas, and X.-L. Qi, "Energy diffusion and the butterfly effect in inhomogeneous sachdev-ye-kitaev chains," *SciPost Physics* **2** no. 3, (2017) 018.

[104] D. Khveshchenko, "Thickening and sickening the syk model," *SciPost Physics* **5** no. 1, (2018) 012.

[105] J. Murugan, D. Stanford, and E. Witten, "More on supersymmetric and 2d analogs of the syk model," *Journal of High Energy Physics* **2017** no. 8, (2017) 146.

[106] S.-K. Jian, Z.-Y. Xian, and H. Yao, "Quantum criticality and duality in the syk/ads _2 chain," *arXiv preprint arXiv:1709.02810* (2017) .

[107] T. Faulkner, N. Iqbal, H. Liu, J. McGreevy, and D. Vegh, "From black holes to strange metals," arXiv:1003.1728 [hep-th].

[108] T. Faulkner, N. Iqbal, H. Liu, J. McGreevy, and D. Vegh, "Charge transport by holographic Fermi surfaces," *Phys. Rev.* **D88** (2013) 045016, arXiv:1306.6396 [hep-th].

[109] A. Mukhopadhyay and G. Policastro, "Phenomenological Characterization of Semiholographic Non-Fermi Liquids," *Phys. Rev. Lett.* **111** no. 22, (2013) 221602, arXiv:1306.3941 [hep-th].

[110] B. Doucot, C. Ecker, A. Mukhopadhyay, and G. Policastro, "Density response and collective modes of semi-holographic non-Fermi liquids," arXiv:1706.04975 [hep-th].

[111] I. Affleck, "Quantum impurity problems in condensed matter physics," *Les Houches 2008 proceedings* (2008) , arXiv:0809.3474 [cond-mat.str-el].

[112] A. Bray and M. Moore, "Replica theory of quantum spin glasses," *Journal of Physics C: Solid State Physics* **13** no. 24, (1980) L655.

[113] G. Refael and J. E. Moore, "Entanglement entropy of random quantum critical points in one dimension," *Physical review letters* **93** no. 26, (2004) 260602, arXiv:cond-mat/0406737.

[114] G. Refael and J. E. Moore, "Criticality and entanglement in random quantum systems," *Journal of physics a: mathematical and theoretical* **42** no. 50, (2009) 504010, arXiv:0908.1986.

[115] A. B. Zamolodchikov, "Irreversibility of the flux of the renormalization group in a 2d field theory," *JETP lett* **43** no. 12, (1986) 730–732.

[116] R. Santachiara, "Increasing of entanglement entropy from pure to random quantum critical chains," *Journal of Statistical Mechanics: Theory and Experiment* **2006** no. 06, (2006) L06002, cond-mat/0602527.

[117] B. Swingle, "Entanglement does not generally decrease under renormalization," *Journal of Statistical Mechanics: Theory and Experiment* **2014** no. 10, (2014) P10041.

[118] T. Grover, "Certain General Constraints on the Many-Body Localization Transition," *ArXiv e-prints* (May, 2014) , arXiv:1405.1471 [cond-mat.dis-nn].

[119] R. A. Davison, W. Fu, A. Georges, Y. Gu, K. Jensen, and S. Sachdev, "Thermoelectric transport in disordered metals without quasiparticles: The Sachdev-Ye-Kitaev models and holography," *Phys. Rev.* **B95** no. 15, (2017) 155131, arXiv:1612.00849 [cond-mat.str-el].

[120] J. Cardy, *Scaling and renormalization in statistical physics*, vol. 5. Cambridge university press, 1996.

[121] S. R. White, "Density matrix formulation for quantum renormalization groups," *Physical review letters* **69** no. 19, (1992) 2863.

[122] U. Schollwöck, "The density-matrix renormalization group in the age of matrix product states," *Annals of Physics* **326** no. 1, (2011) 96–192, 1008.3477.

[123] P. Calabrese and J. Cardy, "Entanglement entropy and conformal field theory," *J.Phys.* **A42** (2009) 504005, arXiv:0905.4013 [cond-mat.stat-mech].

[124] A. M. Goldsborough and G. Evenbly, "Entanglement renormalization for disordered systems," arXiv:1708.07652 [cond-mat].

[125] C. Holzhey, F. Larsen, and F. Wilczek, "Geometric and renormalized entropy in conformal field theory," *Nucl. Phys.* **B424** (1994) 443–467, arXiv:hep-th/9403108 [hep-th].

[126] V. Korepin, "Universality of entropy scaling in one dimensional gapless models," *Physical review letters* **92** no. 9, (2004) 096402.

[127] P. Calabrese and J. Cardy, "Entanglement entropy and quantum field theory," *Journal of Statistical Mechanics: Theory and Experiment* **2004** no. 06, (2004) P06002.

[128] I. Peschel, "Calculation of reduced density matrices from correlation functions," *Journal of Physics A: Mathematical and General* **36** no. 14, (2003) L205.

[129] V. Berezinskii, "Kinetics of a quantum particle in a one-dimensional random potential," *WORLD SCIENTIFIC SERIES IN 20TH CENTURY PHYSICS* **11** (1995) 87–94.

[130] R. Pordes, D. Petravick, B. Kramer, D. Olson, M. Livny, A. Roy, P. Avery, K. Blackburn, T. Wenaus, F. Würthwein, I. Foster, R. Gardner, M. Wilde, A. Blatecky, J. McGee, and R. Quick, "The open science grid," in *Journal of Physics: Conference Series*, vol. 78, p. 012057, IOP Publishing. 2007.

[131] I. Sfiligoi, D. C. Bradley, B. Holzman, P. Mhashilkar, S. Padhi, and F. Wurthwein, "The pilot way to grid resources using glideinwms," in *Computer Science and Information Engineering, 2009 WRI World Congress on*, vol. 2, pp. 428–432, IEEE. 2009.

[132] A. Kitaev and J. Preskill, "Topological entanglement entropy," *Physical review letters* **96** no. 11, (2006) 110404.

[133] M. Levin and X.-G. Wen, "Detecting topological order in a ground state wave function," *Physical review letters* **96** no. 11, (2006) 110405.

[134] H.-C. Jiang, Z. Wang, and L. Balents, "Identifying topological order by entanglement entropy," *Nature Physics* **8** no. 12, (2012) 902.

[135] Y. Zhang, T. Grover, A. Turner, M. Oshikawa, and A. Vishwanath, "Quasiparticle statistics and braiding from ground-state entanglement," *Physical Review B* **85** no. 23, (2012) 235151.

[136] D. A. Huse, R. Nandkishore, and V. Oganesyan, "Phenomenology of fully many-body-localized systems," *Physical Review B* **90** no. 17, (2014) 174202.

[137] J. H. Bardarson, F. Pollmann, and J. E. Moore, "Unbounded growth of entanglement in models of many-body localization," *Physical review letters* **109** no. 1, (2012) 017202.

[138] H.-C. Jiang, Z.-X. Li, A. Seidel, and D.-H. Lee, "Symmetry protected topological luttinger liquids and the phase transition between them," *Science Bulletin* **63** no. 12, (2018) 753–758.

[139] F. D. M. Haldane, "Continuum dynamics of the 1-d heisenberg antiferromagnet: Identification with the o (3) nonlinear sigma model," *Physics Letters A* **93** no. 9, (1983) 464–468.

[140] I. Affleck, T. Kennedy, E. H. Lieb, and H. Tasaki, "Valence bond ground states in isotropic quantum antiferromagnets,".

[141] T. Kennedy and H. Tasaki, "Hidden symmetry breaking and the haldane phase ins= 1 quantum spin chains," *Communications in mathematical physics* **147** no. 3, (1992) 431–484.

[142] F. Pollmann, A. M. Turner, E. Berg, and M. Oshikawa, "Entanglement spectrum of a topological phase in one dimension," *Physical review b* **81** no. 6, (2010) 064439.

[143] R. Verresen, N. G. Jones, and F. Pollmann, "Topology and edge modes in quantum critical chains," *arXiv preprint arXiv:1709.03508* (2017) .

[144] J. R. Garrison, R. V. Mishmash, and M. P. Fisher, "Partial breakdown of quantum thermalization in a hubbard-like model," *Physical Review B* **95** no. 5, (2017) 054204.

[145] L. Vidmar and M. Rigol, "Entanglement Entropy of Eigenstates of Quantum Chaotic Hamiltonians," *Phys. Rev. Lett.* **119** no. 22, (2017) 220603, arXiv:1708.08453 [cond-mat.stat-mech].

[146] D. N. Page, "Average entropy of a subsystem," *Physical review letters* **71** no. 9, (1993) 1291.

[147] C. G. Brell, "Generalized cluster states based on finite groups," *New Journal of Physics* **17** no. 2, (Feb., 2015) 023029, arXiv:1408.6237 [quant-ph].

[148] P. Etingof, D. Nikshych, and V. Ostrik, "Fusion categories and homotopy theory," *Quantum Topology* **1** (2010) 209–273.

[149] P. M. Chaikin and T. C. Lubensky, *Principles of Condensed Matter Physics*. Cambridge Univ. Press, Sept., 2000.